Genetic meta-analysis identifies 10 novel loci and functional pathways for Alzheimer's disease risk

Iris E Jansen[1,2], Jeanne E Savage[1], Kyoko Watanabe[1], Julien Bryois[3], Dylan M Williams[3], Stacy Steinberg[4], Julia Sealock[5], Ida K Karlsson[3], Sara Hägg[3], Lavinia Athanasiu[6,7], Nicola Voyle[8], Petroula Proitsi[9], Aree Witoelar[6,10,], Sven Stringer[1], Dag Aarsland[11,12], Ina S Almdahl[13-15], Fred Andersen[16], Sverre Bergh[17,18], Francesco Bettella[6,10], Sigurbjorn Bjornsson[19], Anne Brækhus[17,20,], Geir Bråthen[21,22], Christiaan de Leeuw[1], Rahul S Desikan[23], Srdjan Djurovic[6,24], Logan Dumitrescu[25], Tormod Fladby[13,14], Timothy Homan[25], Palmi V Jonsson[19,26], Arvid Rongve[27,28], Ingvild Saltvedt[21,29], Sigrid B. Sando[21,22,], Geir Selbæk[17,30], Nathan Skenne[31], Jon Snaedal[19], Eystein Stordal[21,32], Ingun D. Ulstein[10,15], Yunpeng Wang[6,10], Linda R White[21,22], Jens Hjerling-Leffler[31], Patrick F Sullivan[3,33,34], Wiesje M van der Flier[2], Richard Dobson[11,35], Lea K. Davis[36,37], Hreinn Stefansson[4], Kari Stefansson[4], Nancy L Pedersen[3], Stephan Ripke[38-40*], Ole A Andreassen[6,10*], Danielle Posthuma[1,41,*#]

1. Department of Complex Trait Genetics, Center for Neurogenomics and Cognitive Research, Amsterdam Neuroscience, VU University, Amsterdam, The Netherlands.
2. Alzheimer Center and Department of Neurology, Amsterdam Neuroscience, VU University Medical Center, Amsterdam, The Netherlands.
3. Department of Medical Epidemiology and Biostatistics, Karolinska Institutet, Stockholm, Sweden.
4. deCODE Genetics/Amgen, Reykjavik, Iceland.
5. Interdisciplinary Graduate Program, Vanderbilt University, Nashville, USA.
6. NORMENT, K.G. Jebsen Centre for Psychosis Research, Institute of Clinical Medicine, University of Oslo, Oslo, Norway.
7. Division of Mental Health and Addiction, Oslo University Hospital, Oslo, Norway.
8. SGDP Centre, IoPPN, Denmark Hill, London, King's College London, London, UK.
9. Department of Basic and Clinical Neuroscience, Institute of Psychiatry, Psychology and Neuroscience, King's College London, London, UK.
10. Institute of Clinical Medicine, University of Oslo, Oslo, Norway
11. Institute of Psychiatry, Psychology and Neuroscience, King's College London, London, UK.
12. Center for Age-Related Diseases, Stavanger University Hospital, Stavanger, Norway.
13. Department of Neurology, Akershus University Hospital, Lørenskog, Norway.
14. AHUS Campus, University of Oslo, Oslo, Norway.
15. Department of Psychiatry of Old Age, Oslo University Hospital, Oslo, Norway.
16. Department of Community Medicine, University of Tromsø, Tromsø, Norway.
17. Norwegian National Advisory Unit on Ageing and Health, Vestfold Hospital Trust, Tønsberg, Norway.
18. Centre for Old Age Psychiatry Research, Innlandet Hospital Trust, Ottestad, Norway.
19. Department of Geriatric Medicine, Landspitali University Hospital, Reykjavik, Iceland.
20. Geriatric Department, University Hospital Oslo and University of Oslo, Oslo, Norway.
21. Department of Neuroscience, Norwegian University of Science and Technology, Trondheim, Norway.

22. Department of Neurology, St Olav's Hospital, Trondheim University Hospital, Trondheim, Norway.
23. Neuroradiology Section, Department of Radiology and Biomedical Imaging, University of California, San Francisco, USA.
24. Department of Medical Genetics, Oslo University Hospital, Oslo, Norway.
25. Vanderbilt Memory & Alzheimer's Center, Department of Neurology, Vanderbilt University Medical Center, Nashville, USA.
26. Faculty of Medicine, University of Iceland, Reykjavik, Iceland.
27. Department of Research and Innovation, Helse Fonna, Oslo, Norway.
28. Department of Clinical Medicine, University of Bergen, Bergen, Norway.
29. Department of Geriatrics, St. Olav's Hospital, Trondheim University Hospital, Trondheim, Norway.
30. Institute of Health and Society, University of Oslo, Oslo, Norway.
31. Laboratory of Molecular Neurobiology, Department of Medical Biochemistry and Biophysics, Karolinska Institutet, Stockholm, Sweden.
32. Department of Psychiatry, Namsos Hospital, Namsos, Norway.
33. Department of Genetics, University of North Carolina, Chapel Hill, USA.
34. Department of Psychiatry, University of North Carolina, Chapel Hill, USA.
35. Farr Institute of Health Informatics Research, University College London, London, UK.
36. Department of Medicine, Division of Genetic Medicine, Vanderbilt University Medical Center, Nashville, US.
37. Vanderbilt Genetics Institute, Vanderbilt University Medical Center, Nashville, US.
38. Analytic and Translational Genetics Unit, Massachusetts General Hospital, Boston, USA.
39. Stanley Center for Psychiatric Research, Broad Institute of MIT and Harvard, Cambridge, USA.
40. Dept. of Psychiatry and Psychotherapy, Charité - Universitätsmedizin, Berlin, Germany.
41. Department of Clinical Genetics, VU University Medical Center, Amsterdam, The Netherlands.

* These authors contributed equally to this work

#Correspondence to: Danielle Posthuma: Department of Complex Trait Genetics, VU University, De Boelelaan 1085, 1081 HV, Amsterdam, The Netherlands. Phone: +31 20 598 2823, Fax: +31 20 5986926, d.posthuma@vu.nl

Word count: Introductory paragraph: 206; main text: 3,825; Online methods: 5,412

Display items: 5 (Figures 4)

Includes **Supplementary Figures 1-7, Supplementary Tables 1-20.**

Abstract

Alzheimer's disease (AD) is the most frequent neurodegenerative disease with more than 35 million people affected worldwide, and no curative treatment currently available. AD is highly heritable and recent genome-wide meta-analyses have conclusively identified over 20 genomic loci associated with the late onset type of AD, yet only explaining a small proportion of the genetic variance indicating that undiscovered loci exist. Here, we present the largest genome-wide association study of AD and AD-by-proxy (71,880 AD cases, 383,378 controls) AD-by-proxy status is based on parental AD diagnosis, and showed strong genetic correlation with AD (0.81), Genetic meta-analysis identified 29 risk loci (confirming 19, 10 novel), implicating 215 potential causative genes. Independent replication further supports the genetic involvement of the novel loci in AD. Associated genes are strongly expressed in immune related tissues and cell types (spleen, liver and microglia). Furthermore, gene-set analyses confirm the genetic contribution of biological mechanisms involved in lipid-related processes and degradation of amyloid precursor proteins. We show strong genetic correlations with multiple health-related outcomes, and Mendelian randomisation results suggest a protective effect of cognitive ability on AD risk. These results are a step forward in identifying the genetic factors that contribute to AD risk, and add novel insights into the neurobiology of AD.

Main text

Alzheimer's disease (AD) is the most frequent type of dementia with roughly 35 million affected to date.[1] Results from twin studies indicate that AD is highly heritable, with estimates ranging between 60-80%.[2] Genetically, AD can be roughly divided into 2 subgroups: 1) familial early-

105 onset cases that are relatively often explained by rare variants with a strong effect,[3] and 2) late-
106 onset cases that are influenced by multiple common variants with low effect sizes.[4] Segregation
107 analyses have linked several genes to the first subgroup, including *APP*[5], *PSEN1*[6] and *PSEN2*[7].
108 The identification of these genes has resulted in valuable insights into a molecular mechanism
109 with an important role in AD pathogenesis, the amyloidogenic pathway,[8] providing a prominent
110 example of how gene discovery can add to biological understanding of disease aetiology.

111 Besides the identification of a few rare genetic factors (e.g. *TREM2*[9] and *ABCA7*[10]),
112 genome-wide association studies (GWAS) have mostly discovered common risk variants for the
113 more complex late-onset type of AD. *APOE* is the strongest genetic risk locus for late-onset AD,
114 where heterozygous and homozygous Apoε4 carriers are predisposed for a 3-fold and 15-fold
115 increase in risk, respectively.[11] A total of 19 additional GWAS loci have been described using a
116 discovery sample of 17,008 AD cases and 37,154 controls, followed by replication of the
117 implicated loci with 8,572 AD patients and 11,312 controls.[4] The current more than 20 loci do
118 not fully explain the heritability of AD and increasing the sample size is likely to lead to more
119 genome-wide significant risk loci, which will aid in understanding biological mechanisms
120 involved in the risk for AD.

121 In the current study, we included 455,258 individuals of European ancestry meta-
122 analysed in 3 stages (**Figure 1**). These consisted of 24,087 clinically diagnosed late-onset AD
123 cases, paired with 55,058 controls (phase 1). In phase 2, we analysed an AD-by-proxy
124 phenotype, based on individuals in the UK Biobank (UKB) for whom parental AD status was
125 available (N proxy cases=74,793; N proxy controls=328,320; **Online Methods**). In the UKB
126 sample, parental diagnosis for AD was available for N=376,113 individuals, of whom 393

127 individuals had a known diagnosis of AD themselves (identified from medical register data). The
128 high heritability of AD implies that case status for offspring can to some extent be inferred from
129 parental case status and that offspring of AD parents are likely enriched for a higher genetic AD
130 risk load. We thus defined individuals with one or two parents with AD as proxy cases
131 (N=47,793), while putting more weight on the proxy cases with 2 parents. Similarly, the proxy
132 controls include subjects with 2 parents without AD (N=328,320), where older cognitively
133 normal parents were up-weighted as proxy controls to account for the higher likelihood that
134 younger parents may still develop AD. As the proxy phenotype is not a pure measure of an
135 individual's AD status and may include individuals that never develop AD, genetic effect sizes
136 will be somewhat underestimated. However, the proxy case-control sample is very large (N
137 proxy cases=47,793; N proxy controls=328,320), and therefore adds a substantial amount of
138 power to detect genetic effects for AD. We first analysed the clinically defined case-control
139 samples separately from the by-proxy case control sample to allow investigation of overlap in
140 genetic signals for these two measurements of AD risk. Finally in phase 3, we meta-analysed all
141 individuals of phase 1 and phase 2 together.
142
143 *Genome-wide meta-analysis for AD status*
144 Phase 1 involved a genome-wide meta-analysis for AD case-control status using cohorts
145 collected as part of 3 independent main consortia (PGC-ALZ, IGAP and ADSP), totalling 79,145
146 individuals of European ancestry and 9,862,738 genetic variants passing quality control **(Figure**
147 **1, Supplementary Table 1**). The ADSP cohort obtained whole exome sequencing data from
148 4,343 cases and 3,163 controls, while the remaining datasets consisted of genotype SNP array

149 data. AD patients were diagnosed according to generally acknowledged diagnostic criteria, such
150 as the NINCDS-ADRDA (See **Methods**). All cohorts for which we had access to the raw genotypic
151 data were subjected to a standardized quality control pipeline, and GWA analyses were run per
152 cohort and then included in a meta-analysis, alongside one dataset (IGAP) for which only
153 summary statistics were available (see **Methods**). The full sample liability SNP-heritability
154 (h^2_{SNP}), estimated with the more conservative LDSC method, was 0.055 (SE=0.0099), implying
155 that 5.5% of AD heritability can be explained by the tested SNPs. This is in line with previous
156 estimates for IGAP (6.8%) also estimated by LDSC regression method, which is based on
157 summary statistics.[12,13] We do note that previously reported estimates using a method based
158 on raw genotypes (Genome-wide Complex Trait Analysis, GCTA), estimated that up to 53% of
159 total phenotypic variance in AD could be explained by common SNPs, of which up to 6% could
160 be explained by *APOE* alone, up to 13% by the then known variants, and up to 25% by
161 undiscovered loci.[14,15] The conservative LDSC estimate of h^2_{SNP} is presumably a consequence of
162 the underlying LDSC algorithm which is based on common HapMap SNPs and excludes all
163 variants with extreme associations.

164 The λ_{GC}=1.10 indicated the presence of inflated genetic signal compared to the null
165 hypothesis of no association. The linkage disequilibrium (LD) score intercept[13] was 1.044
166 (SE=0.0084) indicating that most inflation could be explained by polygenic signal
167 (**Supplementary Figure 1**). In the meta-analysis of AD case-control status, 1,067 variants
168 indexed by 51 lead SNPs in approximate linkage equilibrium (r^2<0.1) reached genome-wide
169 significance (GWS; $P<5\times10^{-8}$) (**Supplementary Figure 1; Supplementary Table 2)**. These were
170 located in 18 distinct genomic loci **(Table 1)**. 15 of these loci confirmed previous findings

171 (Lambert et al[4]) in a partially overlapping sample of the current study. The 3 remaining loci
172 (lead SNPs* rs7657553, rs11257242 and rs2632516) have been linked more recently to AD in a
173 genetic study[16] of AD-related triglyceride levels while conditioning on lipid levels and in a
174 transethnic genome-wide association study of AD.[17]

175 We next (phase 2) performed a GWAS for AD-by-proxy using 376,113 individuals of
176 European ancestry from the UKB version 2 release using parental AD status weighted by age
177 and corrected for population frequency to construct an AD-by-proxy status (**Figure 1; see**
178 **Methods**). The LD score intercept was 1.022 (SE=0.0099) indicating that most of the inflation in
179 genetic signal (λ_{GC}=1.071) could be explained by polygenic signal (**Supplementary Figure 1b**).
180 For AD-by-proxy, 719 GWS variants were indexed by 61 lead SNPs in approximate linkage
181 equilibrium (r^2<0.1) reached genome-wide significance (P<5×10^{-8}), located in 13 loci
182 (**Supplementary Figure 1a**). Of these, 8 loci overlapped with the significantly associated loci
183 identified for clinical AD case control status (**Table 1**).

184 We observed a strong genetic correlation of 0.81 (SE= 0.185, using LDScore regression)
185 indicating substantial overlap between genetic effects on clinical AD and AD-by-proxy status,
186 beyond shared GWS SNPs. Sign concordance tests indicated that 50.4% of all LD-independent
187 (r^2<0.1) genome-wide SNPs (significant and non-significant) had consistent direction of effects
188 between the two phenotypes (N=344,581 overlapping SNPs), slightly greater than the chance
189 expectation of 50% (exact binomial test P=2.45×10^{-7}). Of the 51 lead SNPs identified by the
190 case-control meta-analysis, all were available in UKB and 96.1% were sign-concordant
191 (P=2.98x10^{-12}), while of the 61 GWS lead SNPs identified in UKB, 48 were available in the case-

*We choose to not report the gene that is in closest proximity to the lead SNP as the ID for the locus, as this incorrectly implies that the gene is the causal gene for AD pathogenesis. We therefore believe it is preferred to use the rs-number as an ID for the locus, and aim to highlight the most likely causal genes with more sophisticated functional interpretation analyses in later sections of this study.

192 control meta-analysis and 99.7% of these were sign-concordant (P=5.98×10^{-14}). Such
193 substantial overlap suggests that the AD-by-proxy phenotype captures a large part of the
194 associated genetic effects on AD.

195 Given the high genetic overlap, in phase 3, we conducted a meta-analysis on the clinical
196 AD case-control GWAS and the AD-by-proxy GWAS (**Figure 1**), comprising a total sample size of
197 455,258 (71,880 (proxy) cases and 383,378 (proxy) controls). The LD score intercept was 1.0018
198 (SE=0.0109) indicating again that most of the inflation in genetic signal (λ_{GC}=1.0833) could be
199 explained by polygenic signal (**Supplementary Figure 1b**). There were 2,357 GWS variants,
200 which were represented by 94 lead SNPs, located in 29 loci (**Table 1**, **Figure 2**). These included
201 15 of the 18 loci detected in our case-control analyses, all of the 13 detected in the AD-by-proxy
202 analyses, as well as 9 loci that were sub-threshold in both individual analyses, but reached
203 significance in the meta-analysis. All 2,160 GWS SNPs that were available in both the case-
204 control and AD-by-proxy sub-samples were sign concordant (exact binomial test P<1×10^{-300}),
205 including all of the 82 available independent lead SNPs (P=1.68x10^{-23}). There was evidence of
206 substantial association signal in both AD and AD-by-proxy for 22 (out of 27 overlapping) loci for
207 which SNP(s) in each locus had a robust P-value (P < .05/94 independent signals). Of the 29
208 associated loci, 16 loci were previously identified by the GWAS of Lambert et al.,[4] and 13 were
209 newly implicated AD loci in our meta-analysis. Three of these (with lead SNPs rs184384746,
210 rs187370608 and rs114360492) were only available in the UKB cohort (**Table 1**). Verifying our
211 results against other[9,18] and more recent[16,19] genetic studies on AD, 3 loci (rs11257238,
212 rs28394864 and rs187370608) were previously discovered, leaving 10 novel loci (rs4575098,

213 rs184384746, rs6448453, rs114360492, rs442495, rs117618017, rs59735493, rs113260531,
214 rs76726049 and rs76320948). Considering all loci of Lambert et al, we were unable to replicate
215 4 loci (*MEF2C, NME8, CELF1* and *FERMT2**) at a genome-wide significance level (observed *P*-
216 values were 1.6 x 10^{-5} to 0.0011), which was mostly caused by a lower association signal in the
217 UKB dataset (**Supplementary Table 3)**. By contrast, Lambert et al. were unable to replicate the
218 *DSG2* and *CD33* locus with their second stage of their study. In our study, *DSG2* locus also
219 lacked significance (meta-analysis *P* = 0.030; UKB analysis *P* = 0.766; **Table 1**), implying
220 invalidation of this locus, while we did observe a significant association (meta-analysis *P* = 6.34
221 x 10^{-9}; UKB analysis *P* = 4.97 x 10^{-5}) for *CD33* (rs3865444 in **Table 1**), implying a genuine genetic
222 association to AD risk.

223 Next, we aimed to find further support for the novel findings of the phase 3 meta-
224 analysis, by using an independent Icelandic cohort (deCODE[20,21]), including 6,593 AD cases and
225 174,289 controls (**Figure 1; see Methods**; **Supplementary Table 4**). We were unable to test
226 support of two loci as the lead SNPs (and SNPs in high LD) were missing in deCODE, which is
227 most likely due to imputation differences (HRC reference for UKB dataset vs. 1000G reference
228 for deCODE dataset). For 7 of the 8 novel loci tested for replication, we observed the same
229 direction of effect in the deCODE cohort. Furthermore, 4 loci (rs6448453, rs442495,
230 rs117618017, rs76320948) showed nominal significant association results (P < 0.05) for the
231 same SNP or a SNP in high LD (r^2 > 0.9) within the same locus (two-tailed binomial test
232 *P*=3.7x10^{-4}). The locus on chromosome 1 (rs45759098) was very close to significance (P =
233 0.053). Apart from the novel loci, we also observed sign concordance for 95.6% of the 90 lead
234 SNPs in all loci from the meta-analysis (*P*=1.60x10^{-20}) that were available in deCODE (out of 94).

* For straightforward comparison to this GWAS, we do here report the genes in closest proximity to the lead SNP. However, we would like to point out that GWAS findings implicate a genomic locus, and that the closest gene is not necessarily the causal gene.

235 As an additional method of testing for replication using genome-wide polygenic score
236 prediction,[22] the current results explain 7.1% of the variance in clinical AD at a low best fitting
237 *P*-threshold of 1.69×10^{-5} ($P=1.80 \times 10^{-10}$) in an independent sample of 761 individuals. When
238 excluding the *APOE*-locus (chr19: 45020859-45844508), the results explain 3.9% of the variance
239 with a best fitting *P*-threshold of 3.5×10^{-5} ($P=1.90 \times 10^{-6}$).
240

241 *Functional interpretation of genetic variants contributing to AD and AD-by-proxy*

242 Next, we conducted a number of in silico follow-up analyses to interpret our findings in a
243 biological context. Functional annotation of all GWS SNPs (*n*=2,178) in the associated loci
244 showed that SNPs were mostly located in intronic/intergenic areas, yet in regions that were
245 enriched for chromatin states 4 and 5, implying effects on active transcription **(Figure 3A, 3B**
246 **and 3C; Supplementary Table 5)**. 24 GWS SNPs were exonic non-synonymous (ExNS) (**Figure**
247 **3A; Supplementary Table 6)** with likely deleterious implications on gene function. Converging
248 evidence of strong association ($Z > |7|$) and a high observed probability of a deleterious variant
249 effect (CADD[23] score≥30) was found for rs75932628 (*TREM2*), rs142412517 (*TOMM40*) and
250 rs7412 (*APOE*). The first two missense mutations are rare (MAF=0.002 and 0.001, respectively)
251 and the alternative alleles were associated with higher risk for AD. The latter *APOE* missense
252 mutation is the well-established protective allele Apoε2. The effect sizes for ExNS ranged from
253 moderate to high. **Supplementary Tables 5 and 6** present a detailed annotation catalogue of
254 variants in the associated genomic loci. Partitioned analysis,[24] excluding SNPs with extremely
255 large effect sizes (i.e. *APOE* variants) showed enrichment for h^2_{SNP} for variants located in
256 H3K27ac marks (Enrichment=3.18, $P=9.63 \times 10^{-5}$), which are associated with activation of

257 transcription, and in Super Enhancers (Enrichment=3.62, P=2.28×10^{-4}), which are genomic
258 regions where multiple epigenetic marks of active transcription are clustered (**Figure 3D;**
259 **Supplementary Table 7)**. Heritability was also enriched in variants on chromosome 17
260 (Enrichment=3.61, P=1.63x10^{-4}) and we observed a trend of enrichment for variants with high
261 minor allele frequencies (Enrichment=3.31, P=2.85x10^{-3}), (**Supplementary Figure 3;**
262 **Supplementary Tables 8 and 9)**. Although a large proportion (23.9%) of the heritability can be
263 explained by SNPs on chromosome 19, this enrichment is not significant, due to the large
264 standard errors around this estimate (**Supplementary Table 8**). Overall these results suggest
265 that, despite some nonsynonymous variants likely contributing to AD risk, most of the GWS
266 SNPs are located in non-coding regions, and are enriched for regions that have an activating
267 effect on transcription of coding regions.
268
269 *Implicated genes*
270 To link the associated variants to genes, we applied three gene-mapping strategies
271 implemented in FUMA[25] (**Online Methods**). We used all SNPs with a P-value < 5x10-8 and r^2 of
272 0.6 with one of the independently associated SNPs for gene-mapping. *Positional* gene-mapping
273 aligned SNPs to 100 genes by their location within or immediately up/downstream (+/-10kb) of
274 known gene boundaries, *eQTL (expression quantitative trait loci)* gene-mapping matched cis-
275 eQTL SNPs to 170 genes whose expression levels they influence in one or more tissues, and
276 c*hromatin interaction* mapping linked SNPs to 21 genes based on three-dimensional DNA-DNA
277 interactions between each SNP's genomic region and nearby or distant genes, which we limited
278 to include only interactions between annotated enhancer and promotor regions (**Figure 3B and**

279 **3C; Supplementary Figure 4; Supplementary Tables 10 and 11**). This resulted in 192 uniquely
280 mapped genes, 80 of which were implicated by at least two mapping strategies and 17 by all 3
281 (**Figure 4E)**. Eight genes (*HLA-DRB5, HLA-DRB1, HLA-DQA, HLA-DQB1, KAT8, PRSS36, ZNF232*
282 and *CEACAM19*) are particularly notable as they are implicated via eQTL association in the
283 hippocampus, a brain region highly affected early in AD pathogenesis (**Supplementary Table**
284 **10**). Of special interest is the locus on chromosome 8 (rs4236673). In the GWAS by Lambert et
285 al.[4], this locus was defined as 2 distinct loci (*CLU* and *PTK2B*), while our meta-analysis specified
286 this locus as a single locus based on LD-patterns. This is also supported by a chromatin
287 interaction between the two regions (**Figure 3E**), which is observed in two immune-related
288 tissues – the spleen and liver (**Supplementary Table 11**). Chromosome 16 contains a locus
289 implicated by long-range eQTL association (**Figure 3F**) clearly illustrating more distant genes can
290 be affected by a genetic factor (**Figure 3F**) and emphasising the relevance of considering
291 putative causal genes or regulatory elements not solely on the physical location but also on
292 epigenetic influences. **Supplementary Figure 4** displays chromatin interactions for all
293 chromosomes containing significant GWAS loci.

294 Although these gene-mapping strategies imply multiple putative causal genes per GWAS
295 locus, several of these genes in the novel loci (and significantly replicated by the deCODE
296 cohort) are of particular interest, as the genes have functional or previous genetic association
297 to AD. For locus 1 in **Supplementary Table 10**, *ADAMTS4* encodes a protein of the ADAMTS
298 family which has a function in neuroplasticity and has been extensively studied for their role in
299 AD pathogenesis.[26] For locus 19, the obvious most likely causal gene is *ADAM10,* as this gene
300 has been conclusively associated to AD through the effect of rare coding variants. However this

301 is the first time that this gene is implicated as a common risk factor for AD. The lead SNP for
302 locus 20 is a nonsynonymous variant in exon 1 of *APH1B,* which encodes for a protein part of
303 the *γ*-secretase complex cleaving *APP.*[27] Although previously reported functional information
304 on genes can be of great value, it is preferable to consider all implicated genes as putative
305 causal factors to guide potential functional follow-up experiments.

306 We next performed genome-wide gene-based association analysis (GWGAS) using
307 MAGMA.[28] This method annotates SNPs to known protein-coding genes to estimate aggregate
308 associations based on all SNPs in a gene. It differs from the gene-mapping strategies in FUMA as
309 it provides a statistical gene-based test, whereas FUMA maps individually significant SNPs to
310 genes. With GWGAS, we identified 97 significantly associated genes (**Supplementary Figure 5;**
311 **Supplementary Table 12)**, of which 74 were also mapped by FUMA **(Figure 4E)**. In total, 16
312 genes were implicated by all four strategies (**Supplementary Table 13),** of which 7 genes (*HLA-*
313 *DRA, HLA-DRB1, PTK2B, CLU, MS4A3, SCIMP* and *RABEP1*) are not located in the *APOE*-locus,
314 and therefore of high interest for further investigation.

315

316 *Gene-sets implicated in AD and AD-by-proxy*

317 Using the gene-based P-values, we performed gene-set analysis for 6,994 biological-pathway-
318 based gene-sets, 53 tissue expression-based gene-sets and 39 brain single cell expression based
319 gene-sets (24 derived from mouse data and 15 derived from human data). We found 4 Gene
320 Ontology[19] gene-sets that were significantly associated with AD risk: *Protein lipid complex*
321 (P=3.93×10^{-10}), *Regulation of amyloid precursor protein catabolic process* (P=8.16×10^{-09}), *High*
322 *density lipoprotein particle* (P=7.81x10^{-8}), and *Protein lipid complex assembly* (P=7.96×10^{-7})

323 **(Figure 4A; Supplementary Tables 14 and 15)**. Conditional analysis on the *APOE* locus showed
324 associations with AD for these four gene-sets independent of the effect of *APOE*, as they
325 remained significantly associated (P<0.0125), yet less strong, suggesting that *APOE* is
326 contributing a substantial part to the association signal, but does not completely drive the
327 signal. There was overlap between genes included in the 4 gene-sets, and conditioning on each
328 significant gene-set association showed that 3 gene-sets were associated with AD
329 independently of each other (**Supplementary Table 14 and 15**). All 25 genes of the *High density*
330 *lipoprotein particle* pathway are also part of the *Protein lipid complex* (conditional analysis
331 *P*=0.18), and these pathways are therefore not interpretable as independent associations.

332 Linking gene-based *P*-values to tissue- and cell-type-specific gene-sets**,** no association
333 survived the stringent Bonferroni correction, which corrected for all tested gene-sets (i.e. 6,994
334 GO categories, 54 tissues and 39 cell types). However, we did observe associations when
335 correcting only for the number of tests within all tissue types or cell-types. This was the case for
336 gene expression across immune-related tissues (**Figure 4C; Supplementary Table 16**),
337 particularly whole blood ($P=5.61\times10^{-6}$), spleen ($P=1.50\text{x}10^{-5}$) and lung ($P=4.67\text{x}10^{-4}$). In brain
338 single-cell expression gene-set analyses, we found associations for microglia, both in the
339 mouse-based expression dataset ($P=1.96\text{x}10^{-3)}$ (**Figure 4B; Supplementary Table 17)** and the
340 human-based expression dataset ($P=2.56\text{x}10^{-3}$) (**Supplementary Figure 6; Supplementary Table**
341 **18).**

342

343 *Cross-trait genetic influences*

For a more comprehensive understanding of the genetic background of AD, we next tested whether AD is likely to share genetic factors with other phenotypes. This might reveal some functional insights about the genetic aetiology of AD. We conducted bivariate LDscore[13] regression to test for genetic correlations between AD and 41 other traits for which large GWAS summary statistics were available. We observed significant negative genetic correlations with adult cognitive ability (r_g=-0.22, P=7.28x10-5), age of first birth (r_g=−0.33, P=1.22×10^{-4}), educational attainment (r_g=−0.25, P=5.01×10^{-4}), and confirmed a very strong positive correlation with previous GWAS of Alzheimer's disease (r_g=0.90, P=3.29x10^{-16}) (**Figure 4D; Supplementary Table 19**).

We then used Generalised Summary-statistic-based Mendelian Randomisation[29] (GSMR; see **Methods**) to test for potential credible causal associations of genetically correlated outcomes which may directly influence the risk for AD. Due to the nature of AD being a late-onset disorder and summary statistics for most other traits being obtained from younger samples, we do not report tests for the opposite direction of potential causality (i.e. we did not test for a causal effect of a late-onset disease on an early onset disease). In this set of analyses, SNPs from the summary statistic of genetically correlated phenotypes were used as instrumental variables to estimate the putative causal effect of these "exposure" phenotypes on AD risk by comparing the ratio of SNPs' associations with each exposure to their associations with AD outcome (see **Methods**). Association statistics were standardized, such that the reported effects reflect the expected difference in odds ratio (OR) for AD as a function of every SD increase in the exposure phenotype. We observed a protective effect of cognitive ability (OR=0.89, 95% confidence interval[CI]: 0.85-0.92, P=5.07x10^{-9}), educational attainment

366 (OR=0.88, 95%CI: 0.81-0.94, P=3.94×10^{-4}), and height (OR=0.96, 95%CI: 0.94-0.97, P=1.84x10^{-8})
367 on risk for AD (**Supplementary Table 20; Supplementary Figure 7)**. No substantial evidence of
368 pleiotropy was observed between AD and these phenotypes, with <1% of overlapping SNPs
369 being filtered as outliers (**Supplementary Figure 7**).
370
371 *Discussion*
372 In conclusion, by using a non-conventional approach of including a by-proxy phenotype for AD
373 to increase sample size, we have identified novel loci and gained novel biological knowledge on
374 AD aetiology. Both the high genetic correlation between the standard case-control status and
375 the UKB by proxy phenotype (r_g=0.81) and the high rate of novel loci replication in the
376 independent deCODE cohort, suggest that this strategy is robust. Through extensive in silico
377 functional follow-up analysis, and in line with previous research,[19,30] we emphasise the crucial
378 causal role of the immune system - rather than immune response as a consequence of disease
379 pathology - by establishing variant enrichments for immune-related body tissues (whole blood,
380 spleen, liver) and for the main immune cells of the brain (microglia). Furthermore, we observe
381 informative eQTL associations and chromatin interactions within immune-related tissues for
382 identified genomic risk loci. Together with the AD-associated genetic effects on lipid
383 metabolism in our study, these biological implications strengthen the hypothesis that AD
384 pathogenesis involves an interplay between inflammation and lipids, as lipid changes might
385 harm immune responses of microglia and astrocytes, and vascular health of the brain.[31]
386 In accordance with previous clinical research, our study suggests an important role for
387 protective effects of several human traits on AD. As an example, cognitive reserve has been

388 proposed as a protective mechanism in which the brain aims to control brain damage with prior
389 existing cognitive processing strategies.[32] Our findings imply that some component of the
390 genetic factors for AD might affect cognitive reserve, rather than being involved in AD-
391 pathology-related damaging processes, influencing AD pathogenesis in an indirect way through
392 cognitive reserve. Similarly, in a largescale community-based study it was observed that AD
393 incidence rates declined over decades, which was specific for individuals with at minimum a
394 high school diploma.[33] Combined with our Mendelian randomization results for educational
395 attainment, this suggests that the protective effect of educational attainment on AD is
396 influenced by genetics.

397 The results of this study could furthermore serve as a valuable resource (e.g.
398 Supplementary Tables 10 and 13) for selection of promising genes for functional follow-up
399 experiments. We anticipate that functional interpretation strategies and follow-up experiments
400 will result in a comprehensive understanding of sporadic late-onset AD aetiology, which will
401 serve as a solid foundation for future AD drug development and stratification approaches.

402

403 **URLs:**

404 http://ukbiobank.ac.uk

405 https://www.ncbi.nlm.nih.gov/gap

406 http://fuma.ctglab.nl

407 http://ctg.cncr.nl/software/magma

408 http://genome.sph.umich.edu/wiki/METAL_Program

409 https://github.com/bulik/ldsc

410 http://ldsc.broadinstitute.org/

411 https://data.broadinstitute.org/alkesgroup/LDSCORE/

412 http://www.genecards.org

413 http://www.med.unc.edu/pgc/results-and-downloads

414 http://software.broadinstitute.org/gsea/msigdb/collections.jsp

415 https://www.ebi.ac.uk/gwas/

416 https://github.com/ivankosmos/RegionAnnotator

417 http://cnsgenomics.com/software/gsmr/

418

419 **Acknowledgments:** This work was funded by The Netherlands Organization for Scientific
420 Research (NWO VICI 453-14-005) and the Sophia Foundation for Scientific Research (grant nr:
421 S14-27). The analyses were carried out on the Genetic Cluster Computer, which is financed by
422 the Netherlands Scientific Organization (NWO: 480-05-003), by the VU University, Amsterdam,
423 The Netherlands, and by the Dutch Brain Foundation, and is hosted by the Dutch National
424 Computing and Networking Services SurfSARA. This research has been conducted using the UK
425 Biobank resource under application number 16406 and the public ADSP dataset, obtained
426 through the Database of Genotypes and Phenotypes (dbGaP) under accession number
427 phs000572. We thank the International Genomics of Alzheimer's Project (IGAP) for providing
428 summary results data for these analyses. The investigators within IGAP contributed to the
429 design and implementation of IGAP and/or provided data but did not participate in analysis or
430 writing of this report. IGAP was made possible by the generous participation of the control
431 subjects, the patients, and their families. The i–Select chips was funded by the French National

Foundation on Alzheimer's disease and related disorders. EADI was supported by the LABEX (laboratory of excellence program investment for the future) DISTALZ grant, Inserm, Institut Pasteur de Lille, Université de Lille 2 and the Lille University Hospital. GERAD was supported by the Medical Research Council (Grant n° 503480), Alzheimer's Research UK (Grant n° 503176), the Wellcome Trust (Grant n° 082604/2/07/Z) and German Federal Ministry of Education and Research (BMBF): Competence Network Dementia (CND) grant n° 01GI0102, 01GI0711, 01GI0420. CHARGE was partly supported by the NIH/NIA grant R01 AG033193 and the NIA AG081220 and AGES contract N01–AG–12100, the NHLBI grant R01 HL105756, the Icelandic Heart Association, and the Erasmus Medical Center and Erasmus University. ADGC was supported by the NIH/NIA grants: U01 AG032984, U24 AG021886, U01 AG016976, and the Alzheimer's Association grant ADGC–10–196728. This paper represents independent research funded by the National Institute for Health Research (NIHR) Biomedical Research Centre at South London and Maudsley NHS Foundation Trust and King's College London. The views expressed are those of the author(s) and not necessarily those of the NHS, the NIHR or the Department of Health.

Genotyping for the Swedish Twin Studies of Aging was supported by NIH/NIA grant R01 AG037985. Genotyping in TwinGene was supported by NIH/NIDDK U01 DK066134. WvdF is recipient of Joint Programming for Neurodegenerative Diseases (JPND) grants PERADES (ANR-13-JPRF-0001) and EADB (733051061). JB was supported by a grant from the Swiss National Science Foundation. JHL was supported by the Swedish Research Council (Vetenskapsrådet, award 2014-3863), the Wellcome Trust (108726/Z/15/Z), and the Swedish Brain Foundation (Hjärnfonden). NS was supported by the Wellcome Trust (108726/Z/15/Z). RD was supported

454 by National Institute for Health Research University College London Hospital's Biomedical
455 Research Centre, Arthritis Research UK, the British Heart Foundation, Cancer Research UK, the
456 Chief Scientist Office, the Economic and Social Research Council, the Engineering and Physical
457 Sciences Research Council, the National Institute for Social Care and Health Research, and the
458 Wellcome Trust (grant number MR/K006584/1).
459 We thank the numerous participants, researchers, and staff from many studies who collected
460 and contributed to the data. Additional acknowledgments can be found in the Supplementary
461 Information file. Summary statistics will be made available for download upon publication from
462 http://ctglab.vu.nl.
463

464 **Author Contributions:** I.E.J. and J.E.S. performed the analyses. D.P. and O.E.A. conceived the
465 idea of the study. D.P. and S.R. supervised analyses. S.St. performed QC on the UK Biobank data
466 and wrote the analysis pipeline. K.W. constructed and applied the FUMA pipeline for
467 performing follow-up analyses. J.B. conducted the single cell enrichment analyses. J.H.L and
468 N.S. contributed data. D.P. and I.E.J. wrote the paper. All authors critically reviewed the paper.
469

470 **Author Information**: PF Sullivan reports the following potentially competing financial interests:
471 Lundbeck (advisory committee), Pfizer (Scientific Advisory Board member), and Roche (grant
472 recipient, speaker reimbursement). JHL: Cartana (Scientific Advisor) and Roche (grant recipient).
473 All other authors declare no financial interests or potential conflicts of interest.
474 Correspondence and requests for materials should be addressed to d.posthuma@vu.nl.
475
476

Table 1. Summary statistics for the meta-analysis of case-control status, by proxy phenotype and both.
Note: Independent lead SNPs are defined by r2 < .1; distinct genomic loci are >250kb apart. Allele1 is the effect allele for the meta association statistic. Meta-analysis effect direction (column AL) is in the following order: ADSP, IGAP, UKB, PGC-ALZ, note that the first cohort is often missing as this concerns exome sequencing data. Corrected P value for significance = 5E-08 (marked as boldfaced and underlined values). Note that the lead SNP can differ between the distinct analyses, while it tags the same locus

		Case-control status						By proxy AD						Overall						
Locus	Chr	SNP	bp	Allele 1	Allele 2	Z	*p*	SNP	bp	Allele 1	Allele 2	Z	*p*	SNP	bp	Allele 1	Allele 2	Z	*p*	direction
1	1	rs4575098	161155392	A	G	3.78	0.000157	rs4575098	161155392	A	G	5.39	6.88E-08	rs4575098	161155392	A	G	6.36	**2.05E-10**	?+++
2	1	rs6656401	207692049	A	G	8.54	**1.39E-17**	rs679515	207750568	T	C	6.13	**8.85E-10**	rs2093760	207786828	A	G	8.82	**1.10E-18**	++++
3	2	rs4663105	127891427	C	A	11.21	**3.58E-29**	rs4663105	127891427	C	A	10.54	**5.46E-26**	rs4663105	127891427	C	A	13.94	**3.38E-44**	?+++
4	2	rs10933431	233981912	G	C	-4.79	1.67E-06	rs10933431	233981912	G	C	-4.71	2.51E-06	rs10933431	233981912	G	C	-6.13	**8.92E-10**	?---
5	3	NA						rs184384746	57226150	T	C	5.70	**1.24E-08**	rs184384746	57226150	T	C	5.69	**1.24E-08**	??+?
6	4	rs6448453	11026028	A	G	2.26	0.023641	rs6448451	11024682	G	C	5.70	**1.19E-08**	rs6448453	11026028	A	G	6.00	**1.93E-09**	?++-
7	4	rs7657553	11723235	A	G	5.60	**2.16E-08**	rs7657553	11723235	A	G	-0.27	0.79	rs7657553	11723235	A	G	1.95	0.051	?+-+
8	6	rs9269853	32550322	A	C	5.56	**2.66E-08**	rs6931277	32583357	T	A	-5.22	1.78E-07	rs6931277	32583357	T	A	-6.49	**8.41E-11**	?---
9	6	NA						rs187370608	40942196	A	G	8.26	**1.45E-16**	rs187370608	40942196	A	G	8.26	**1.45E-16**	??+?
10	6	rs9381563	47432637	C	T	5.84	**5.35E-09**	rs9381563	47432637	C	T	4.46	8.10E-06	rs9381563	47432637	C	T	6.33	**2.52E-10**	?+++
11	7	rs1859788	99971834	A	G	-5.82	**6.05E-09**	rs7384878	99932049	C	T	-6.34	**2.38E-10**	rs1859788	99971834	A	G	-7.93	**2.22E-15**	----
12	7	rs11763230	143108841	T	C	-6.67	**2.58E-11**	rs7810606	143108158	T	C	-4.89	1.01E-06	rs7810606	143108158	T	C	-6.62	**3.59E-11**	?---
13	7	NA						rs114360492	145950029	T	C	5.99	**2.1E-09**	rs114360492	145950029	T	C	5.99	**2.10E-09**	??+?
14	8	rs4236673	27464929	A	G	-9.14	**6.36E-20**	rs1532278	27466315	T	C	-5.78	**7.45E-09**	rs4236673	27464929	A	G	-8.98	**2.61E-19**	----
15	10	rs11257242	11721119	C	G	-5.58	**2.38E-08**	rs11257238	11717397	C	T	4.02	5.84E-05	rs11257238	11717397	C	T	5.69	**1.26E-08**	?+++
16	11	rs7935829	59942815	G	A	-7.16	**8.21E-13**	rs1582763	60021948	A	G	-5.86	**4.72E-09**	rs2081545	59958380	A	C	-7.97	**1.55E-15**	----
17	11	rs10792832	85867875	A	G	-8.56	**1.12E-17**	rs3844143	85850243	C	T	-6.56	**5.31E-11**	rs867611	85776544	G	A	-8.75	**2.19E-18**	?---
18	11	rs11218343	121435587	C	T	-6.55	**5.57E-11**	rs11218343	121435587	C	T	-4.68	2.81E-06	rs11218343	121435587	C	T	-6.79	**1.09E-11**	?---
19	14	rs12590654	92938855	A	G	-5.61	**1.98E-08**	rs12590654	92938855	A	G	-4.63	3.70E-06	rs12590654	92938855	A	G	-6.39	**1.65E-10**	?---
20	15	rs442495	59022615	C	T	-3.61	0.000309	rs442495	59022615	C	T	-5.15	2.65E-07	rs442495	59022615	C	T	-6.07	**1.31E-09**	?---
21	15	rs117618017	63569902	T	C	2.29	0.022178	rs117618017	63569902	T	C	5.15	2.64E-07	rs117618017	63569902	T	C	5.52	**3.35E-08**	++++
22	16	rs59735493	31133100	A	G	-3.34	0.000825	rs59735493	31133100	A	G	-4.63	3.72E-06	rs59735493	31133100	A	G	-5.49	**3.98E-08**	?---
23	17	rs113260531	5138980	A	G	4.66	3.21E-06	rs9916042	4984447	A	G	5.46	**4.73E-08**	rs113260531	5138980	A	G	6.12	**9.16E-10**	?+++
24	17	rs28394864	47450775	A	G	3.97	7.29E-05	rs28394864	47450775	A	G	4.50	6.80E-06	rs28394864	47450775	A	G	5.62	**1.87E-08**	?+++
25	17	rs2632516	56409089	C	G	-6.05	**1.42E-09**	rs2632516	56409089	C	G	-2.79	0.005288	rs2632516	56409089	C	G	-4.90	9.66E-07	?---
26	18	rs8093731	29088958	T	C	-5.46	**4.63E-08**	rs8093731	29088958	T	C	-0.30	0.7656	rs8093731	29088958	T	C	-2.17	0.030	?--?
27	18	rs76726049	56189459	C	T	2.06	0.039261	rs76726049	56189459	C	T	5.22	1.83E-07	rs76726049	56189459	C	T	5.52	**3.30E-08**	?+++
28	19	rs4147929	1063443	A	G	5.76	**8.64E-09**	rs3752241	1053524	G	C	-5.55	**2.87E-08**	rs111278892	1039323	G	C	6.50	**7.93E-11**	?+++
29	19	rs41289512	45351516	G	C	29.74	**2.70E-194**	rs75627662	45413576	T	C	36.79	**9.5E-296**	rs41289512	45351516	G	C	35.50	**5.79E-276**	?+++
30	19	rs76320948	46241841	T	C	4.32	1.54E-05	rs76320948	46241841	T	C	4.29	1.80E-05	rs76320948	46241841	T	C	5.46	**4.64E-08**	?++?
31	19	rs3865444	51727962	A	C	-5.48	**4.25E-08**	rs3865444	51727962	A	C	-4.06	4.97E-05	rs3865444	51727962	A	C	-5.81	**6.34E-09**	?---
32	20	rs6014724	54998544	G	A	-5.35	8.72E-08	rs6014724	54998544	T	C	-4.52	6.32E-06	rs6014724	54998544	G	A	-6.18	**6.56E-10**	?---

525 **Figure 1. Overview of analyses steps.** The main genetic analysis encompasses the procedures to detect
526 GWAS risk loci for AD. The functional analysis part includes the *in silico* functional follow-up procedures
527 with the aim to put the genetic findings in biological context. The Mendelian randomisation analysis has
528 been performed on the results of phase 1 to account for sample overlap between our study and other
529 traits for which they have used the UKB dataset.
530
531

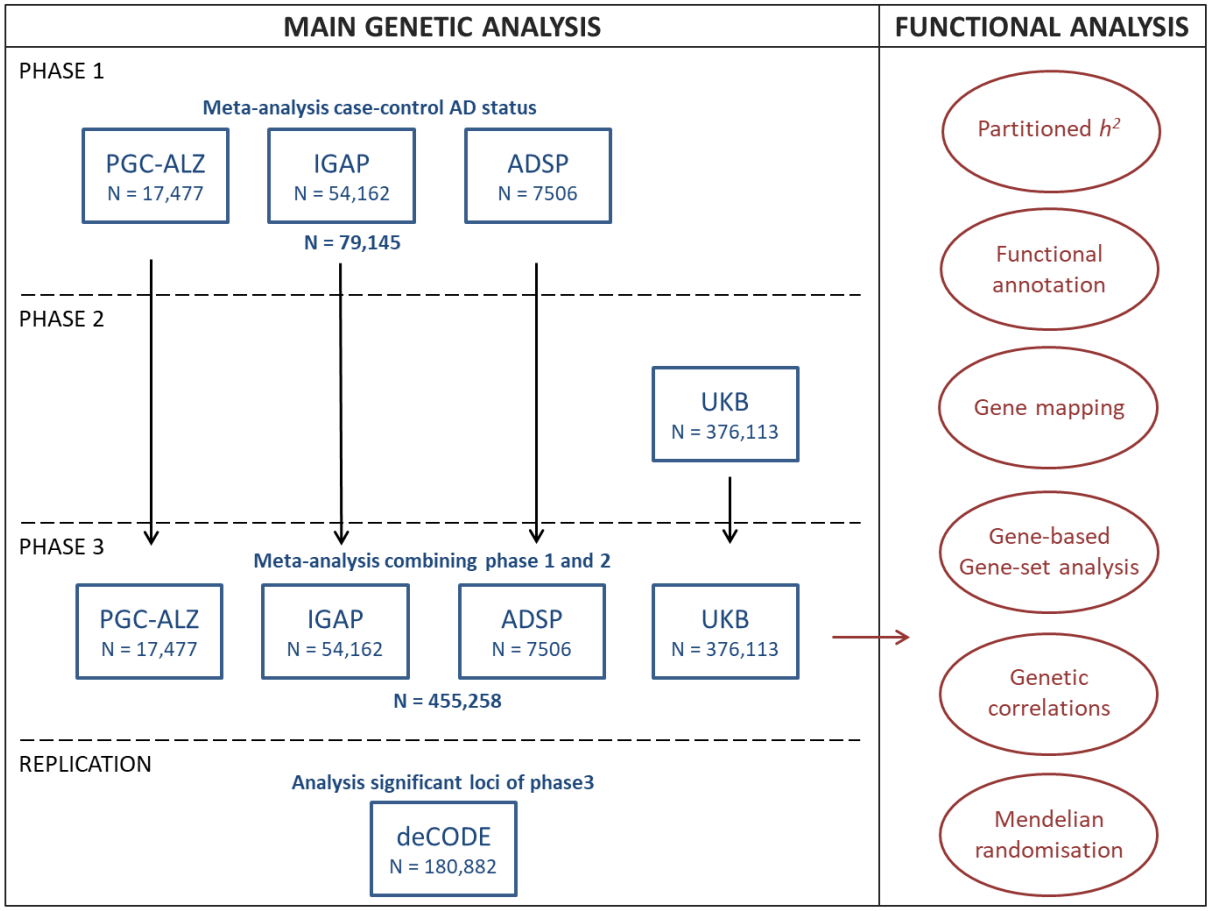

532
533
534
535
536
537
538
539
540

Figure 2. GWAS results for AD risk (N=455,258). Manhattan plot displays all associations per variant ordered according to their genomic position on the x-axis and showing the strength of the association with the –log10 transformed P-values on the y-axis. The y-axis is limited to enable visualization of non-APOE loci.

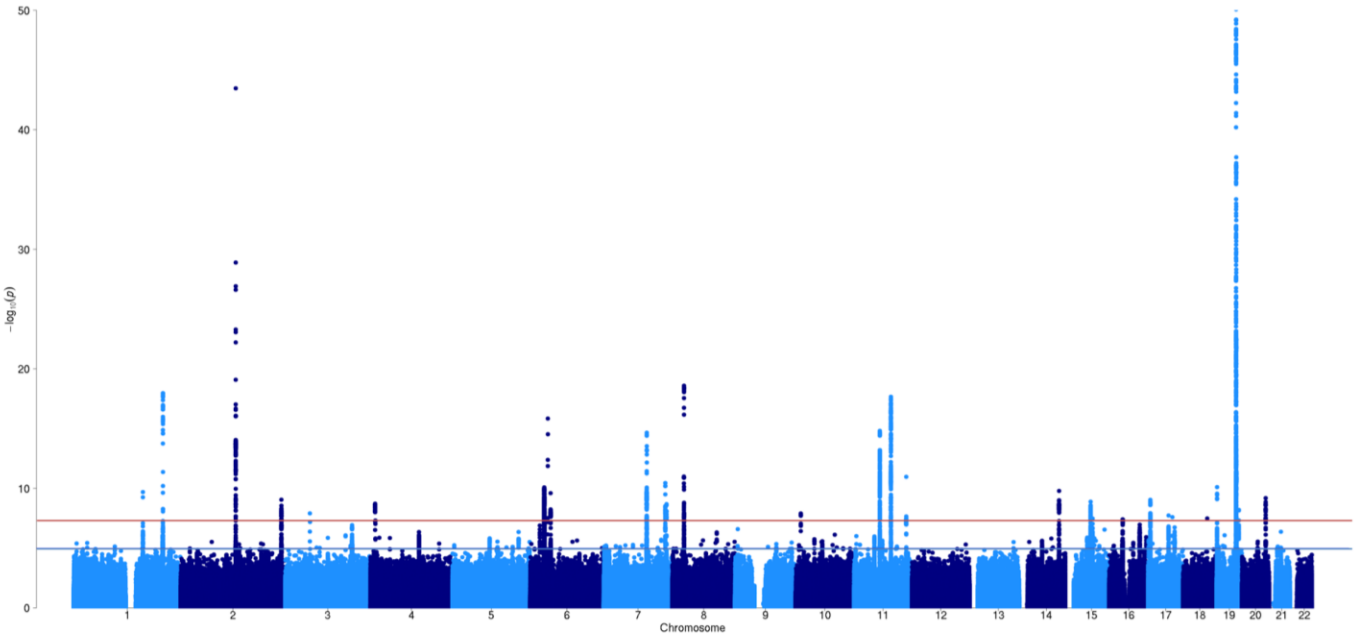

Figure 3. Functional annotation of association results. a) Heritability enrichment of 28 functional variant annotations calculated with stratified LD score regression. UTR=untranslated region; CTCF=CCCTC-binding factor; DHS=DNaseI Hypersensitive Site; TFBS=transcription factor binding site; DGF=DNAaseI digital genomic footprint; **b)** Functional effects of variants in genomic risk loci of the meta-analysis – the second bar shows distribution for exonic variants only; **c)** Distribution of RegulomeDB score for variants in genomic risk loci, with a low score indicating a higher probability of having a regulatory function. **d)** Distribution of minimum chromatin state across 127 tissue and cell types for variants in genomic risk loci, with lower states indicating higher accessibility and states 1-7 referring to open chromatin states. **e)** Zoomed-in circos plot of chromosome 8. **f) Z**oomed-in circos plot of chromosome 16. Circos plots show implicated genes by significant loci, where blue areas indicate genomic risk loci, green indicates eQTL associations and orange indicates chromatin interactions. Genes mapped by both eQTL and chromatin interactions are red. The outer layer shows a Manhattan plot containing the negative log10-transformed P-value of each SNP in the GWAS meta-analysis of AD. Full circos plots of all autosomal chromosomes are provided in Supplementary Figures 4.

565

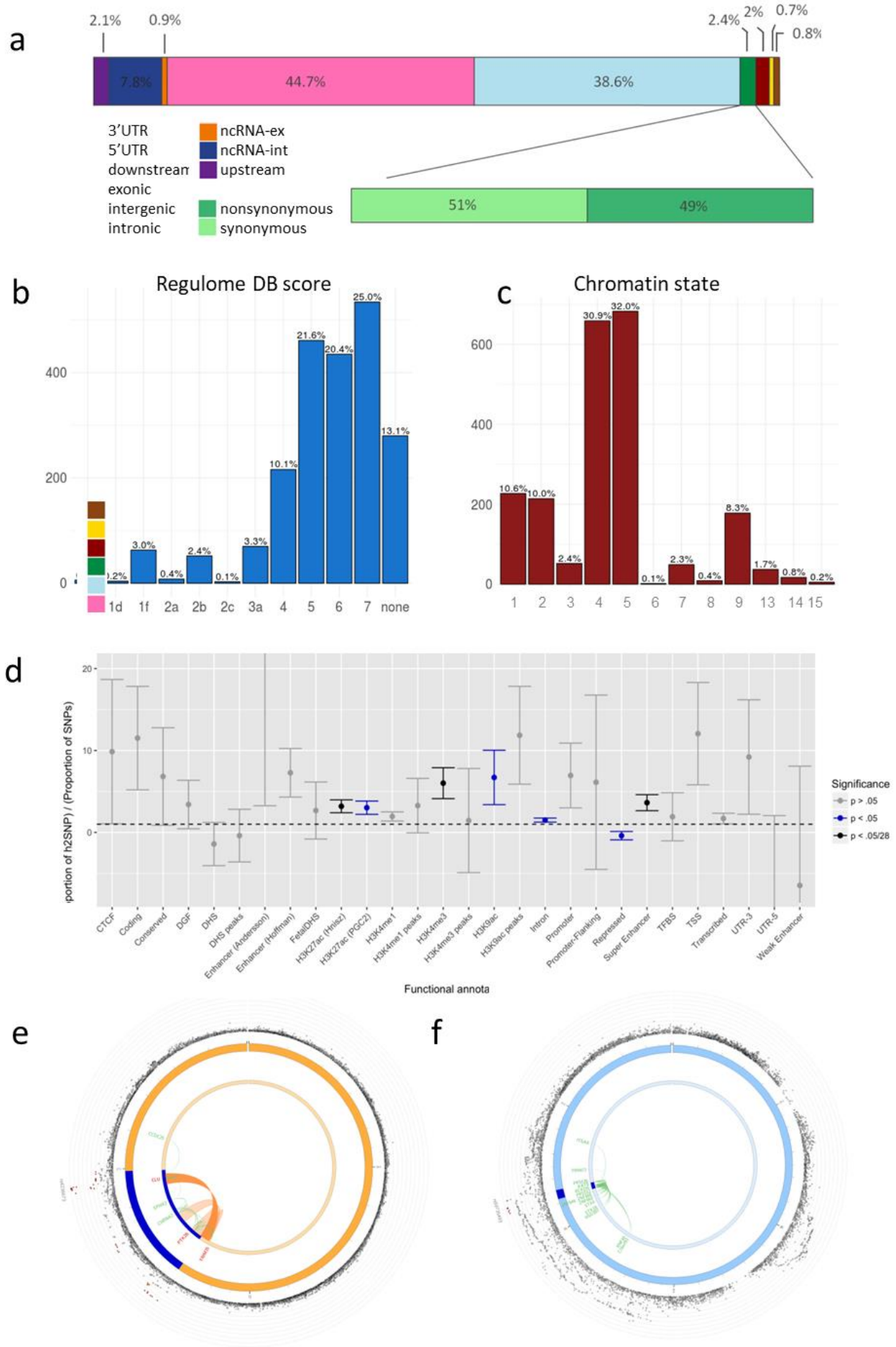
a
2.1%
0.9%
2.4%
2%
0.7%
0.8%
7.8%
44.7%
38.6%
3'UTR
5'UTR
downstream
exonic
intergenic
intronic
ncRNA-ex
ncRNA-int
upstream
nonsynonymous
synonymous
51%
49%
b
Regulome DB score
1d
1f
2a
2b
2c
3a
4
5
6
7
none
c
Chromatin state
d
Functional annota
Significance
p > .05
p < .05
p < .05/28
e
f

Figure 4. Functional implications based on gene-set analysis, genetic correlations and functional annotations. The gene-set results are displayed per category of biological mechanisms (A), brain cell-types (B) and tissue types (C). The red horizontal lines indicates the significance threshold corrected for all gene-set tests of all categories, while the blue horizontal lines display the significance threshold corrected only for the number of tests within the three categories (i.e. gene-ontology, tissue expression, single cell expression). (D) Genetic correlations between AD and other heritable traits. (E) Venn diagram showing the number of genes mapped by four distinct strategies.

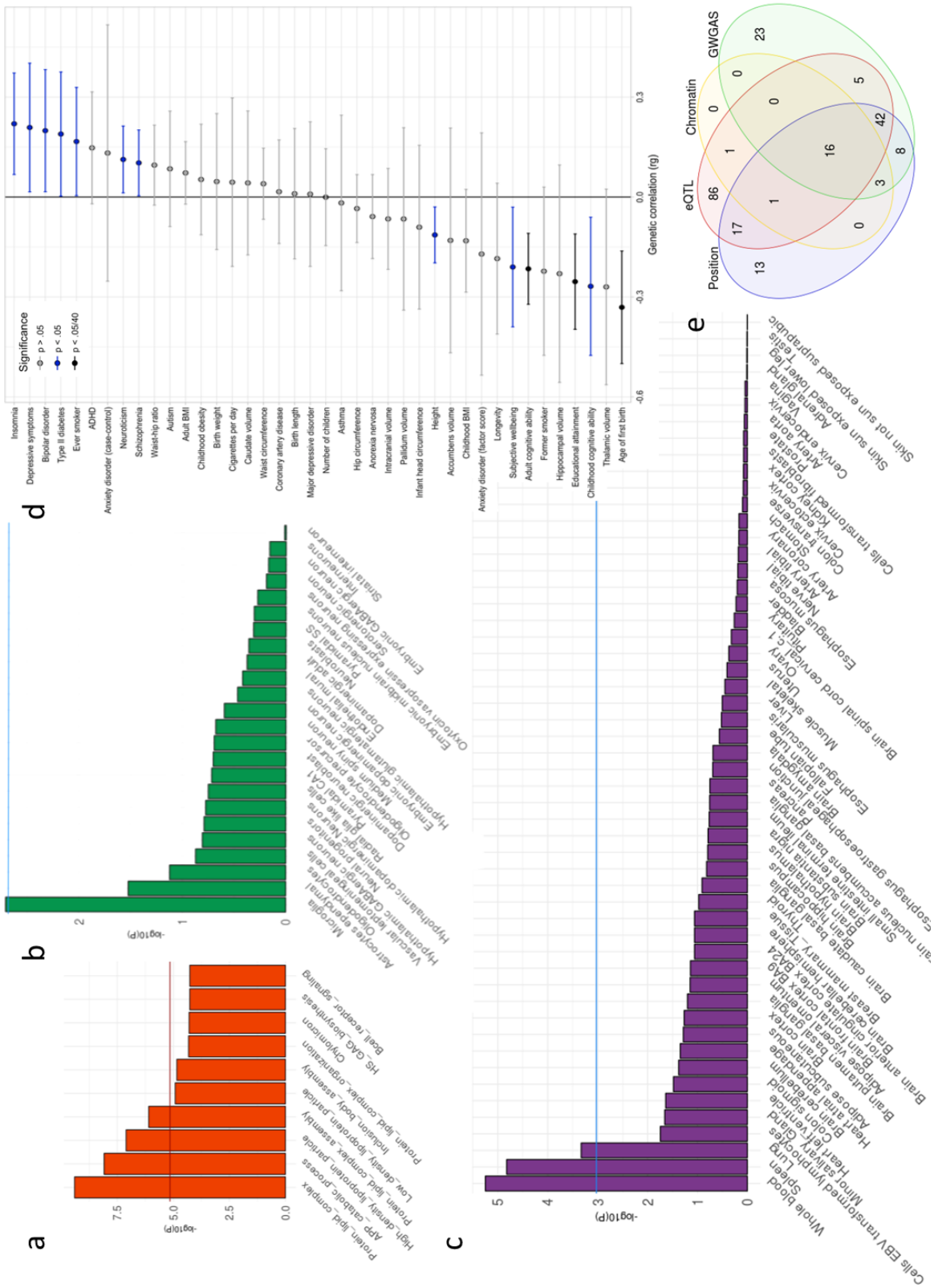

591 **Online methods**

592

593 1.1 Study Cohorts

594 *1.1.1 PGC-ALZ cohorts*

595 Three non-public datasets (the Norwegian DemGene network, The Swedish Twin Studies of
596 Aging and TwinGene) were meta-analyzed as part of the Alzheimer workgroup initiative of the
597 Psychiatric Genomic Consortium (PGC-ALZ).

598 We collected genotype data from the Norwegian DemGene Network consisting of 2,224
599 cases and 1,855 healthy controls. The DemGene Study is a Norwegian network of clinical sites
600 collecting cases from Memory Clinics based on standardised examination of cognitive,
601 functional and behavioural measures and data on progression of most patients. We diagnosed
602 2,224 cases of AD from 7 studies: the Norwegian Register of persons with Cognitive Symptoms
603 (NorCog), the Progression of Alzheimer's Disease and Resource use (PADR), the Dementia Study
604 of Western Norway (DemVest), the AHUS study, the Dementia Study in Rural Northern Norway
605 (NordNorge), HUNT Dementia Study and Nursing Home study, and the TrønderBrain study.
606 These cases were diagnosed according to the recommendations from the National Institute on
607 Aging–Alzheimer's Association (NIA/AA) (AHUS), the NINCDS-ADRDA criteria (DemVest and
608 TrønderBrain) or the ICD-10 research criteria (NorCog, PADR, NordNorge and HUNT). The
609 controls from Norway were obtained through the AHUS, NordNorge, HUNT and TrønderBrain
610 studies. Controls were screened with standardized interview and cognitive tests. Genotypes of
611 the 4079 individuals from the DemGene Study were obtained with Human Omni Express-24
612 v.1.1 (Illumina Inc., San Diego, CA, USA) at deCODE Genetics (Reykjavik, Iceland). To increase

613 the statistical power of our association analysis, the controls were combined with additional
614 5786 population controls from Norwegian blood donor samples (Oslo University Hospital,
615 Ullevål Hospital, Oslo) and controls from Thematically Organized Psychosis Research (TOP)
616 Study27 (between 25-65 years). Control subjects of TOP Study were of Caucasian origin without
617 history of moderate/severe head injury, neurological disorder, mental retardation and were
618 excluded if they or any of their close relatives had a lifetime history of a severe psychiatric
619 disorder, a history of medical problems thought to interfere with brain function or significant
620 illicit drug use.

621 The Swedish Twin Studies of Aging (STSA) (n cases = 398, n controls = 1079) includes
622 three sub-studies of aging within the Swedish Twin Registry[34]: The Swedish Adoption/Twin
623 Study of Aging (SATSA)[35], Aging in Women and MEN (GENDER)[36], and The Study of Dementia in
624 Swedish Twins (HARMONY)[37]. Informed consent was obtained from all participants and the
625 studies were approved by the Regional Ethics Board in Stockholm and the Institutional Review
626 Board at the University of Southern California. DNA was extracted from blood samples and
627 genotyped using Illumina Infinium PsychArray. Alzheimer's disease patients were diagnosed as
628 part of the studies according to the NINCDS/ADRDA criteria[38]. In addition, information on
629 disease after last study participation was retrieved from three population-based health care
630 registers: The National Patient Register, the Causes of Death Register, and the Prescribed Drug
631 Register.

632 TwinGene[34] is a population-based study of older twins drawn from the Swedish Twin
633 Registry. Written informed consent was obtained from all participants and the study was
634 approved by the Regional Ethics Board in Stockholm. DNA was extracted from blood samples

635 and genotyped using Illumina Human OmniExpress for 1791 individuals. Information about
636 Alzheimer's disease (n cases = 343, n controls = 9070) was extracted from the National Patient
637 Register, the Causes of Death Register, and the Prescribed Drug Register, all of which are
638 population-based health care registers with nationwide coverage.
639
640 *1.1.2 IGAP*
641 Publically available (http://web.pasteur-lille.fr/en/recherche/u744/igap/igap_download.php)
642 genome-wide association analysis results of the International Genomics of Alzheimer's Project
643 (IGAP)[4] were included as one of the four cohorts that were meta-analysed in our effort. IGAP is
644 a large two-stage study based upon genome-wide association studies (GWAS) on individuals of
645 European ancestry. We focused on results of stage 1, for which IGAP used genotyped and
646 imputed data of 7,055,881 single nucleotide polymorphisms (SNPs) to meta-analyse four
647 previously-published GWAS datasets consisting of 17,008 Alzheimer's disease cases and 37,154
648 controls (The European Alzheimer's disease Initiative – EADI the Alzheimer Disease Genetics
649 Consortium – ADGC The Cohorts for Heart and Aging Research in Genomic Epidemiology
650 consortium – CHARGE The Genetic and Environmental Risk in AD consortium – GERAD). As the
651 purpose of stage 2 (2, 11,632 SNPs were genotyped and tested for association in an
652 independent set of 8,572 Alzheimer's disease cases and 11,312 controls) was replication of the
653 significantly associated loci of stage 1, we limited the inclusion of the summary statistics for our
654 own analyses to stage 1. Written informed consent was obtained from study participants or, for
655 those with substantial cognitive impairment, from a caregiver, legal guardian or other proxy,

656 and the study protocols for all populations were reviewed and approved by the appropriate
657 institutional review boards.
658
659 *1.1.3 ADSP*
660 The Alzheimer's Disease Sequencing Project (ADSP) collaboration has the aim to identify novel
661 genetic factors that contribute to AD risk by studying genetic sequencing data. ADSP has made
662 their sequencing data available through the Genotypes and Phenotyps database (dbGaP) under
663 the study accession: phs000572.v7.p (https://www.ncbi.nlm.nih.gov/projects/gap/cgi-
664 bin/study.cgi?study_id=phs000572.v1 .p1). We have obtained access to 10,907 individuals
665 (5,771 cases, 5,136 controls) with whole-exome sequencing data to include as the second
666 cohort within our meta-analysis. A substantial proportion of the ADSP individuals were
667 previously also included in IGAP. We applied two strategies to prevent inflated meta-analysis
668 results due to sample overlap: (1) exclusion of ADSP individuals that were duplicates based on
669 genotype data comparison of individual level genetic data between IGAP and ADSP, (2) perform
670 meta-analysis while correcting for cross-study LD score regression intercept (see section 1.4.).
671 To accomplish the first approach we obtained access for all IGAP datasets for which individual
672 level genotype data was available through dbGaP (phs000160.v1.p1 - https://
673 www.ncbi.nlm.nih.gov/projects/gap/cgi-bin/study.cgi?study_id= phs000160.v1.p1;
674 phs000219.v1.p1 - https://www.ncbi.nlm.nih.gov/projects/gap/cgi-
675 bin/study.cgi?study_id=phs000219.v1.p1; phs000372.v1.p1 -
676 https://www.ncbi.nlm.nih.gov/projects/gap/cgi-bin/study.cgi?study_id=phs000372.v1 .p1;
677 phs000168.v2.p2 - https://www.ncbi.nlm.nih.gov/projects/gap/cgi-bin/study.cgi?study_id=

678 phs000168.v2.p2; phs000234.v1.p1 - https://www.ncbi.nlm.nih.gov/projects/gap/cgi-
679 bin/study.cgi? study_id=phs000234.v1.p1) or NIAGADS (NG00026 -
680 https://www.niagads.org/datasets/ng00026; NG00028 -
681 https://www.niagads.org/datasets/ng00028; NG00029 - https://www.niagads.org/
682 datasets/ng00029; NG00031 - https://www.niagads.org/datasets/ng00030 ; NG00031 -
683 https://www.niagads.org/datasets/ng00031; NG00034 -
684 https://www.niagads.org/datasets/ng00034). By calculating identity-by-descent using PLINK[39],
685 we identified duplicates, which were excluded from the ADSP WES dataset for subsequent
686 analyses.
687
688 *1.1.1 UK Biobank study*
689 The current study used data from the UK Biobank[40] (UKB; www.ukbiobank.ac.uk), a large
690 population-based cohort that includes over 500,000 participants and aims to improve insight
691 into a wide variety of health-related determinants and outcomes across the UK. Between 2006
692 and 2010, approximately 9.2 million invitations to participate in the study were sent to
693 individuals aged 40-69 years who were registered with the National Health Service (NHS) and
694 were living within 25 miles from one of the 22 study research centers. In total, 503,325
695 participants were recruited in the study, from which we used a subsample of individuals of
696 European ancestry with available phenotypic and genotypic data (*M* age = 56.5, 54.0% female),
697 described in more detail below. Besides phenotypic information obtained from the NHS
698 registries and associated medical records, participants completed an in-person visit at one of
699 the study research centers where extensive self-report data were collected by questionnaire in

700 addition to anthropometric assessments, DNA collection from blood samples, and magnetic
701 resonance imaging of body and brain. All participants provided written informed consent; the
702 UKB received ethical approval from the National Research Ethics Service Committee North
703 West-Haydock (reference 11/NW/0382), and all study procedures were in accordance with the
704 World Medical Association for medical research. Access to the UK Biobank data was obtained
705 under application number 16406.
706
707 1.2 UKB by proxy phenotype
708 A proxy phenotype for Alzheimer's disease case-control status in UKB was assessed as part of
709 the self-report questionnaire administered during the in-person assessment. Participants were
710 asked to report whether their biological mother or father ever suffered from Alzheimer's
711 disease/dementia, and to report each parent's current age (or age at death, if applicable). Of
712 376,113 individuals in our analytic subsample who completed these questions, a diagnosis was
713 reported for 32,327 mothers (8.6%) and 17,014 fathers (4.5%), resulting in 47,793 participants
714 (12.7%) with one or both parents affected. We created a proxy phenotype from these questions
715 to index genetic risk for Alzheimer's based on parents' diagnoses. The phenotype was
716 constructed as a linear count of the number of affected biological parents (0, 1, or 2). The
717 contribution for each unaffected parent to this count was weighted by the parent's age/age at
718 death to account for the fact that they may not yet have passed through the period of risk for
719 this late-onset disease. Specifically, each affected parent contributed one full unit of "risk" to
720 the count, while each unaffected parent contributed a proportion of one unit of "risk" inversely
721 related to their age. This was calculated as the ratio of parent's age to age 100 (approximately

722 the 95th percentile for life expectancy in developed countries, such that weight=(100-age)/100.
723 The weight for unaffected parents was capped at 0.32, corresponding to a risk equivalent to
724 that of the maximum population prevalence of AD.[41] The phenotype thus ranged from
725 approximately 0-2, with values near zero when both parents were unaffected (lower for older
726 parents and possible values below zero if both parents were over age 100) and values of two
727 when both parents were affected. Participants who were uncertain or chose not to answer
728 questions about either parent's disease status or age were excluded from analyses, resulting in
729 a final N=364,859.

730 Additional information on Alzheimer's disease risk was obtained from national medical
731 records linked to participant data. This information pertained to the participants themselves
732 (not their parents), and was extracted from hospital records obtained between 1996 and the
733 present or from national death registries in the case of participants who passed away after
734 initial enrolment in the study, as described in more detail in the UKB resources
735 (http://biobank.ctsu.ox.ac.uk/crystal/refer.cgi?id=146641;
736 http://biobank.ctsu.ox.ac.uk/crystal/refer.cgi?id=115559). Briefly, primary and secondary
737 diagnoses from inpatient hospital stays and primary and secondary causes of death from death
738 records were recorded using ICD-10 codes. Participants with a diagnosis of "Alzheimer's
739 disease" (diseases of the nervous system chapter; code G30) or "Dementia in Alzheimer's
740 disease" (mental and behavioral disorders chapter; code F00) from any record of a hospital stay
741 or as a cause of death were treated as Alzheimer's cases as given the maximum possible "risk"
742 score of 2, regardless of affectation status of their parents. The reported rate of Alzheimer's in
743 parents of cases (27.4%) was more than double that of non-cases (12.7%; $\chi^2(1)=71.7$, $P=2.45E-$

744 17). There were 393 individuals in the analytic subsample classified as affected by these
745 records; due to the small number of cases and the limited representativeness of these types of
746 health records, we use this information to supplement the proxy parent phenotype rather than
747 as a primary outcome. This information reduces the possibility of misclassification in the proxy
748 phenotype method, and also allows us to evaluate the performance of the proxy phenotype
749 method.

750

751 1.3 Genome-wide association analysis

752 Except for IGAP (obtained summary statistics), we performed genome-wide association
753 analyses for the ADSP, PGC-ALZ and UKB cohorts. For the UKB dataset, quality control and
754 imputation procedures were slightly different, and therefore described separately in the
755 sections below.

756

757 *1.3.1a Quality control and imputation procedures for ADSP and PGC-ALZ datasets*

758 Prior to individual quality control steps, all datasets were filters on a max missingness of 5%.
759 Individuals were excluded when identified as a low quality sample (individual call rate < 0.98),
760 heterozygosity outlier (F +/-.20), gender mismatch (females: F >0.2, males: F < 0.2) when
761 comparing phenotypic and genotypic data, population outlier (defined by principal component
762 boundaries of 1000 Genomes European samples) or being related (PI_HAT > 0.2). Inclusion
763 criteria for variants encompassed a call rate > 0.98, a case-control missingness difference <
764 0.02, a Hardy-Weinberg equilibrium *p*-value < 10e-6 for controls (<10e-10 for cases) and a valid
765 association *p*-value (excluding the variants with low allele frequencies).

766 Pre-imputation, the ADSP and PGC-ALZ datasets were checked for palindromic variants
767 with allele frequency close to 0.5, incorrect reference allele definitions, false strand designation
768 and extreme deviations from expected allele frequencies. Subsequently the ADSP and PGC-ALZ
769 datasets were imputed with the 1000 Genomes Phase 3[42] reference panel. The reported SNPs
770 all have a considerable imputation quality (INFO score>0.591) and variants with a low allele
771 frequency (MAF<0.01) were excluded, resulting in a total of 7508 individuals (4343 cases and
772 3165 controls) and 260,934 variants for the ADSP cohort and 17477 individuals (2,736 cases and
773 14,471 controls) and 9,629,492 variants for the PGC-ALZ cohort.
774
775 *1.3.1b Quality control and imputation for UKB dataset*
776 We used second-release genotype data that were made available by UKB in July 2017.
777 Genotype data collection and processing are described by the UKB in a previous overview
778 paper[43]. DNA was extracted from blood samples and genotyping was completed for 488,366
779 individuals on one of two Affymetrix genotyping arrays with custom content, the UK BiLEVE
780 Axiom array (n=49,949) or UK Biobank Axiom array (n=438,417), covering 812,428 genetic
781 markers common to both arrays. Of these, 488,377 individuals and 805,426 markers passed
782 genotype quality control checks conducted by UKB (see
783 http://www.biorxiv.org/content/early/2017/07/20/166298 for details). Samples were excluded
784 for low DNA concentration, call rate < 95%, excess heterozygosity, sex chromosome
785 abnormality, or sample duplication. Variants were excluded if they exhibited poor clustering of
786 allele calls, batch, plate, array, or sex effects, departures from HWE, or discordance between
787 technical replicate samples.

788 After quality control, samples were imputed to approximately 92 million SNPs using
789 both the reference panel of the Haplotype Reference Consortium (HRC)[44] as well as a combined
790 reference panel of the 1000 Genomes Project[42] and UK10K. As recommended by UKB, we
791 removed variants that were not imputed on the HRC reference panel due to technical errors in
792 the imputation process of the combined panel. We converted imputed variants to hard calls
793 (certainty > 0.9), filtered by imputation quality (INFO score >0.9), and excluded multi-allelic
794 SNPs, indels, SNPs without unique rsID, and SNPs with minor allele frequency (MAF) <0.0001,
795 resulting in 10,847,151 SNPs available for analysis.

796 For the present study, we selected unrelated individuals of European ancestry. To
797 empirically determine ancestry, we projected genetic principal components from known
798 ancestral populations in the 1000 Genomes Project onto the UKB genotypes and assigned
799 individuals to the continental ancestral superpopulation with the closest Mahalanobis
800 distance.[45] Within-ancestry principal components were created using FlashPCA2[46] to correct for
801 any residual population stratification within the European ancestry subset. Unrelated
802 individuals (less than 3rd degree relatives, as indicated by genomic relatedness coefficients
803 calculated by UKB) were selected by sequentially removing participants with the greatest
804 number of relatives until no related pairs remained. After applying these filtering criteria and
805 removing any participants with missing phenotypic or covariate data and participants who
806 withdrew consent, 364,859 individuals remained for analysis in the UKB sample.

807

808 *1.3.2 Single-marker association analysis*

809 Genome-wide association analysis (GWAS) for the ADSP, PGC-ALZ and UKB datasets was
810 performed in PLINK[39], using logistic regression for dichotomous phenotypes (cases versus
811 controls for ADSP and PGC-ALZ cohorts), and linear regression for phenotypes analysed as
812 continuous outcomes (by proxy parental AD phenotype for UKB cohort). For the ADSP and PGC-
813 ALZ cohorts, association tests were adjusted for gender, batch (if applicable), and the first 4
814 principal components. Twenty principal components were calculated, and depending on the
815 dataset being tested, additional principal components (on top of the standard inclusion of 4
816 PCAs) were added if significantly associated to the phenotype. Furthermore, for the PGC-ALZ
817 cohorts age was included as a covariate. For 4,537 controls of the DemGene cohort, no detailed
818 age information was available, besides the age range the subjects were in (20-45 years). We
819 therefore set the age of these individuals conservatively to 20 years. For the ADSP dataset, age
820 was not included as a covariate due to the enrichment for older controls (mean age cases =
821 73.1 years (SE=7.8); mean age controls = 86.1 years (SE=4.5)) in their collection procedures.
822 Correcting for age in ADSP would remove a substantial part of genuine association signals (e.g.
823 well-established *APOE* locus rs11556505 is strongly associated to AD (P=1.08x10^{-99}), which is
824 lost when correcting for age (P=0.0054). For the UKB dataset, 12 components were included as
825 covariates, as well as age, sex, genotyping array, and assessment centre. We used the genome-
826 wide threshold for significance of P<5×10-8).
827
828 1.3.3 *Multivariate genome-wide meta-analysis*
829 Two meta-analyses were performed, including: 1) cohorts with case-control phenotypes (IGAP,
830 ADSP and PGC-ALZ datasets), 2) all cohorts, also including the by proxy phenotype of UKB.

The per SNP test statistics is defined by

$$Z_k = \frac{\sum_i w_i Z_i}{\sqrt{\sum_i w_i^2 + \sum_i \sum_j w_i w_j \left| CTI_{ij} \right| (i \neq j)}}$$

where w_i and Z_i are squared root of the sample size and the test statistics of SNP *k* of cohort *i*, respectively. CTI is cross trait LD score intercept estimated by LDSC using genome-wide summary statistics as

$$CTI_{ij} = \frac{N_{sij}\rho_{ij}}{\sqrt{N_i N_j}}$$

where N_{sij} and r_{ij} are overlapping samples and phenotypic correlation between cohort *i* and *j*, respectively.[13] Test statistics per SNP per GWAS was converted from P-value by taking sign of either beta or odds ratio. When direction is aligned the conversion is two-sided. To avoid infinite value, we replaced P-value 1 with 0.999999 and P-value < 1e-323 to 1e-323 (the minimum >0 value in Python).

The effective sample size (N_{eff}) is computed for each SNP *k* from the matrix *M*, containing the sample size N_i of each cohort *i* on the diagonal and the estimated number of shared data points $N_{sij} \mathrm{x} \rho_{ij} = CTI_{ij} \mathrm{x} \sqrt{N_i N_j}$ for each pair of cohorts *i* and *j* as the off-diagonal values. N_{eff} is computed recursively as follows. Starting with the first cohort in *M*, N_{eff} is first increased by $M_{1,1}$, corresponding to the sample size of that cohort. The proportion of samples shared between cohort 1 and each other cohort *j* is them computed as $p_{1,j} = M_{1,j}/M_{j,j}$, and *M* is then adjusted to remove this overlap, multiplying all values in each column *j* by $1\text{-}p_{1,j}$. This amounts to reducing the sample size of each other cohort *j* by the number of samples it shares

853 with cohort 1, and reducing the shared samples between cohort *j* and subsequent cohorts by
854 the same proportion. After this, the first row and column of *M* are discarded, and the same
855 process is applied to the new *M* matrix. This is repeated until *M* is empty. The script for the
856 multivariate GWAS is available from https://github.com/Kyoko-wtnb/mvGWAMA.
857
858 1.5 Replication of meta-analysis result in Icelandic sample
859 The study group included 6,593 Alzheimer's disease cases (4,923 of whom were chip-typed) and
860 174,289 controls (88,581 of whom were chip-typed). In 16% of patients, the diagnosis of
861 Alzheimer's disease was established according to the criteria for definite, probable, or possible
862 Alzheimer's disease of the National Institute of Neurological and Communicative Disorders and
863 Stroke and the Alzheimer's Disease and Related Disorders Association (NINCDS-ADRDA). In 77%
864 of patients, the diagnosis was established according to the criteria for code 331.0 in ICD-9, or
865 for F00 and G30 in ICD-10. Seven percent of the patients were identified in the Directorate of
866 Health medication database as having been prescribed Donepezil (Aricept), a palliative
867 treatment for Alzheimer's disease. The controls were drawn from various research projects at
868 deCODE Genetics, excluding those in whom Alzheimer's disease had been diagnosed.
869 The study was approved by the National Bioethics Committee and the Icelandic Data Protection
870 Authority. Written informed consent was obtained from all participants or their guardians
871 before blood samples were drawn. All sample identifiers were encrypted in accordance with
872 the regulations of the Icelandic Data Protection Authority.
873 Chip-typing and long-range phasing of 155,250 individuals was carried out as described
874 previously.[20] Imputation of the variants found in 28,075 whole-genome sequenced individuals

875 into the chip-typed individuals and 285,664 close relatives was performed as detailed earlier.[20]
876 Association analysis was carried out using logistic regression with Alzheimer's disease status as
877 the response and genotype counts and a set of nuisance variables including sex, county of birth,
878 and current age as predictors.[21] Correction for inflation of test statistics due to relatedness and
879 population stratification was performed using the intercept estimate from LD score regression
880 (1.29) as described in.[13]
881
882 1.6 Genomic risk loci definition
883 We used FUMA[25], an online platform for functional mapping and annotation of genetic variants,
884 to define genomic risk loci and obtain functional information of relevant SNPs in these loci. We
885 first identified independent significant SNPs that have a genome-wide significant P-value
886 (<5×10-8) and are independent from each other at r^2<0.6. These SNPs were further represented
887 by lead SNPs, which are a subset of the independent significant SNPs that are in approximate
888 linkage equilibrium with each other at r^2>0.6. We then defined associated genomic risk loci by
889 merging any physically overlapping lead SNPs (LD blocks <250kb apart). Borders of the genomic
890 risk loci were defined by identifying all SNPs in LD (r^2>0.6) with one of the independent
891 significant SNPs in the locus, and the region containing all these candidate SNPs was considered
892 to be a single independent genomic risk locus. LD information was calculated using the UK
893 Biobank genotype data as a reference.
894
895 1.7 Cohort Heritability and Genetic Correlation

896 LD score regression[13] was used to estimate genomic inflation and heritability of the AD in each
897 of the 7 cohorts (PGC-ALZ, ADSP, IGAP, UKB, DemGene, STSA, TwinGene) using their post-
898 quality control summary statistics, and to estimate the cross-cohort genetic correlations.[47] Pre-
899 calculated LD scores from the 1000 Genomes European reference population were obtained
900 from https://data.broadinstitute.org/alkesgroup/LDSCORE/. Genetic correlations were
901 calculated on HapMap3 SNPs only. LD score regression was also used on the case-control and
902 by-proxy phenotype result to estimate heritability and genetic correlations for the two
903 phenotype definitions.
904
905 1.8 Polygenic risk scoring
906 We calculated polygenic scores (PGS) based on the SNP effect sizes of meta-analyses. PGS were
907 calculated using an independent genotype dataset of 761 individuals (379 cases and 382
908 controls) from the ADDNeuroMed study.[48] The same QC and imputation approach was applied
909 as for the other datasets with genotype-level data (see Method section 1.3.1a). PRSice PGS
910 were calculated on hard-called imputed genotypes using *P*-value thresholds from 0.0 to 0.5 in
911 steps ranging from $5x10^{-8}$ to 0.001. The explained variance (ΔR^2) was derived from a linear
912 model in which the AD phenotype was regressed on each PGS while controlling for the same
913 covariates as in each cohort-specific GWAS, compared to a linear model with GWAS covariates
914 only.
915
916 1.9 Stratified Heritability

917 To test whether specific categories of SNP annotations were enriched for heritability, we
918 partitioned SNP heritability for binary annotations using stratified LD score regression
919 (https://github.com/bulik/ldsc)[13]. Heritability enrichment was calculated as the proportion of
920 heritability explained by a SNP category divided by the proportion of SNPs that are in that
921 category. Partitioned heritability was computed by 28 functional annotation categories, by
922 minor allele frequency (MAF) in six percentile bins and by 22 chromosomes. Annotations for
923 binary categories of functional genomic characteristics (e.g. coding or regulatory regions) were
924 obtained from the LD score website (https://github.com/bulik/ldsc). The Bonferroni-corrected
925 significance threshold for 56 annotations was set at: $P<0.05/56=8.93\times10^{-4}$.
926

927 1.10 Functional Annotation of SNPs

928 Functional annotation of SNPs implicated in the meta-analysis was performed using FUMA[25]
929 (http://fuma.ctglab.nl/). We selected all *candidate SNPs* in associated genomic loci having an
930 $r^2 \geqq 0.6$ with one of the independent significant SNPs (see above), a *P*-value ($P<1\text{x}10^{-8}$) and a
931 MAF>0.0001 for annotations. Functional consequences for these SNPs were obtained by
932 matching SNPs' chromosome, base-pair position, and reference and alternate alleles to
933 databases containing known functional annotations, including ANNOVAR[49] categories,
934 Combined Annotation Dependent Depletion (CADD) scores[23], RegulomeDB[50] (RDB) scores, and
935 chromatin states[51,52]. ANNOVAR annotates functional consequence of SNPs on genes (e.g.
936 intron, exon, intergenic). CADD scores predict how deleterious the effect of a SNP with higher
937 scores referring to higher deleteriousness. A CADD score above 12.37 is the threshold to be
938 potentially pathogenic[53]. The RegulomeDB score is a categorical score based on information

939 from expression quantitative trait loci (eQTLs) and chromatin marks, ranging from 1a to 7 with
940 lower scores indicating an increased likelihood of having a regulatory function. Scores are as
941 follows: 1a=eQTL + Transciption Factor (TF) binding + matched TF motif + matched DNase
942 Footprint + DNase peak; 1b=eQTL + TF binding + any motif + DNase Footprint + DNase peak;
943 1c=eQTL + TF binding + matched TF motif + DNase peak; 1d=eQTL + TF binding + any motif +
944 DNase peak; 1e=eQTL + TF binding + matched TF motif; 1f=eQTL + TF binding / DNase peak;
945 2a=TF binding + matched TF motif + matched DNase Footprint + DNase peak; 2b=TF binding +
946 any motif + DNase Footprint + DNase peak; 2c=TF binding + matched TF motif + DNase peak;
947 3a=TF binding + any motif + DNase peak; 3b=TF binding + matched TF motif; 4=TF binding +
948 DNase peak; 5=TF binding or DNase peak; 6=other;7=None. The chromatin state represents the
949 accessibility of genomic regions (every 200bp) with 15 categorical states predicted by a hidden
950 Markov model based on 5 chromatin marks for 127 epigenomes in the Roadmap Epigenomics
951 Project[39]. A lower state indicates higher accessibility, with states 1-7 referring to open
952 chromatin states. We annotated the minimum chromatin state across tissues to SNPs. The 15-
953 core chromatin states as suggested by Roadmap are as follows: 1=Active Transcription Start Site
954 (TSS); 2=Flanking Active TSS; 3=Transcription at gene 5' and 3'; 4=Strong transcription; 5= Weak
955 Transcription; 6=Genic enhancers; 7=Enhancers; 8=Zinc finger genes & repeats;
956 9=Heterochromatic; 10=Bivalent/Poised TSS; 11=Flanking Bivalent/Poised TSS/Enh; 12=Bivalent
957 Enhancer; 13=Repressed PolyComb; 14=Weak Repressed PolyComb; 15=Quiescent/Low.
958

959 1.11 Gene-mapping

960 Genome-wide significant loci obtained by GWAS were mapped to genes in FUMA[25] using three
961 strategies:

962 1. Positional mapping maps SNPs to genes based on physical distance (within a 10kb
963 window) from known protein coding genes in the human reference assembly
964 (GRCh37/hg19).

965 2. eQTL mapping maps SNPs to genes with which they show a significant eQTL association
966 (i.e. allelic variation at the SNP is associated with the expression level of that gene).
967 eQTL mapping uses information from 45 tissue types in 3 data repositories (GTEx[54],
968 Blood eQTL browser[55], BIOS QTL browser[56]), and is based on cis-eQTLs which can map
969 SNPs to genes up to 1Mb apart. We used a false discovery rate (FDR) of 0.05 to define
970 significant eQTL associations.

971 3. Chromatin interaction mapping was performed to map SNPs to genes when there is a
972 three-dimensional DNA-DNA interaction between the SNP region and another gene
973 region. Chromatin interaction mapping can involve long-range interactions as it does not
974 have a distance boundary. FUMA currently contains Hi-C data of 14 tissue types from
975 the study of Schmitt et al[57]. Since chromatin interactions are often defined in a certain
976 resolution, such as 40kb, an interacting region can span multiple genes. If a SNPs is
977 located in a region that interacts with a region containing multiple genes, it will be
978 mapped to each of those genes. To further prioritize candidate genes, we selected only
979 genes mapped by chromatin interaction in which one region involved in the interaction
980 overlaps with a predicted enhancer region in any of the 111 tissue/cell types from the

981 Roadmap Epigenomics Project[52] and the other region is located in a gene promoter
982 region (250bp up and 500bp downstream of the transcription start site and also
983 predicted by Roadmap to be a promoter region). This method reduces the number of
984 genes mapped but increases the likelihood that those identified will have a plausible
985 biological function. We used a FDR of 1×10^{-5} to define significant interactions, based on
986 previous recommendations[44] modified to account for the differences in cell lines used
987 here.
988
989 1.12 Gene-based analysis
990 To account for the distinct types of genetic data in this study, genotype array (PGC-ALZ, IGAP,
991 UKB) and whole-exome sequencing data (ADSP), we first performed two gene-based genome-
992 wide association analysis (GWGAS) using MAGMA[28], followed by a meta-analysis. SNP-based P-
993 values from the meta-analysis of the 3 genotype-array-based datasets were used as input for
994 the first GWGAS, while the unimputed individual-level sequence data of ADSP was used as
995 input for the second GWGAS. 18,233 protein-coding genes (each containing at least one SNP in
996 the GWAS) from the NCBI 37.3 gene definitions were used as basis for GWGAS in MAGMA.
997 Bonferroni correction was applied to correct for multiple testing ($P<2.74\times10^{-6}$).
998
999 1.13 Gene-set analysis
1000 Results from the GWGAS analyses were used to test for association in three types of 7,087
1001 predefined gene-sets:

1002 1. 6,994 curated gene-sets representing known biological and metabolic pathways derived
1003 from Gene Ontology (5917 gene-sets), Biocarta (217 gene-sets), KEGG (186 gene-sets),
1004 Reactome (674 gene-sets) catalogued by and obtained from the MsigDB version 6.1[58]
1005 (http://software.broadinstitute.org/gsea/msigdb/collections.jsp)
1006 2. Gene expression values from 54 (53 + 1 calculated 1st PC of three tissue subtypes)
1007 tissues obtained from GTEx[54], log2 transformed with pseudocount 1 after winsorization
1008 at 50 and averaged per tissue.
1009 3. Cell-type specific expression in 173 types of brain cells (24 broad categories of cell types,
1010 'level 1' and 129 specific categories of cell types 'level 2'), which were calculated
1011 following the method described in [30]. Briefly, brain cell-type expression data was drawn
1012 from single-cell RNA sequencing data from mouse brains. For each gene, the value for
1013 each cell-type was calculated by dividing the mean Unique Molecular Identifier (UMI)
1014 counts for the given cell type by the summed mean UMI counts across all cell types.
1015 Single-cell gene-sets were derived by grouping genes into 40 equal bins based on
1016 specificity of expression.
1017 4. Nucleus specific gene expression of 15 distinct human brain cell-types of study
1018 described in[59]. The value for each cell-type was calculated with the same method as
1019 explained in point 3 above.

1020 These gene-sets were tested using MAGMA. We computed competitive *P*-values, which
1021 represent the test of association for a specific gene-set compared with genes not in the gene-
1022 set to correct for baseline level of genetic association in the data. The Bonferroni-corrected
1023 significance threshold was 0.05/7,087 gene-sets=7.06×10^{-6}. The suggestive significance

1024 threshold was defined by the number of tests within the category. Conditional analyses were
1025 performed as a follow-up using MAGMA to test whether each significant association observed
1026 was independent of all others and of *APOE* (a gene-set including all genes within genomic
1027 region chr19:45,020,859-45,844,508). Furthermore, the association between each of the
1028 significant gene-set was tested conditional on each of the other significantly associated gene-
1029 sets. Gene-sets that retained their association after correcting for other sets were considered to
1030 represent independent signals. We note that this is not a test of association per se, but rather a
1031 strategy to identify, among gene-sets with known significant associations and overlap in genes,
1032 which set (s) are responsible for driving the observed association.

1033

1034 1.14 Cross-Trait Genetic Correlation

1035 Genetic correlations (r_g) between AD and 41 phenotypes were computed using LD score
1036 regression[13], as described above, based on GWAS summary statistics obtained from publicly
1037 available databases (http://www.med.unc.edu/pgc/results-and-downloads; http://
1038 ldsc.broadinstitute.org/; **Supplementary Table 19**). The Bonferroni-corrected significance
1039 threshold was 0.05/41 traits=1.22×10^{-3}.

1040

1041 1.15 Mendelian Randomisation

1042 To infer credible causal associations between AD and traits that are genetically correlated with
1043 AD, we performed Generalised Summary-data based Mendelian Randomisation[29] (GSMR;
1044 http://cnsgenomics.com/software/gsmr/). This method utilizes summary-level data to test for
1045 putative causal associations between a risk factor (exposure) and an outcome by using

independent genome-wide significant SNPs as instrumental variables as an index of the exposure. HEIDI-outlier detection was used to filter genetic instruments that showed clear pleiotropic effects on the exposure phenotype and the outcome phenotype. We used a threshold p-value of 0.01 for the outlier detection analysis in HEIDI which removes 1% of SNPs by chance if there is no pleiotropic effect. To test for a potential causal effect of various outcomes on risk for AD, we selected phenotypes in non-overlapping samples that showed (suggestive) significant (P<0.05) genetic correlations (r_g) with AD. With this method it is typical to test for bi-directional causation by repeating the analyses while switching the role of the exposure and the outcome; however, because AD is a late-onset disease, it makes little sense to estimate its causal effect on outcomes that develop earlier in life, particularly when the summary statistics for these outcomes were derived mostly from younger samples than those of AD cases. Therefore, we conducted these analyses only in one direction. For genetically correlated phenotypes, we selected independent (r^2=<0.1), GWS lead SNPs as instrumental variables in the analyses. The method estimates a putative causal effect of the exposure on the outcome (b_{xy}) as a function of the relationship between the SNPs' effects on the exposure (b_{zx}) and the SNPs' effects on the outcome (b_{zy}), given the assumption that the effect of non-pleiotropic SNPs on an exposure (x) should be related to their effect on the outcome (y) in an independent sample only via mediation through the phenotypic causal pathway (b_{xy}). The estimated causal effect coefficients (b_{xy}) are approximately equal to the natural log odds ratio (OR)[29] for a case-control trait. An OR of 2 can be interpreted as a doubled risk compared to the population prevalence of a binary trait for every SD increase in the exposure trait. For quantitative traits the b_{zx} and b_{zy} can be interpreted as a one standard deviation increase

1068 explained in the outcome trait for every SD increase in the exposure trait. This method can help
1069 differentiate the causal direction of association between two traits, but cannot make any
1070 statement about the intermediate mechanisms involved in any potential causal process.

1071

1072 *Data availability*

1073 Summary statistics will be made available for download upon publication (https://ctg.cncr.nl).

1074

1075 **References**

1076

1077 1. Prince M, Bryce R, Albanese E, Wimo A, Ribeiro W, Ferri CP. The global prevalence of
1078 dementia: a systematic review and metaanalysis. *Alzheimer's & dementia : the journal of the*
1079 *Alzheimer's Association* 2013; **9**(1): 63-75.e2.
1080 2. Gatz M, Reynolds CA, Fratiglioni L, et al. Role of genes and environments for explaining
1081 Alzheimer disease. *Archives of general psychiatry* 2006; **63**(2): 168-74.
1082 3. Cacace R, Sleegers K, Van Broeckhoven C. Molecular genetics of early-onset Alzheimer's
1083 disease revisited. *Alzheimer's & dementia : the journal of the Alzheimer's Association* 2016;
1084 **12**(6): 733-48.
1085 4. Lambert JC, Ibrahim-Verbaas CA, Harold D, et al. Meta-analysis of 74,046 individuals
1086 identifies 11 new susceptibility loci for Alzheimer's disease. *Nature genetics* 2013; **45**(12): 1452-
1087 8.
1088 5. Goate A, Chartier-Harlin MC, Mullan M, et al. Segregation of a missense mutation in the
1089 amyloid precursor protein gene with familial Alzheimer's disease. *Nature* 1991; **349**(6311): 704-
1090 6.
1091 6. Sherrington R, Rogaev EI, Liang Y, et al. Cloning of a gene bearing missense mutations in
1092 early-onset familial Alzheimer's disease. *Nature* 1995; **375**(6534): 754-60.
1093 7. Sherrington R, Froelich S, Sorbi S, et al. Alzheimer's disease associated with mutations in
1094 presenilin 2 is rare and variably penetrant. *Human molecular genetics* 1996; **5**(7): 985-8.
1095 8. Karran E, Mercken M, De Strooper B. The amyloid cascade hypothesis for Alzheimer's
1096 disease: an appraisal for the development of therapeutics. *Nature reviews Drug discovery* 2011;
1097 **10**(9): 698-712.
1098 9. Jonsson T, Stefansson H, Steinberg S, et al. Variant of TREM2 associated with the risk of
1099 Alzheimer's disease. *The New England journal of medicine* 2013; **368**(2): 107-16.
1100 10. Steinberg S, Stefansson H, Jonsson T, et al. Loss-of-function variants in ABCA7 confer risk
1101 of Alzheimer's disease. *Nature genetics* 2015; **47**(5): 445-7.
1102 11. Liu CC, Liu CC, Kanekiyo T, Xu H, Bu G. Apolipoprotein E and Alzheimer disease: risk,
1103 mechanisms and therapy. *Nature reviews Neurology* 2013; **9**(2): 106-18.
1104 12. Zheng J, Erzurumluoglu AM, Elsworth BL, et al. LD Hub: a centralized database and web
1105 interface to perform LD score regression that maximizes the potential of summary level GWAS

1106 data for SNP heritability and genetic correlation analysis. *Bioinformatics (Oxford, England)*
1107 2017; **33**(2): 272-9.
1108 13. Bulik-Sullivan BK, Loh PR, Finucane HK, et al. LD Score regression distinguishes
1109 confounding from polygenicity in genome-wide association studies. *Nature genetics* 2015;
1110 **47**(3): 291-5.
1111 14. Ridge PG, Mukherjee S, Crane PK, Kauwe JS. Alzheimer's disease: analyzing the missing
1112 heritability. *PloS one* 2013; **8**(11): e79771.
1113 15. Ridge PG, Hoyt KB, Boehme K, et al. Assessment of the genetic variance of late-onset
1114 Alzheimer's disease. *Neurobiology of aging* 2016; **41**: 200.e13-.e20.
1115 16. Desikan RS, Schork AJ, Wang Y, et al. Polygenic Overlap Between C-Reactive Protein,
1116 Plasma Lipids, and Alzheimer Disease. *Circulation* 2015; **131**(23): 2061-9.
1117 17. Jun GR, Chung J, Mez J, et al. Transethnic genome-wide scan identifies novel Alzheimer's
1118 disease loci. *Alzheimer's & dementia : the journal of the Alzheimer's Association* 2017; **13**(7):
1119 727-38.
1120 18. Guerreiro R, Wojtas A, Bras J, et al. TREM2 variants in Alzheimer's disease. *The New*
1121 *England journal of medicine* 2013; **368**(2): 117-27.
1122 19. Sims R, van der Lee SJ, Naj AC, et al. Rare coding variants in PLCG2, ABI3, and TREM2
1123 implicate microglial-mediated innate immunity in Alzheimer's disease. *Nature genetics* 2017;
1124 **49**(9): 1373-84.
1125 20. Gudbjartsson DF, Helgason H, Gudjonsson SA, et al. Large-scale whole-genome
1126 sequencing of the Icelandic population. *Nature genetics* 2015; **47**(5): 435-44.
1127 21. Steinthorsdottir V, Thorleifsson G, Sulem P, et al. Identification of low-frequency and
1128 rare sequence variants associated with elevated or reduced risk of type 2 diabetes. *Nature*
1129 *genetics* 2014; **46**(3): 294-8.
1130 22. Euesden J, Lewis CM, O'Reilly PF. PRSice: Polygenic Risk Score software. *Bioinformatics*
1131 *(Oxford, England)* 2015; **31**(9): 1466-8.
1132 23. Kircher M, Witten DM, Jain P, O'Roak BJ, Cooper GM, Shendure J. A general framework
1133 for estimating the relative pathogenicity of human genetic variants. *Nature genetics* 2014;
1134 **46**(3): 310-5.
1135 24. Finucane HK, Bulik-Sullivan B, Gusev A, et al. Partitioning heritability by functional
1136 annotation using genome-wide association summary statistics. *Nature genetics* 2015; **47**(11):
1137 1228-35.
1138 25. Watanabe K, Taskesen E, van Bochoven A, Posthuma D. Functional mapping and
1139 annotation of genetic associations with FUMA. *Nature communications* 2017; **8**(1): 1826.
1140 26. Gurses MS, Ural MN, Gulec MA, Akyol O, Akyol S. Pathophysiological Function of
1141 ADAMTS Enzymes on Molecular Mechanism of Alzheimer's Disease. *Aging and disease* 2016;
1142 **7**(4): 479-90.
1143 27. Dries DR, Yu G. Assembly, maturation, and trafficking of the gamma-secretase complex
1144 in Alzheimer's disease. *Current Alzheimer research* 2008; **5**(2): 132-46.
1145 28. de Leeuw CA, Mooij JM, Heskes T, Posthuma D. MAGMA: generalized gene-set analysis
1146 of GWAS data. *PLoS computational biology* 2015; **11**(4): e1004219.
1147 29. Zhu Z, Zheng Z, Zhang F, et al. Causal associations between risk factors and common
1148 diseases inferred from GWAS summary data. *Nature communications* 2018; **9**(1): 224.

1149 30. Skene NG, Grant SG. Identification of Vulnerable Cell Types in Major Brain Disorders
1150 Using Single Cell Transcriptomes and Expression Weighted Cell Type Enrichment. *Frontiers in*
1151 *neuroscience* 2016; **10**: 16.
1152 31. Loewendorf A, Fonteh A, Mg H, Me C. Inflammation in Alzheimer's Disease: Cross-talk
1153 between Lipids and Innate Immune Cells of the Brain; 2015.
1154 32. Stern Y. Cognitive reserve in ageing and Alzheimer's disease. *The Lancet Neurology*
1155 2012; **11**(11): 1006-12.
1156 33. Satizabal C, Beiser AS, Seshadri S. Incidence of Dementia over Three Decades in the
1157 Framingham Heart Study. *The New England journal of medicine* 2016; **375**(1): 93-4.
1158 34. Magnusson PK, Almqvist C, Rahman I, et al. The Swedish Twin Registry: establishment of
1159 a biobank and other recent developments. *Twin research and human genetics : the official*
1160 *journal of the International Society for Twin Studies* 2013; **16**(1): 317-29.
1161 35. Finkel D, Pedersen NL. Processing Speed and Longitudinal Trajectories of Change for
1162 Cognitive Abilities: The Swedish Adoption/Twin Study of Aging. *Aging, Neuropsychology, and*
1163 *Cognition* 2004; **11**(2-3): 325-45.
1164 36. Gold CH, Malmberg B, McClearn GE, Pedersen NL, Berg S. Gender and health: a study of
1165 older unlike-sex twins. *The journals of gerontology Series B, Psychological sciences and social*
1166 *sciences* 2002; **57**(3): S168-76.
1167 37. Gatz M, Fratiglioni L, Johansson B, et al. Complete ascertainment of dementia in the
1168 Swedish Twin Registry: the HARMONY study. *Neurobiology of aging* 2005; **26**(4): 439-47.
1169 38. McKhann G, Drachman D, Folstein M, Katzman R, Price D, Stadlan EM. Clinical diagnosis
1170 of Alzheimer's disease: report of the NINCDS-ADRDA Work Group under the auspices of
1171 Department of Health and Human Services Task Force on Alzheimer's Disease. *Neurology* 1984;
1172 **34**(7): 939-44.
1173 39. Chang CC, Chow CC, Tellier LC, Vattikuti S, Purcell SM, Lee JJ. Second-generation PLINK:
1174 rising to the challenge of larger and richer datasets. *GigaScience* 2015; **4**: 7.
1175 40. Sudlow C, Gallacher J, Allen N, et al. UK biobank: an open access resource for identifying
1176 the causes of a wide range of complex diseases of middle and old age. *PLoS medicine* 2015;
1177 **12**(3): e1001779.
1178 41. Hebert LE, Weuve J, Scherr PA, Evans DA. Alzheimer disease in the United States (2010-
1179 2050) estimated using the 2010 census. *Neurology* 2013; **80**(19): 1778-83.
1180 42. The Genomes Project C. A global reference for human genetic variation. *Nature* 2015;
1181 **526**: 68.
1182 43. Davies G, Marioni RE, Liewald DC, et al. Genome-wide association study of cognitive
1183 functions and educational attainment in UK Biobank (N=112 151). *Molecular psychiatry* 2016;
1184 **21**(6): 758-67.
1185 44. McCarthy S, Das S, Kretzschmar W, et al. A reference panel of 64,976 haplotypes for
1186 genotype imputation. *Nature genetics* 2016; **48**(10): 1279-83.
1187 45. Peterson RE, Edwards AC, Bacanu SA, Dick DM, Kendler KS, Webb BT. The utility of
1188 empirically assigning ancestry groups in cross-population genetic studies of addiction. *The*
1189 *American journal on addictions* 2017; **26**(5): 494-501.
1190 46. Abraham G, Qiu Y, Inouye M. FlashPCA2: principal component analysis of Biobank-scale
1191 genotype datasets. *Bioinformatics (Oxford, England)* 2017; **33**(17): 2776-8.

1192 47. Bulik-Sullivan B, Finucane HK, Anttila V, et al. An atlas of genetic correlations across
1193 human diseases and traits. *Nature genetics* 2015; **47**(11): 1236-41.
1194 48. Lovestone S, Francis P, Kloszewska I, et al. AddNeuroMed--the European collaboration
1195 for the discovery of novel biomarkers for Alzheimer's disease. *Annals of the New York Academy*
1196 *of Sciences* 2009; **1180**: 36-46.
1197 49. Wang K, Li M, Hakonarson H. ANNOVAR: functional annotation of genetic variants from
1198 high-throughput sequencing data. *Nucleic acids research* 2010; **38**(16): e164.
1199 50. Boyle AP, Hong EL, Hariharan M, et al. Annotation of functional variation in personal
1200 genomes using RegulomeDB. *Genome research* 2012; **22**(9): 1790-7.
1201 51. Ernst J, Kellis M. ChromHMM: automating chromatin-state discovery and
1202 characterization. *Nature methods* 2012; **9**(3): 215-6.
1203 52. Kundaje A, Meuleman W, Ernst J, et al. Integrative analysis of 111 reference human
1204 epigenomes. *Nature* 2015; **518**(7539): 317-30.
1205 53. Amendola LM, Dorschner MO, Robertson PD, et al. Actionable exomic incidental findings
1206 in 6503 participants: challenges of variant classification. *Genome research* 2015; **25**(3): 305-15.
1207 54. Human genomics. The Genotype-Tissue Expression (GTEx) pilot analysis: multitissue
1208 gene regulation in humans. *Science (New York, NY)* 2015; **348**(6235): 648-60.
1209 55. Westra HJ, Peters MJ, Esko T, et al. Systematic identification of trans eQTLs as putative
1210 drivers of known disease associations. *Nature genetics* 2013; **45**(10): 1238-43.
1211 56. Zhernakova DV, Deelen P, Vermaat M, et al. Identification of context-dependent
1212 expression quantitative trait loci in whole blood. *Nature genetics* 2017; **49**(1): 139-45.
1213 57. Schmitt AD, Hu M, Jung I, et al. A Compendium of Chromatin Contact Maps Reveals
1214 Spatially Active Regions in the Human Genome. *Cell reports* 2016; **17**(8): 2042-59.
1215 58. Subramanian A, Tamayo P, Mootha VK, et al. Gene set enrichment analysis: a
1216 knowledge-based approach for interpreting genome-wide expression profiles. *Proceedings of*
1217 *the National Academy of Sciences of the United States of America* 2005; **102**(43): 15545-50.
1218 59. Habib N, Avraham-Davidi I, Basu A, et al. Massively parallel single-nucleus RNA-seq with
1219 DroNc-seq. *Nature methods* 2017; **14**(10): 955-8.
1220

Supplementary Figure 1. Manhattan and QQ plots of single variant association results per main cohort. For each cohort, Manhattan and QQ plots are shown. A) The Manhattan plot displays all associations per variant ordered according to their genomic position on the x-axis and showing the strength of the association with the –log10 transformed *P*-values on the y-axis. The y-axis is limited to enable visualization of non-*APOE* loci. B) The QQ plot displays the expected –log10 transformed *p*-values on the x-axis and the observed –log10 transformed *p*-values on the y-axis.

A

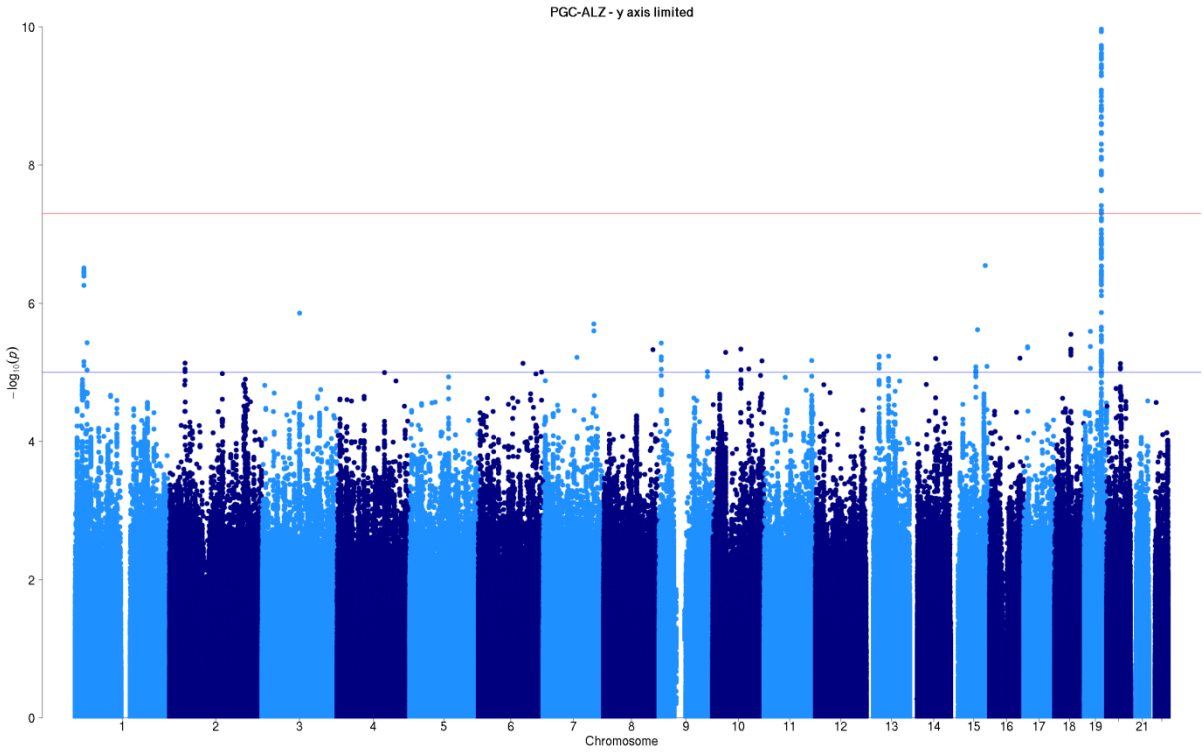

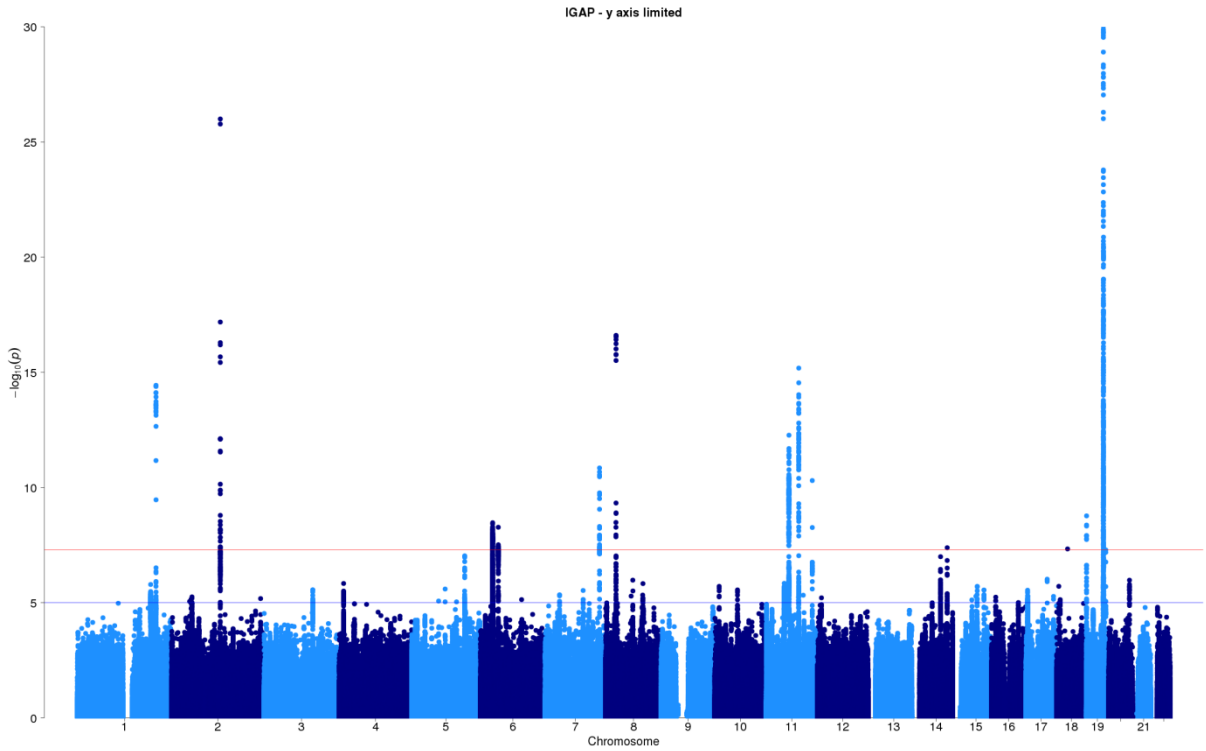

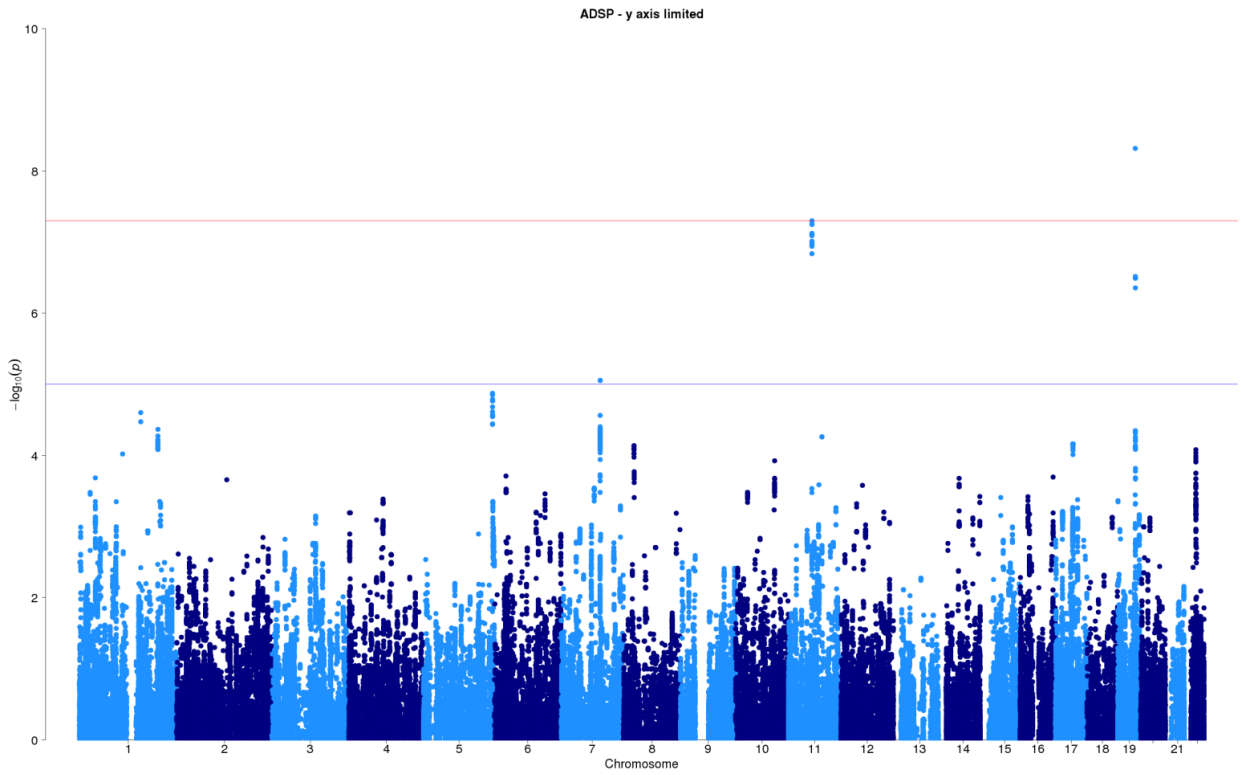
ADSP - y axis limited
$-\log_{10}(p)$
Chromosome

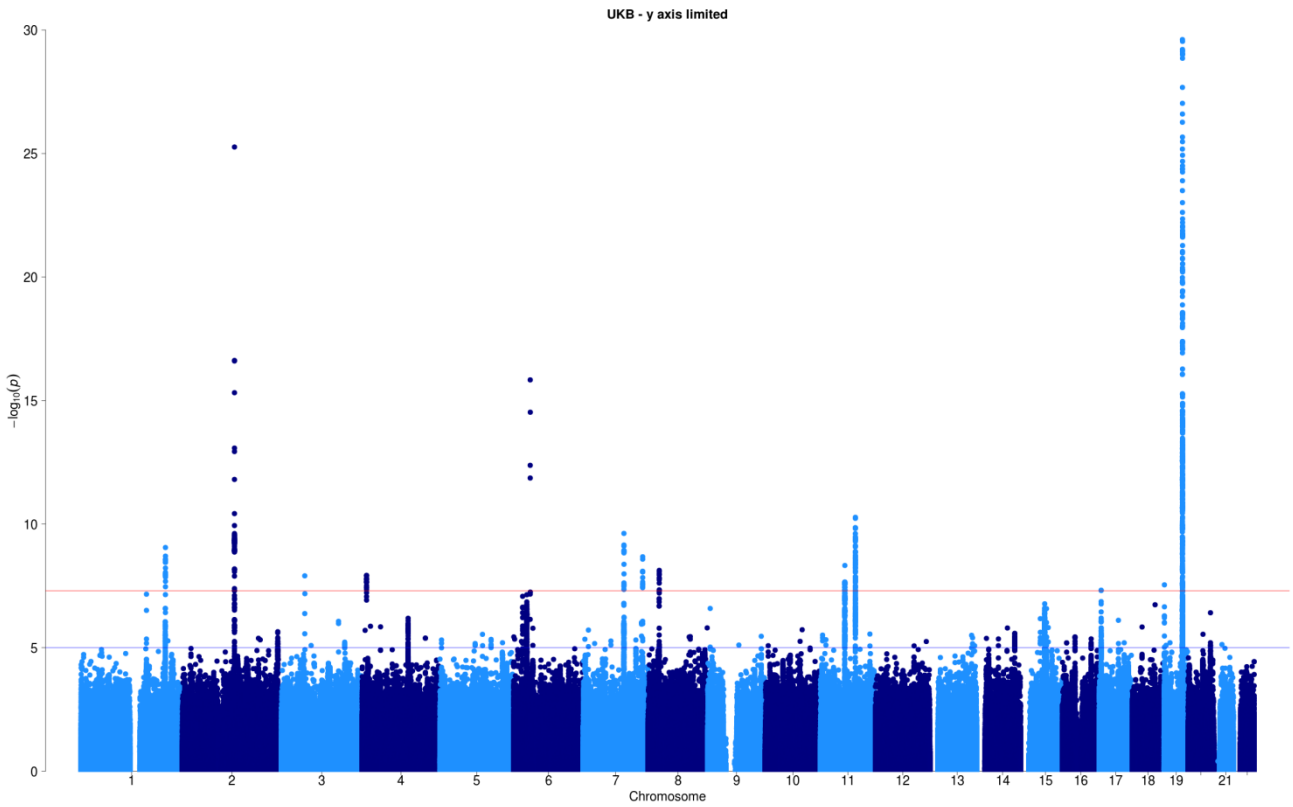
UKB - y axis limited
$-\log_{10}(p)$
Chromosome

B

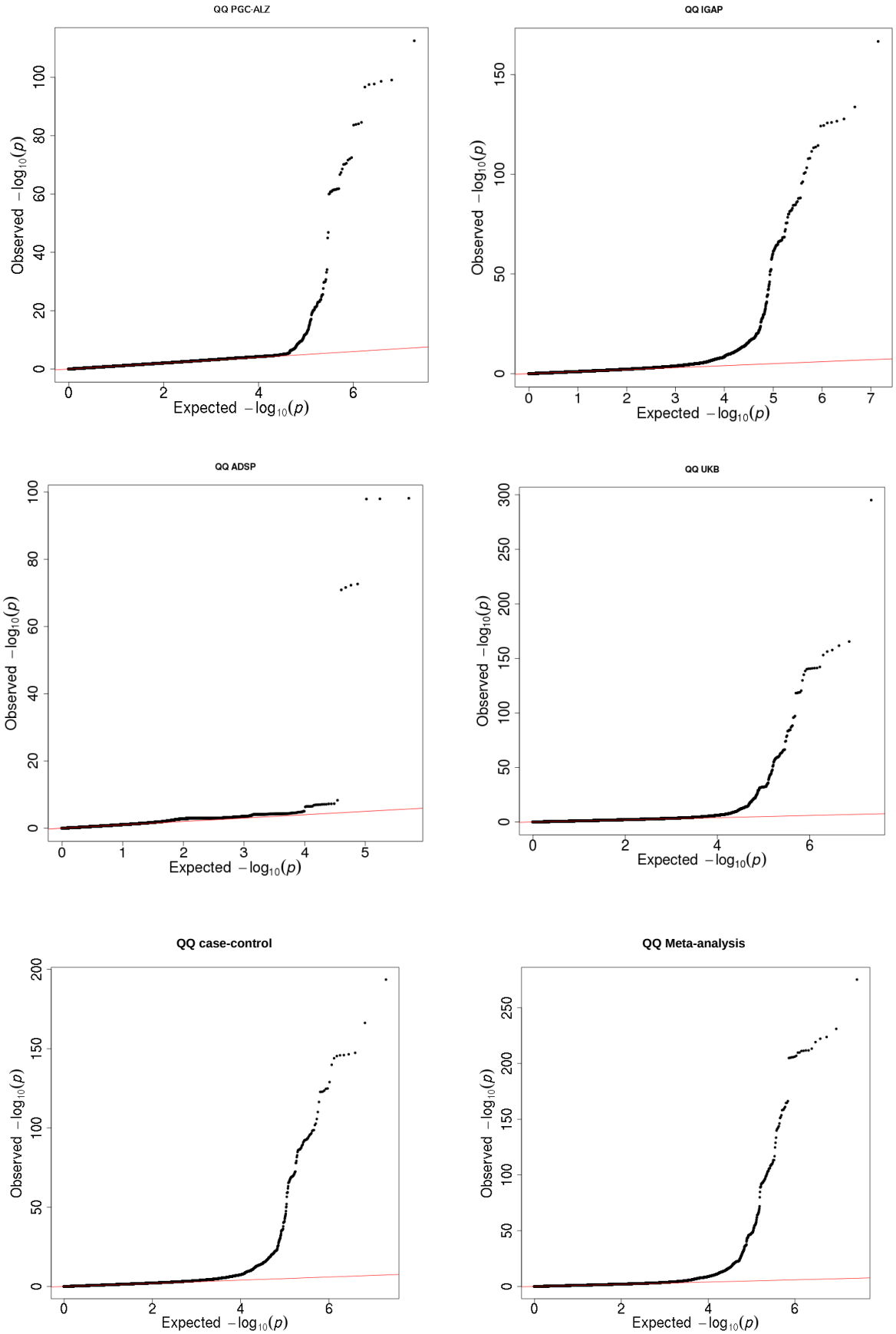
QQ PGC-ALZ
QQ IGAP
QQ ADSP
QQ UKB
QQ case-control
QQ Meta-analysis
Observed $-\log_{10}(p)$
Expected $-\log_{10}(p)$

Supplementary Figure 2. Regional plot for the 29 significant loci of the meta-analysis. Every point represents a SNP, which are colour-coded based on the highest r2 to one of the most significant SNPs, if greater or equal to r2 of 0.6. Other SNPs are coloured in grey.

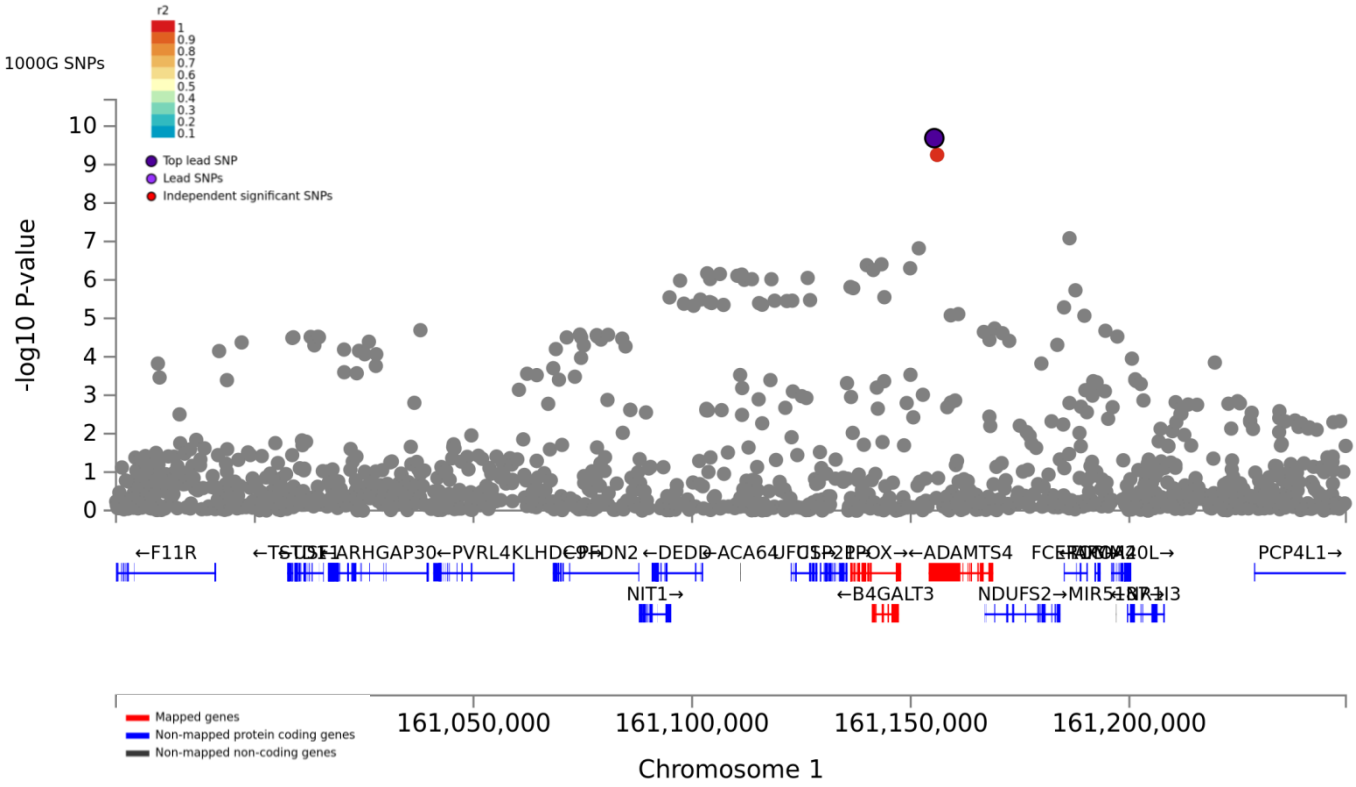

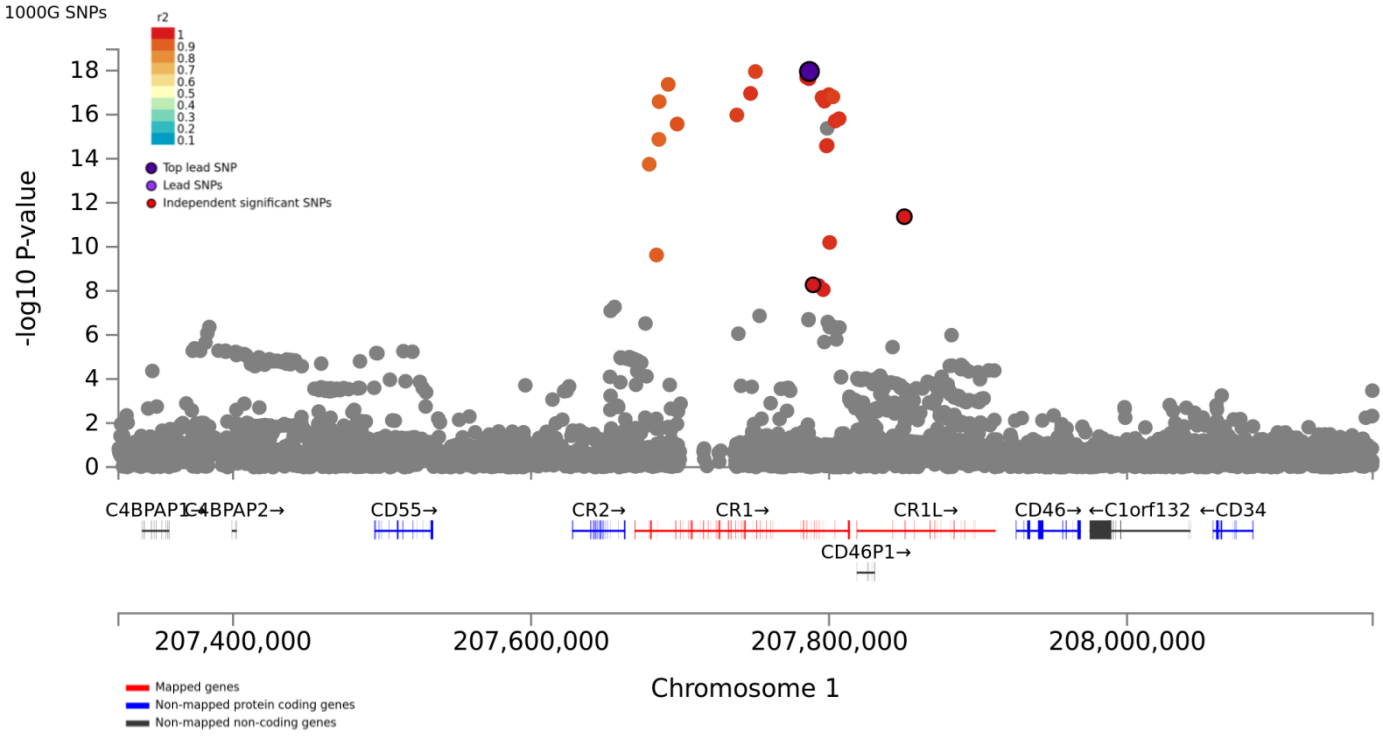

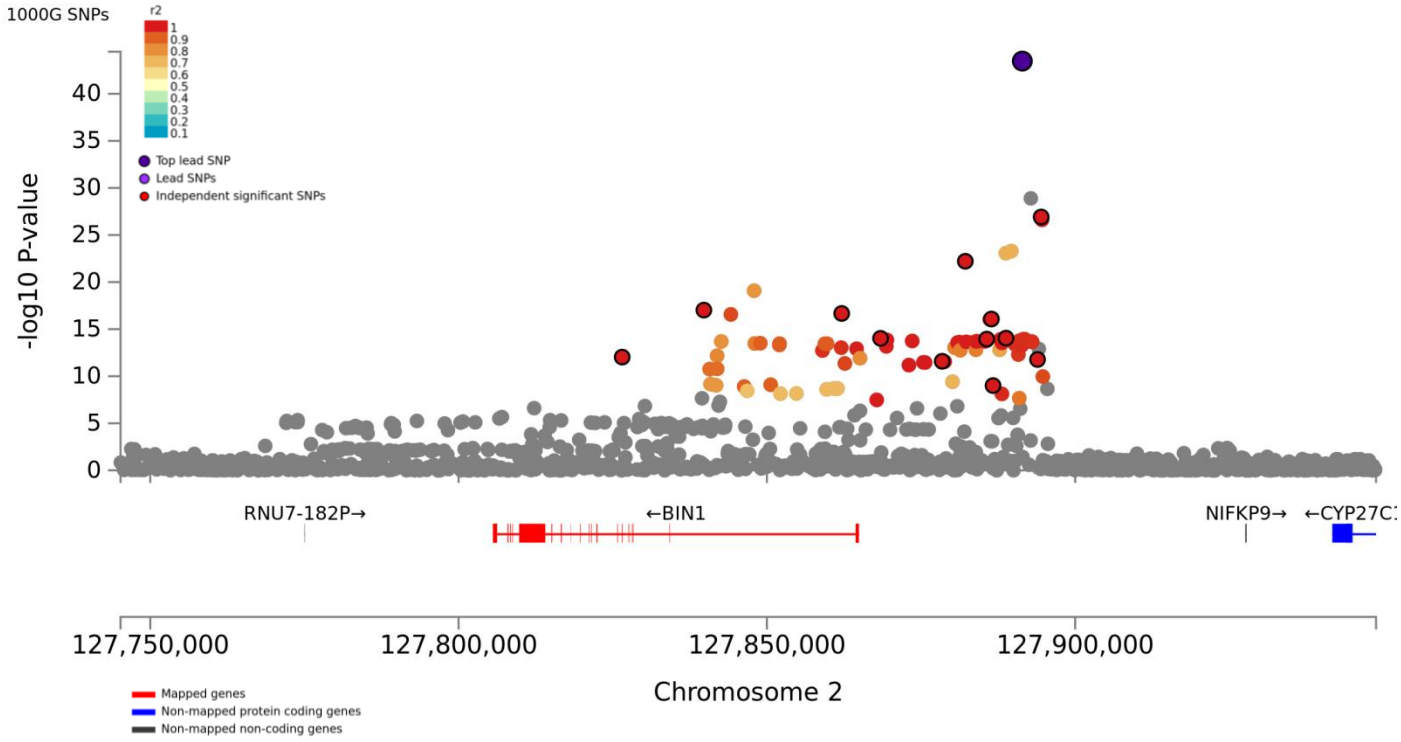
1000G SNPs
r2
1
0.9
0.8
0.7
0.6
0.5
0.4
0.3
0.2
0.1
Top lead SNP
Lead SNPs
Independent significant SNPs
-log10 P-value
40
35
30
25
20
15
10
5
0
RNU7-182P→
←BIN1
NIFKP9→
←CYP27C1
127,750,000
127,800,000
127,850,000
127,900,000
Chromosome 2
Mapped genes
Non-mapped protein coding genes
Non-mapped non-coding genes

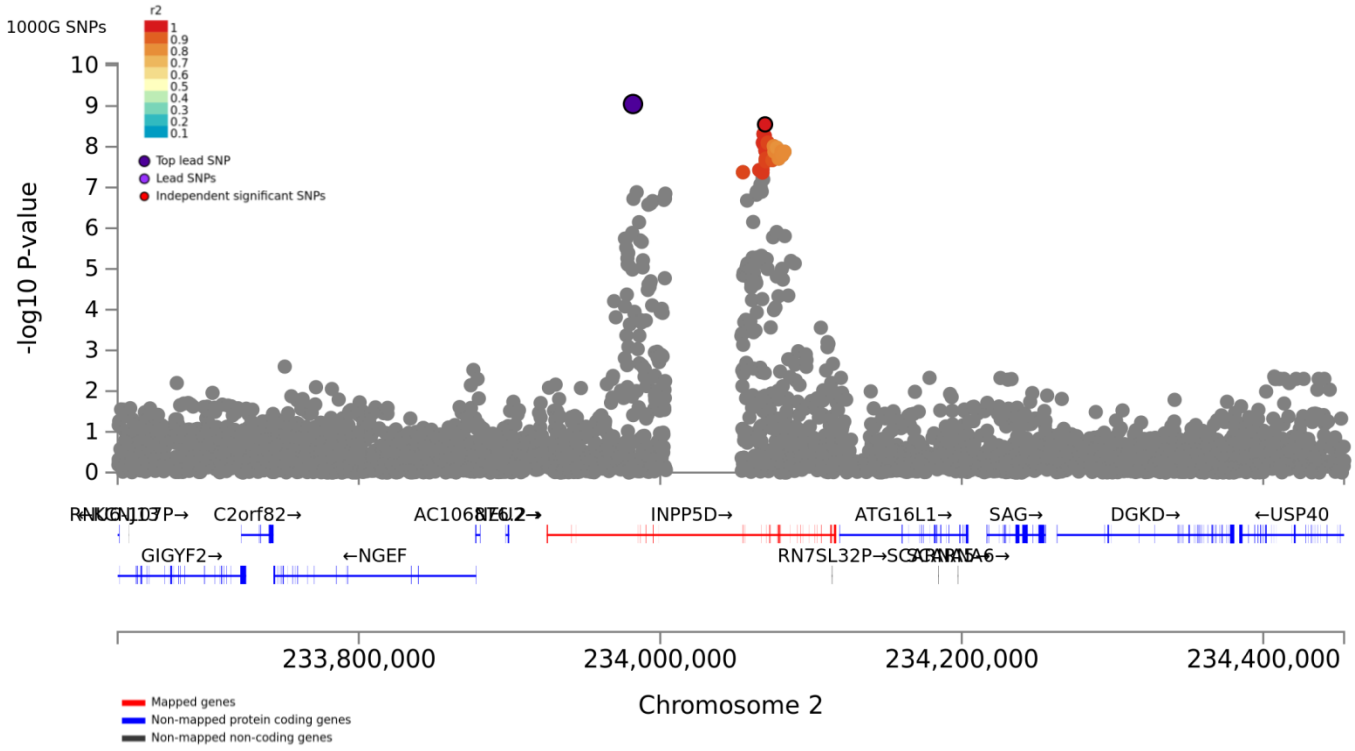
1000G SNPs
r2
1
0.9
0.8
0.7
0.6
0.5
0.4
0.3
0.2
0.1
Top lead SNP
Lead SNPs
Independent significant SNPs
-log10 P-value
10
9
8
7
6
5
4
3
2
1
0
C2orf82→
INPP5D→
ATG16L1→
SAG→
DGKD→
←USP40
GIGYF2→
←NGEF
233,800,000
234,000,000
234,200,000
234,400,000
Chromosome 2
Mapped genes
Non-mapped protein coding genes
Non-mapped non-coding genes

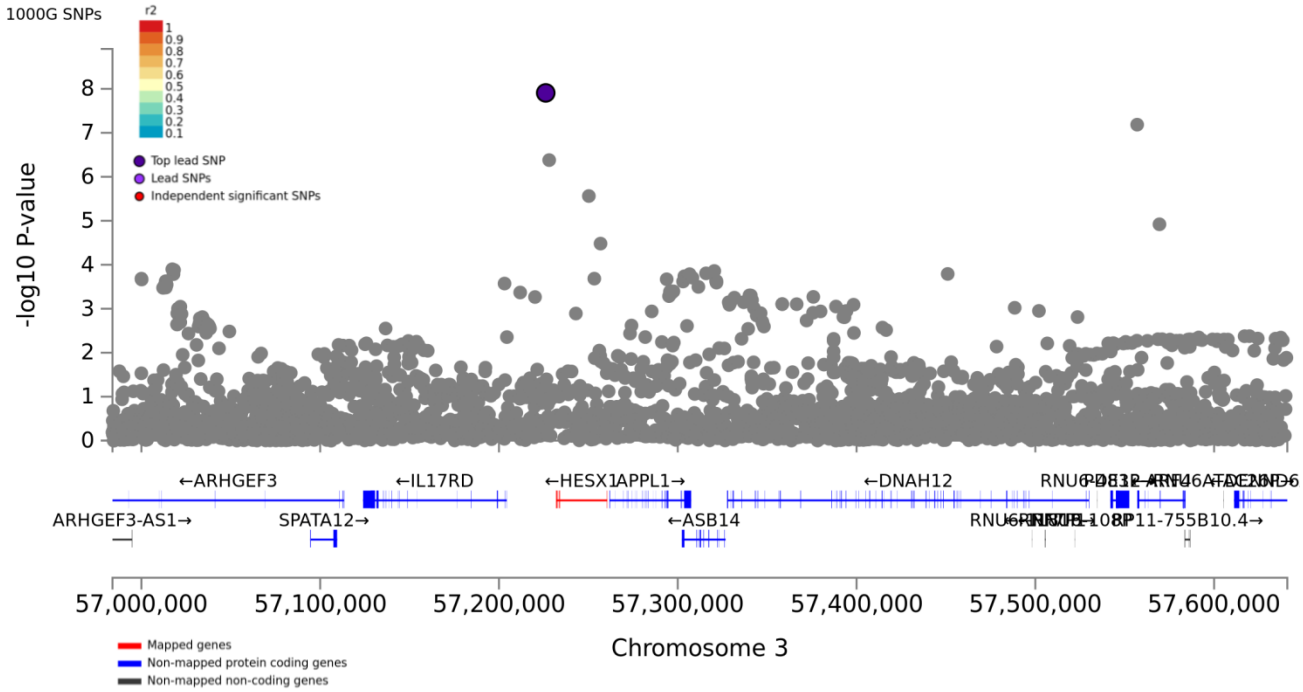
1000G SNPs
r2
1
0.9
0.8
0.7
0.6
0.5
0.4
0.3
0.2
0.1
Top lead SNP
Lead SNPs
Independent significant SNPs
-log10 P-value
0
1
2
3
4
5
6
7
8
←ARHGEF3
←IL17RD
←HESX1
APPL1→
←DNAH12
ARHGEF3-AS1→
SPATA12→
←ASB14
RP11-755B10.4→
57,000,000
57,100,000
57,200,000
57,300,000
57,400,000
57,500,000
57,600,000
Chromosome 3
Mapped genes
Non-mapped protein coding genes
Non-mapped non-coding genes

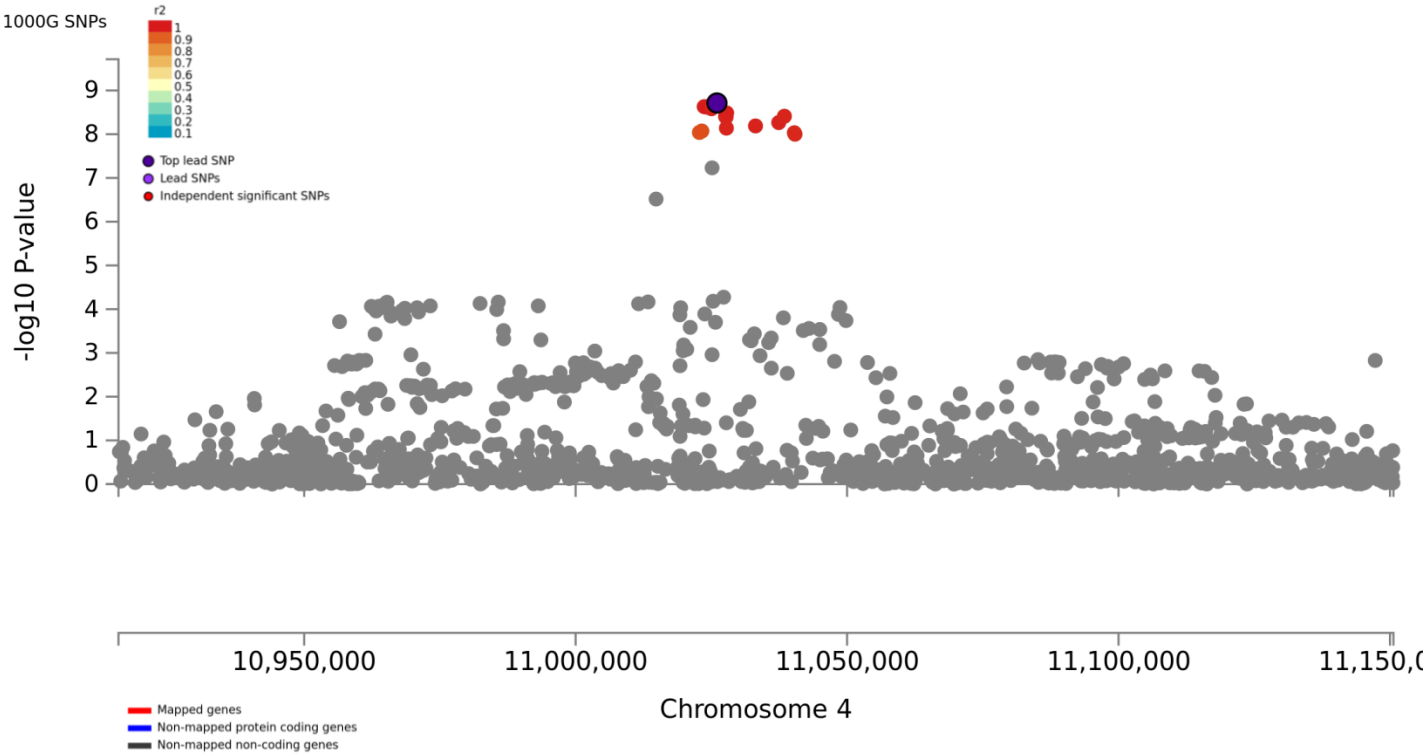
1000G SNPs
r2
1
0.9
0.8
0.7
0.6
0.5
0.4
0.3
0.2
0.1
Top lead SNP
Lead SNPs
Independent significant SNPs
-log10 P-value
0
1
2
3
4
5
6
7
8
9
10,950,000
11,000,000
11,050,000
11,100,000
Chromosome 4
Mapped genes
Non-mapped protein coding genes
Non-mapped non-coding genes

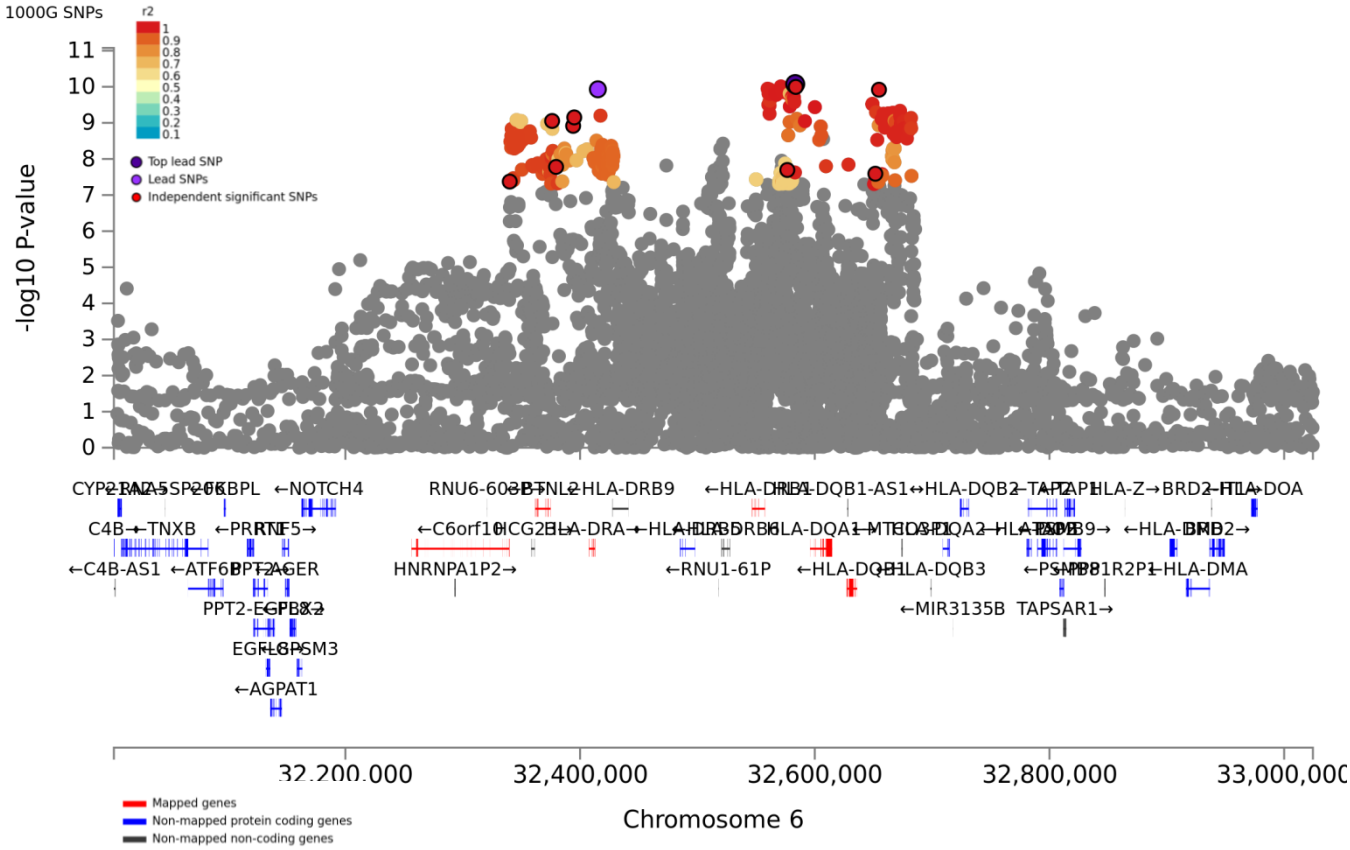
1000G SNPs
r2
Top lead SNP
Lead SNPs
Independent significant SNPs
-log10 P-value
Chromosome 6
Mapped genes
Non-mapped protein coding genes
Non-mapped non-coding genes

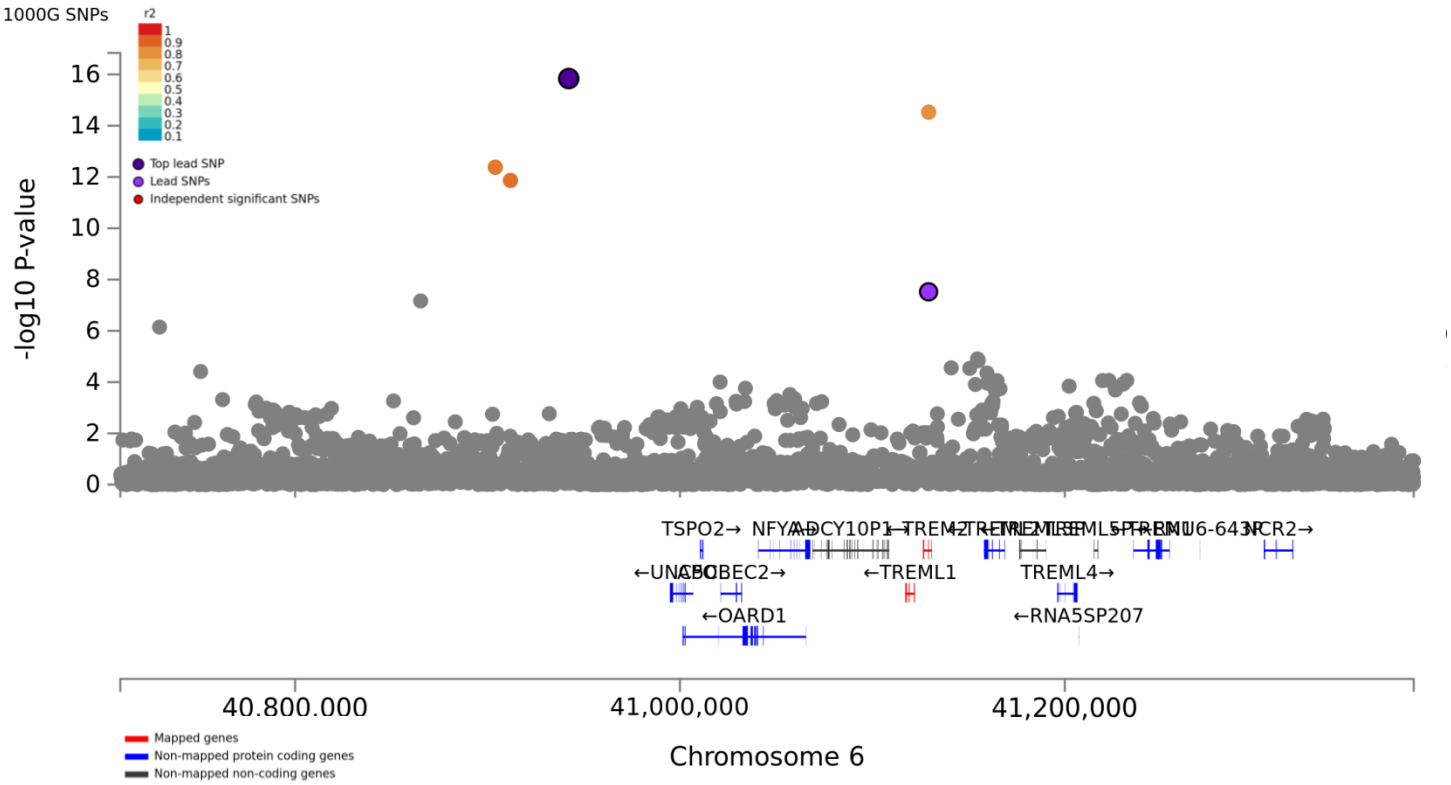
1000G SNPs
r2
Top lead SNP
Lead SNPs
Independent significant SNPs
-log10 P-value
Chromosome 6
Mapped genes
Non-mapped protein coding genes
Non-mapped non-coding genes

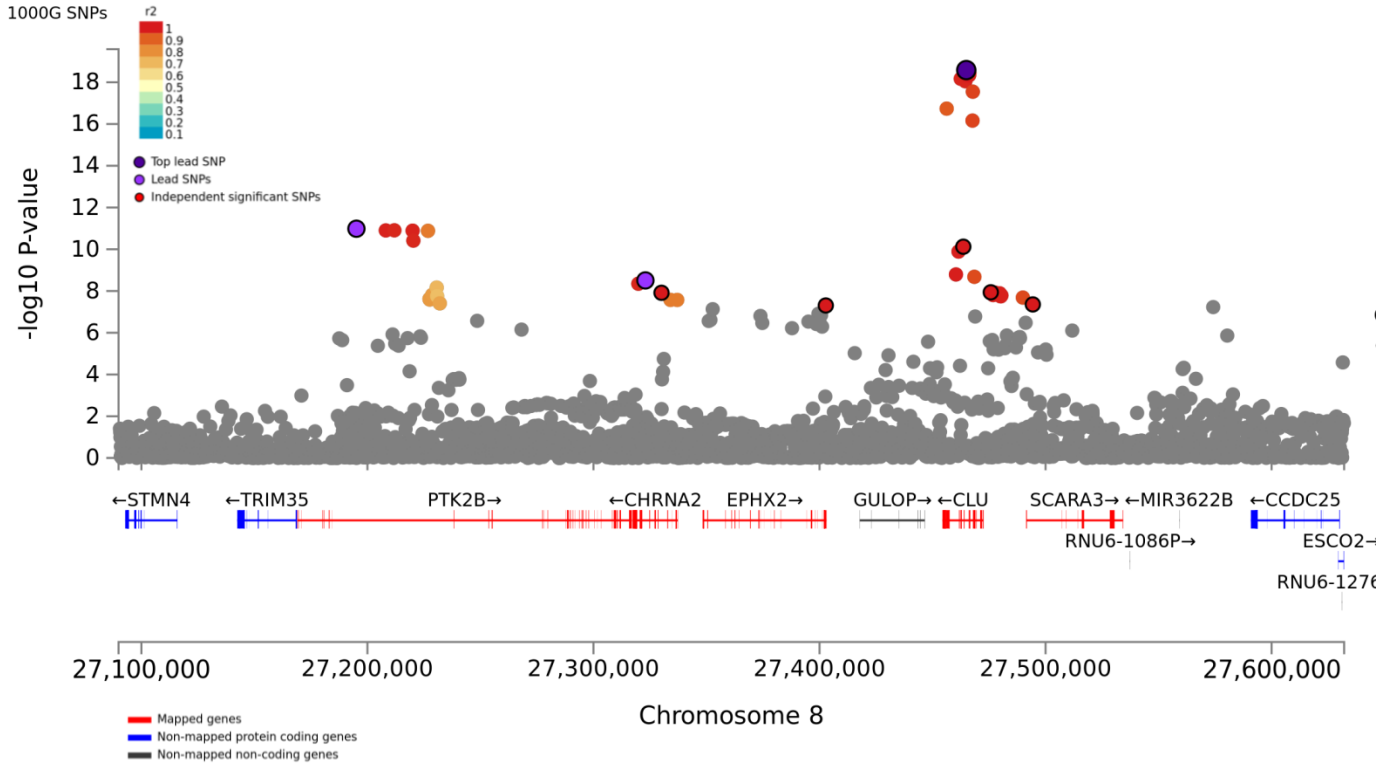
1000G SNPs
r2
1
0.9
0.8
0.7
0.6
0.5
0.4
0.3
0.2
0.1
Top lead SNP
Lead SNPs
Independent significant SNPs
-log10 P-value
0
2
4
6
8
10
12
14
16
18
←STMN4
←TRIM35
PTK2B→
←CHRNA2
EPHX2→
GULOP→
←CLU
SCARA3→
←MIR3622B
←CCDC25
RNU6-1086P→
ESCO2→
27,100,000
27,200,000
27,300,000
27,400,000
27,500,000
27,600,000
Chromosome 8
Mapped genes
Non-mapped protein coding genes
Non-mapped non-coding genes

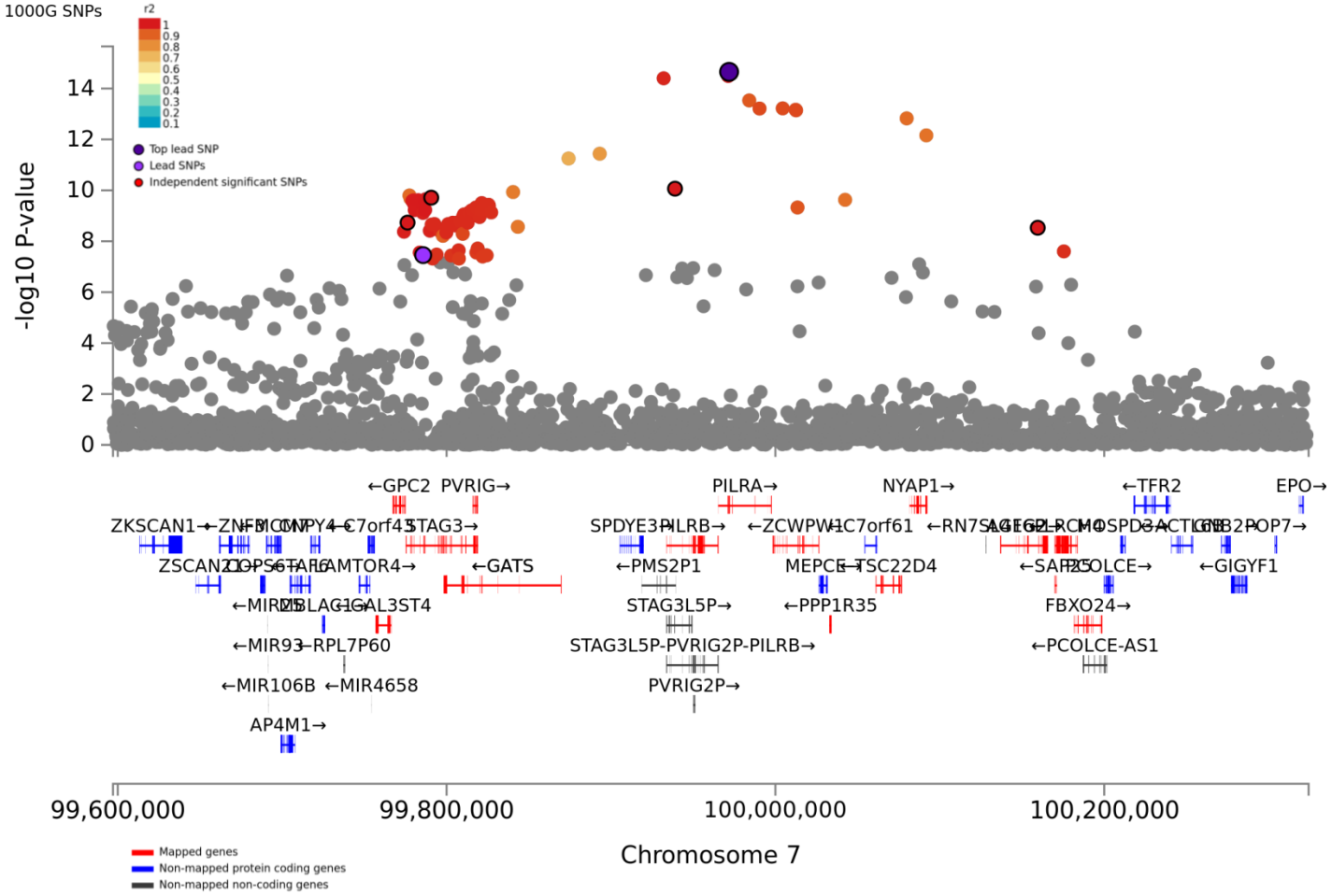
1000G SNPs
r2
1
0.9
0.8
0.7
0.6
0.5
0.4
0.3
0.2
0.1
Top lead SNP
Lead SNPs
Independent significant SNPs
-log10 P-value
0
2
4
6
8
10
12
14
←GPC2
PVRIG→
PILRA→
NYAP1→
←TFR2
EPO→
ZKSCAN1→
STAG3→
SPDYE3
PILRB→
←ZCWPW1
C7orf61
POP7→
←GATS
←PMS2P1
MEPCE
TSC22D4
←GIGYF1
STAG3L5P→
←PPP1R35
FBXO24→
←MIR93
RPL7P60
STAG3L5P-PVRIG2P-PILRB→
←PCOLCE-AS1
←MIR106B
←MIR4658
PVRIG2P→
AP4M1→
99,600,000
99,800,000
100,000,000
100,200,000
Chromosome 7
Mapped genes
Non-mapped protein coding genes
Non-mapped non-coding genes

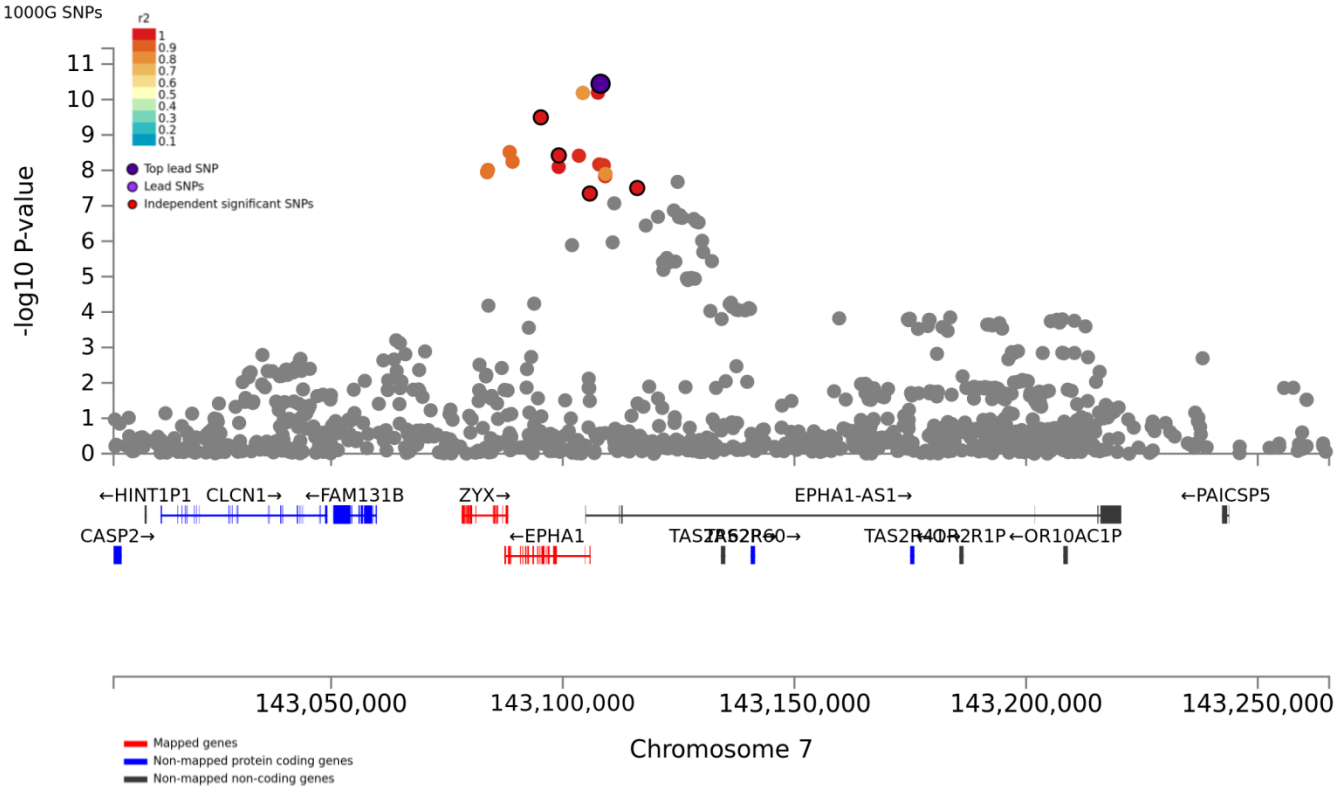
1000G SNPs
r2
1
0.9
0.8
0.7
0.6
0.5
0.4
0.3
0.2
0.1
Top lead SNP
Lead SNPs
Independent significant SNPs
-log10 P-value
11
10
9
8
7
6
5
4
3
2
1
0
←HINT1P1
CLCN1→
←FAM131B
ZYX→
EPHA1-AS1→
←PAICSP5
CASP2→
←EPHA1
TAS2R60→
TAS2R40
OR2R1P
←OR10AC1P
143,050,000
143,100,000
143,150,000
143,200,000
143,250,000
Chromosome 7
Mapped genes
Non-mapped protein coding genes
Non-mapped non-coding genes

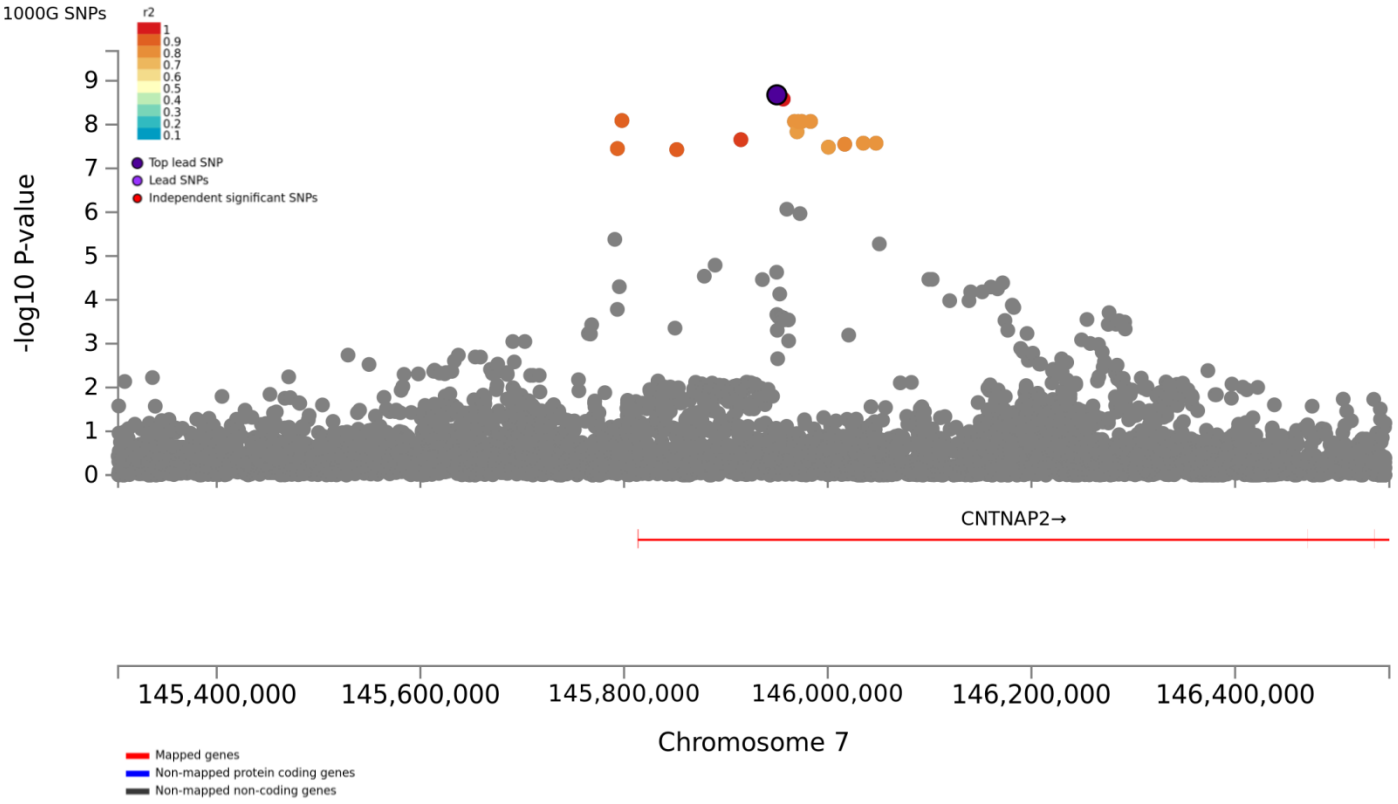
1000G SNPs
r2
1
0.9
0.8
0.7
0.6
0.5
0.4
0.3
0.2
0.1
Top lead SNP
Lead SNPs
Independent significant SNPs
-log10 P-value
9
8
7
6
5
4
3
2
1
0
CNTNAP2→
145,400,000
145,600,000
145,800,000
146,000,000
146,200,000
146,400,000
Chromosome 7
Mapped genes
Non-mapped protein coding genes
Non-mapped non-coding genes

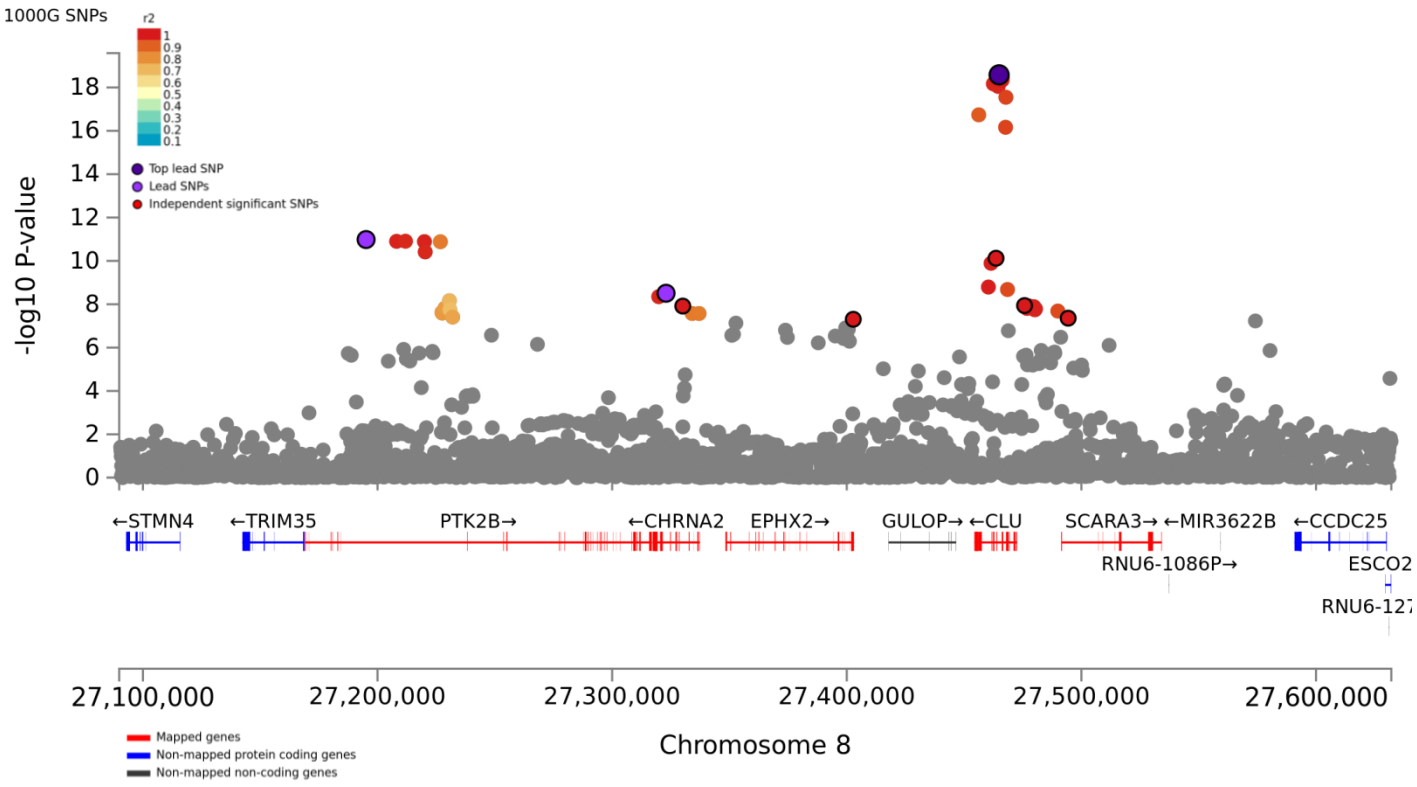
1000G SNPs
r2
1
0.9
0.8
0.7
0.6
0.5
0.4
0.3
0.2
0.1
Top lead SNP
Lead SNPs
Independent significant SNPs
-log10 P-value
18
16
14
12
10
8
6
4
2
0
←STMN4
←TRIM35
PTK2B→
←CHRNA2
EPHX2→
GULOP→
←CLU
SCARA3→
←MIR3622B
←CCDC25
RNU6-1086P→
ESCO2
27,100,000
27,200,000
27,300,000
27,400,000
27,500,000
27,600,000
Chromosome 8
Mapped genes
Non-mapped protein coding genes
Non-mapped non-coding genes

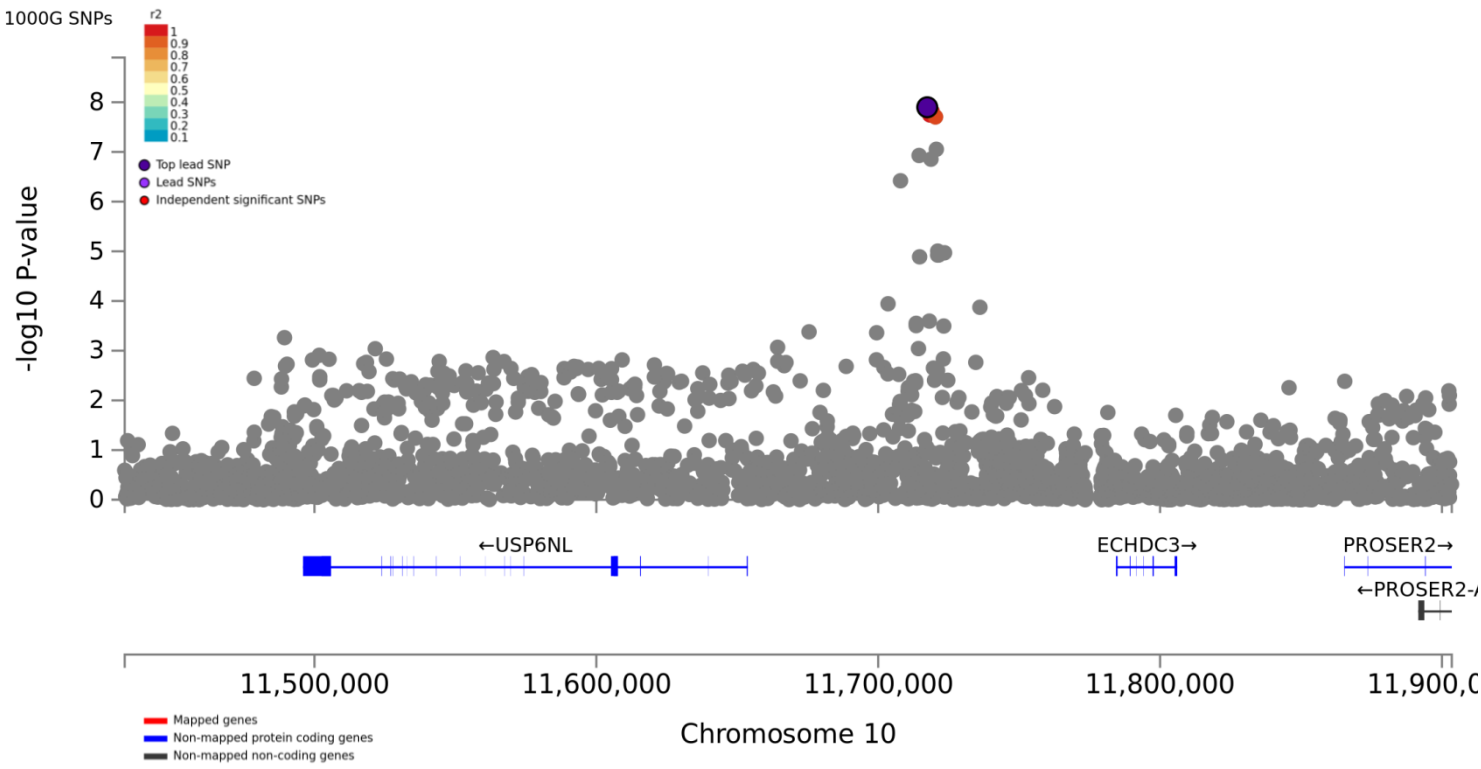
1000G SNPs
r2
1
0.9
0.8
0.7
0.6
0.5
0.4
0.3
0.2
0.1
Top lead SNP
Lead SNPs
Independent significant SNPs
-log10 P-value
8
7
6
5
4
3
2
1
0
←USP6NL
ECHDC3→
PROSER2→
11,500,000
11,600,000
11,700,000
11,800,000
Chromosome 10
Mapped genes
Non-mapped protein coding genes
Non-mapped non-coding genes

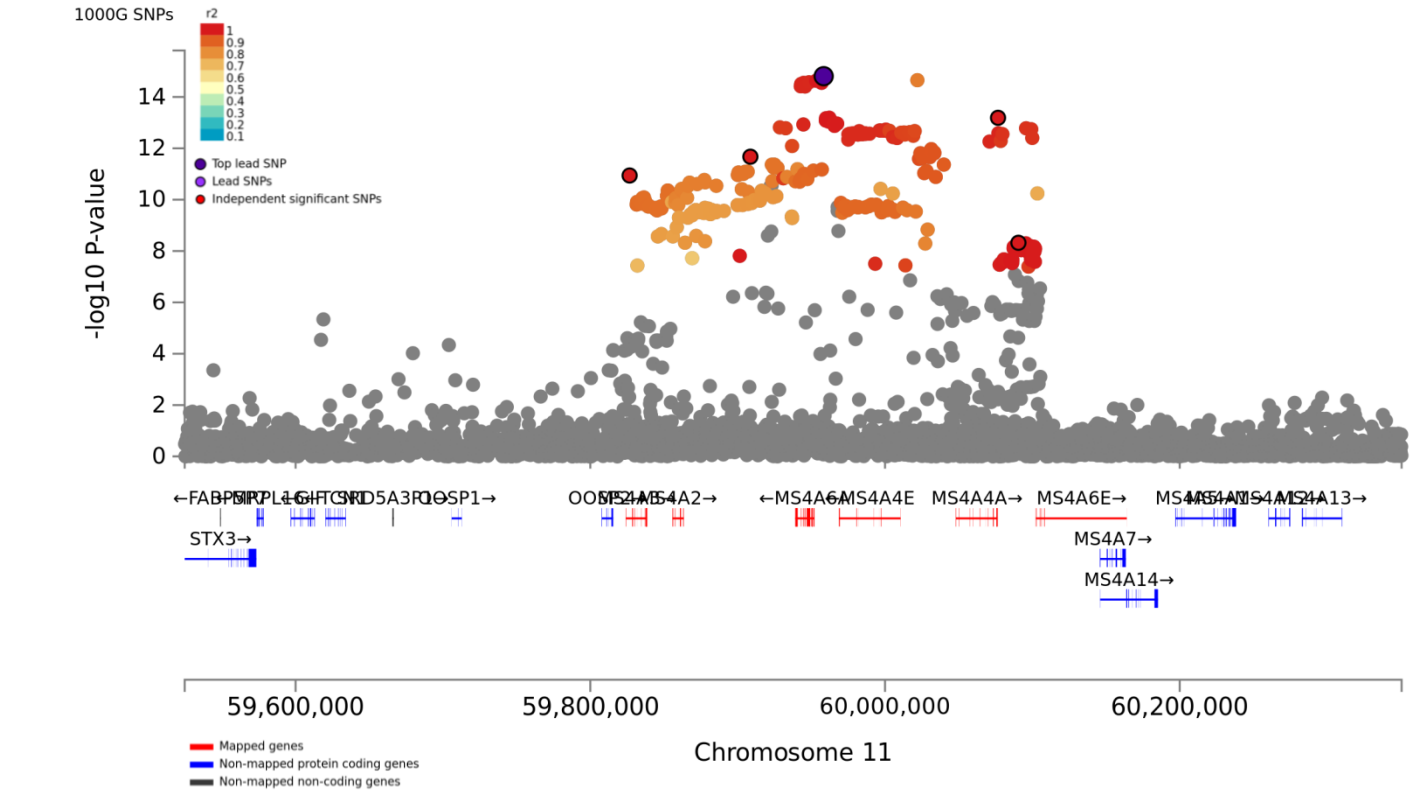
1000G SNPs
r2
1
0.9
0.8
0.7
0.6
0.5
0.4
0.3
0.2
0.1
Top lead SNP
Lead SNPs
Independent significant SNPs
-log10 P-value
14
12
10
8
6
4
2
0
←MS4A6A
MS4A4E
MS4A4A→
MS4A6E→
STX3→
MS4A7→
MS4A14→
59,600,000
59,800,000
60,000,000
60,200,000
Chromosome 11
Mapped genes
Non-mapped protein coding genes
Non-mapped non-coding genes

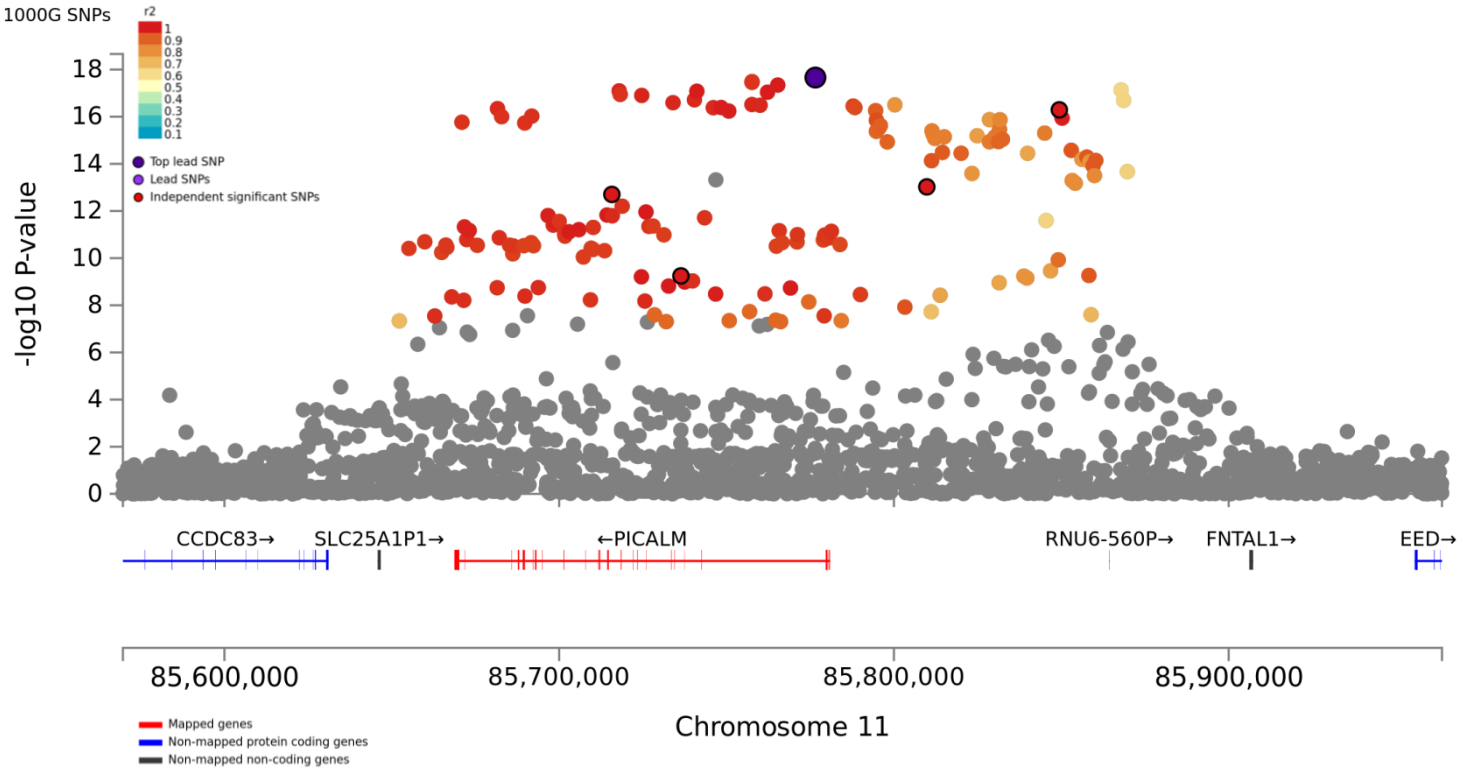
1000G SNPs
r2
1
0.9
0.8
0.7
0.6
0.5
0.4
0.3
0.2
0.1
Top lead SNP
Lead SNPs
Independent significant SNPs
-log10 P-value
18
16
14
12
10
8
6
4
2
0
CCDC83→
SLC25A1P1→
←PICALM
RNU6-560P→
FNTAL1→
EED→
85,600,000
85,700,000
85,800,000
85,900,000
Chromosome 11
Mapped genes
Non-mapped protein coding genes
Non-mapped non-coding genes

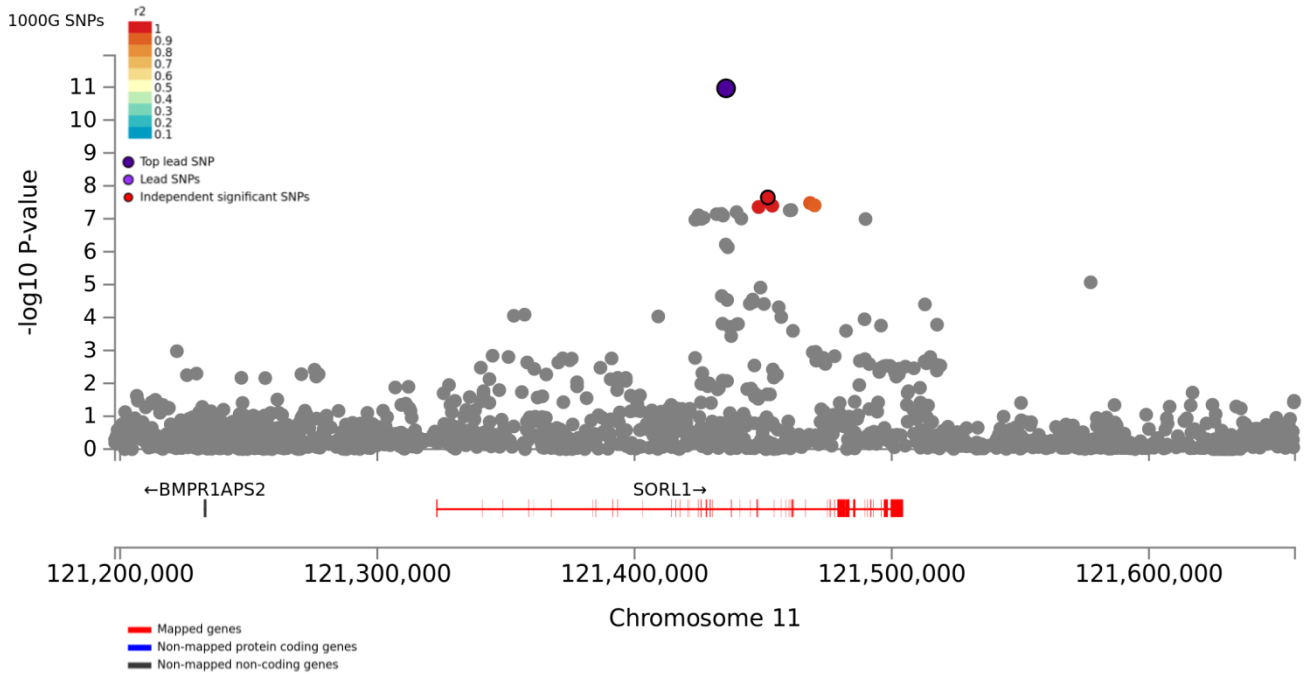
1000G SNPs
r2
1
0.9
0.8
0.7
0.6
0.5
0.4
0.3
0.2
0.1
Top lead SNP
Lead SNPs
Independent significant SNPs
-log10 P-value
←BMPR1APS2
SORL1→
121,200,000
121,300,000
121,400,000
121,500,000
121,600,000
Chromosome 11
Mapped genes
Non-mapped protein coding genes
Non-mapped non-coding genes

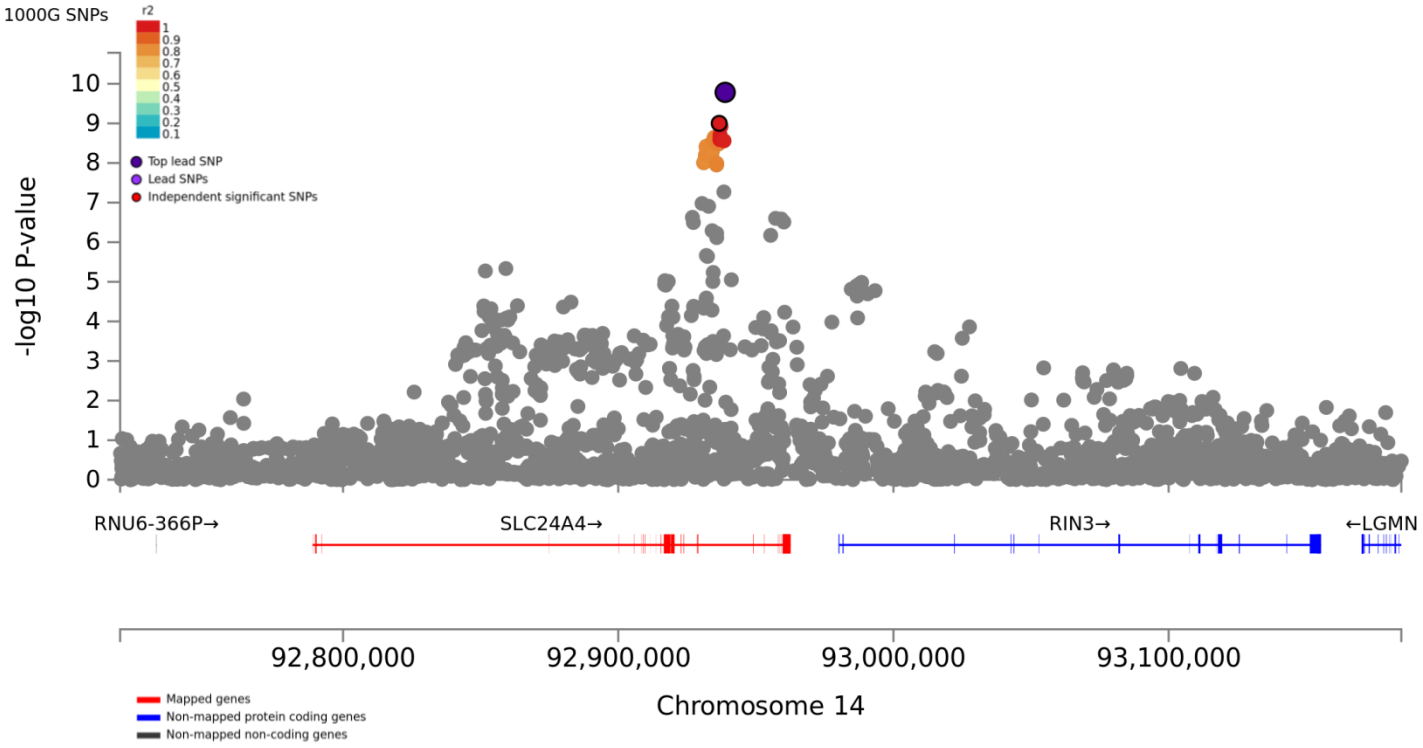
1000G SNPs
r2
1
0.9
0.8
0.7
0.6
0.5
0.4
0.3
0.2
0.1
Top lead SNP
Lead SNPs
Independent significant SNPs
-log10 P-value
RNU6-366P→
SLC24A4→
RIN3→
←LGMN
92,800,000
92,900,000
93,000,000
93,100,000
Chromosome 14
Mapped genes
Non-mapped protein coding genes
Non-mapped non-coding genes

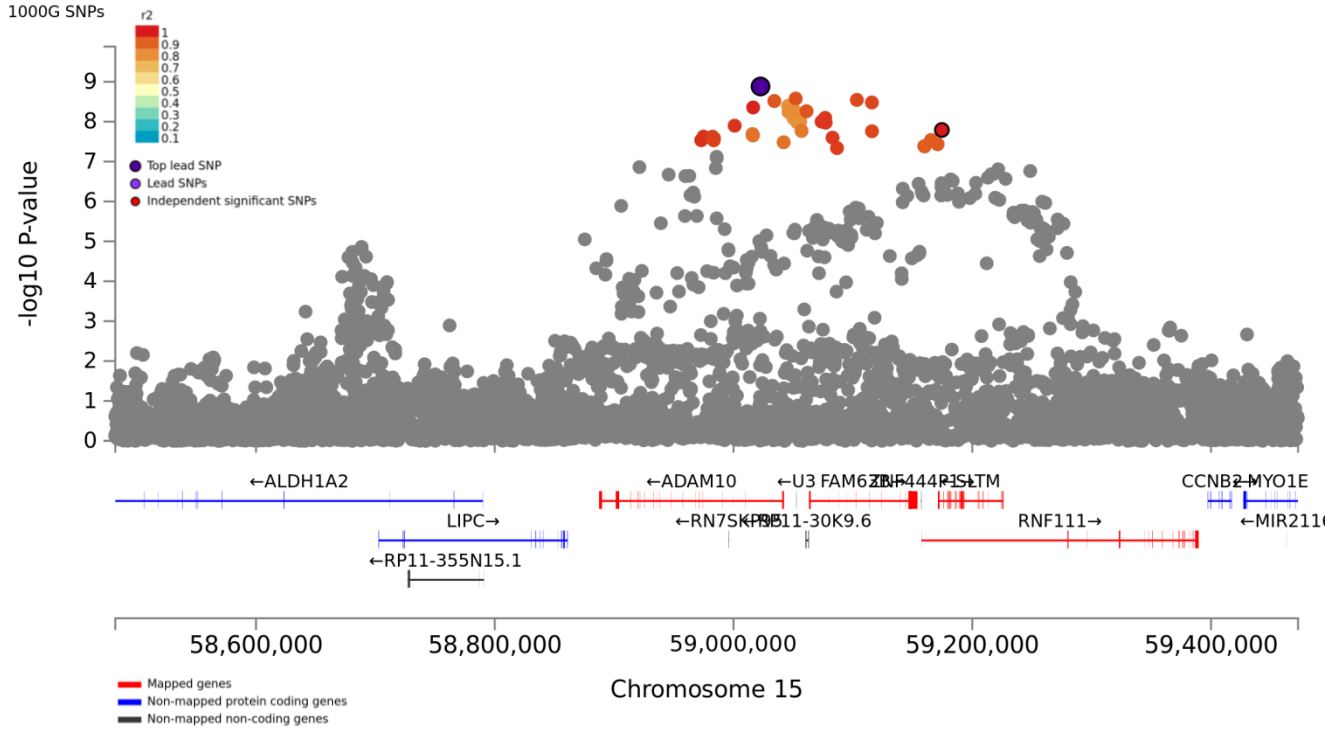
1000G SNPs
r2
Top lead SNP
Lead SNPs
Independent significant SNPs
-log10 P-value
←ALDH1A2
←ADAM10
←U3
LIPC→
←RN7SK
←RP11-30K9.6
RNF111→
←RP11-355N15.1
CCNB2
←MYO1E
58,600,000
58,800,000
59,000,000
59,200,000
59,400,000
Chromosome 15
Mapped genes
Non-mapped protein coding genes
Non-mapped non-coding genes

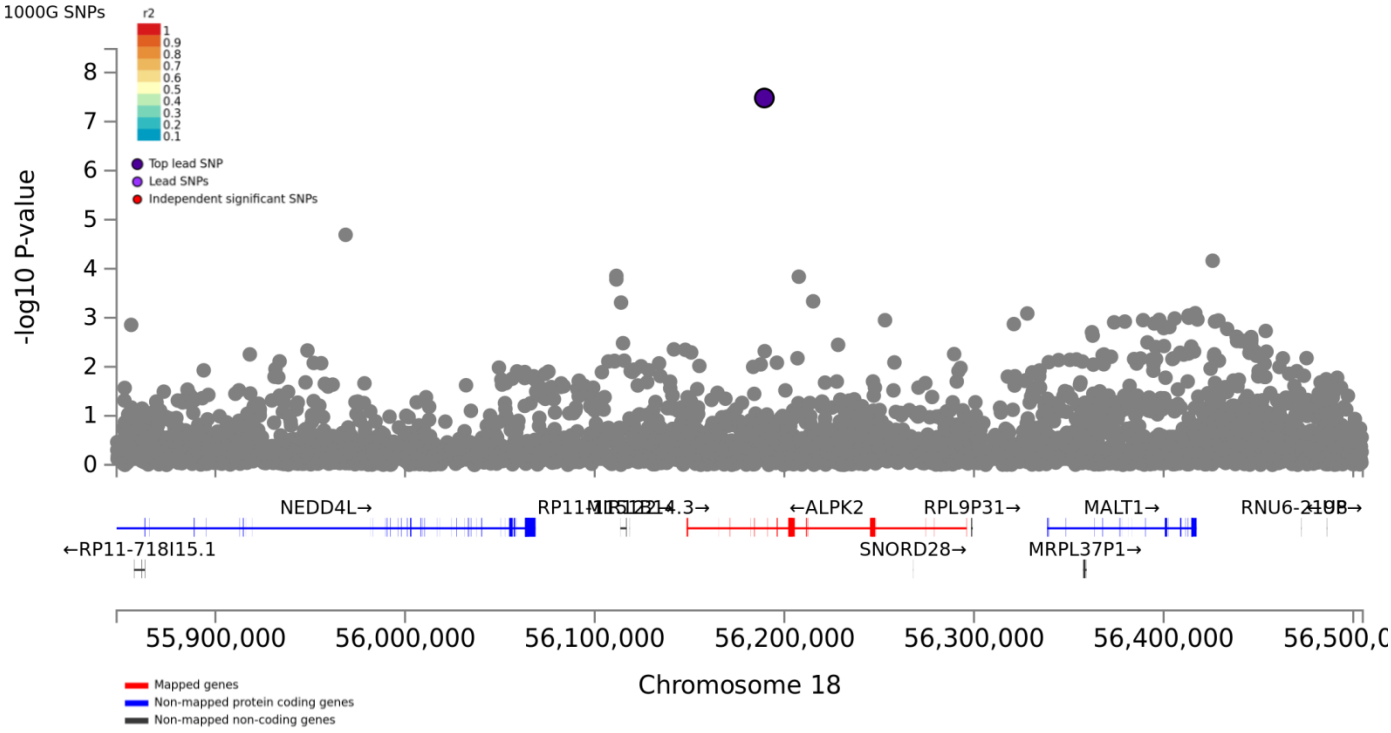
1000G SNPs
r2
Top lead SNP
Lead SNPs
Independent significant SNPs
-log10 P-value
NEDD4L→
←ALPK2
RPL9P31→
MALT1→
←RP11-718I15.1
SNORD28→
MRPL37P1→
55,900,000
56,000,000
56,100,000
56,200,000
56,300,000
56,400,000
Chromosome 18
Mapped genes
Non-mapped protein coding genes
Non-mapped non-coding genes

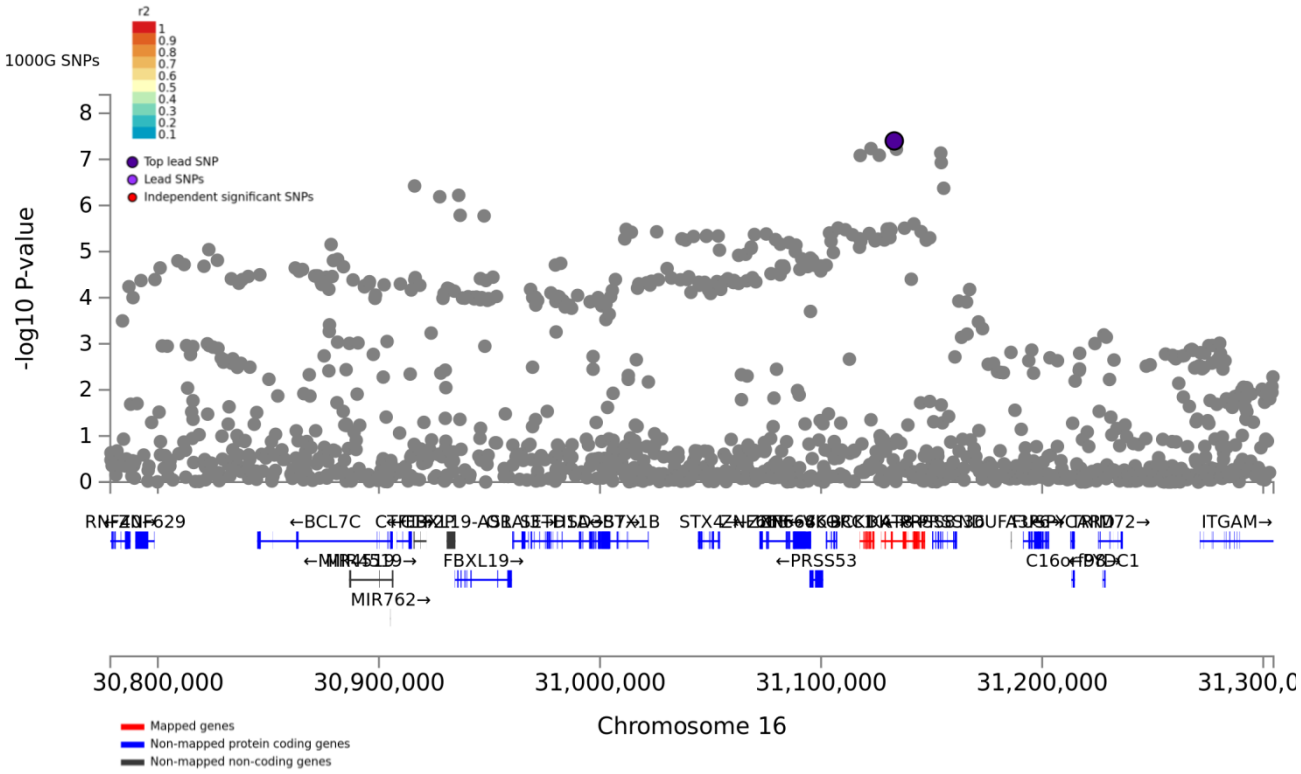
1000G SNPs
r2
1
0.9
0.8
0.7
0.6
0.5
0.4
0.3
0.2
0.1
Top lead SNP
Lead SNPs
Independent significant SNPs
-log10 P-value
0
1
2
3
4
5
6
7
8
←BCL7C
FBXL19→
←PRSS53
MIR762→
ITGAM→
30,800,000
30,900,000
31,000,000
31,100,000
31,200,000
Chromosome 16
Mapped genes
Non-mapped protein coding genes
Non-mapped non-coding genes

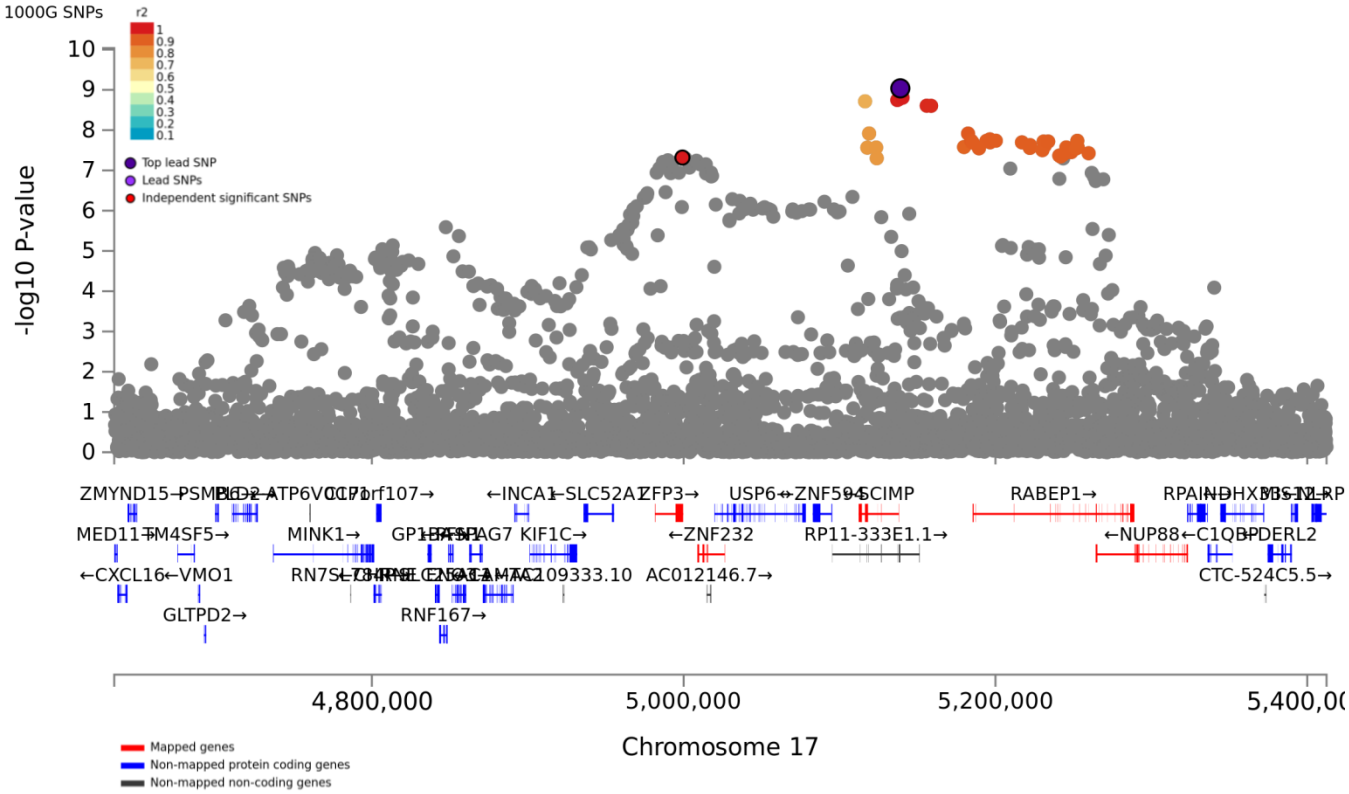
1000G SNPs
r2
1
0.9
0.8
0.7
0.6
0.5
0.4
0.3
0.2
0.1
Top lead SNP
Lead SNPs
Independent significant SNPs
-log10 P-value
0
1
2
3
4
5
6
7
8
9
10
←INCA1
USP6
RABEP1→
MINK1→
KIF1C→
←ZNF232
RP11-333E1.1→
←NUP88
←CXCL16
←VMO1
AC012146.7→
CTC-524C5.5→
GLTPD2→
RNF167→
4,800,000
5,000,000
5,200,000
Chromosome 17
Mapped genes
Non-mapped protein coding genes
Non-mapped non-coding genes

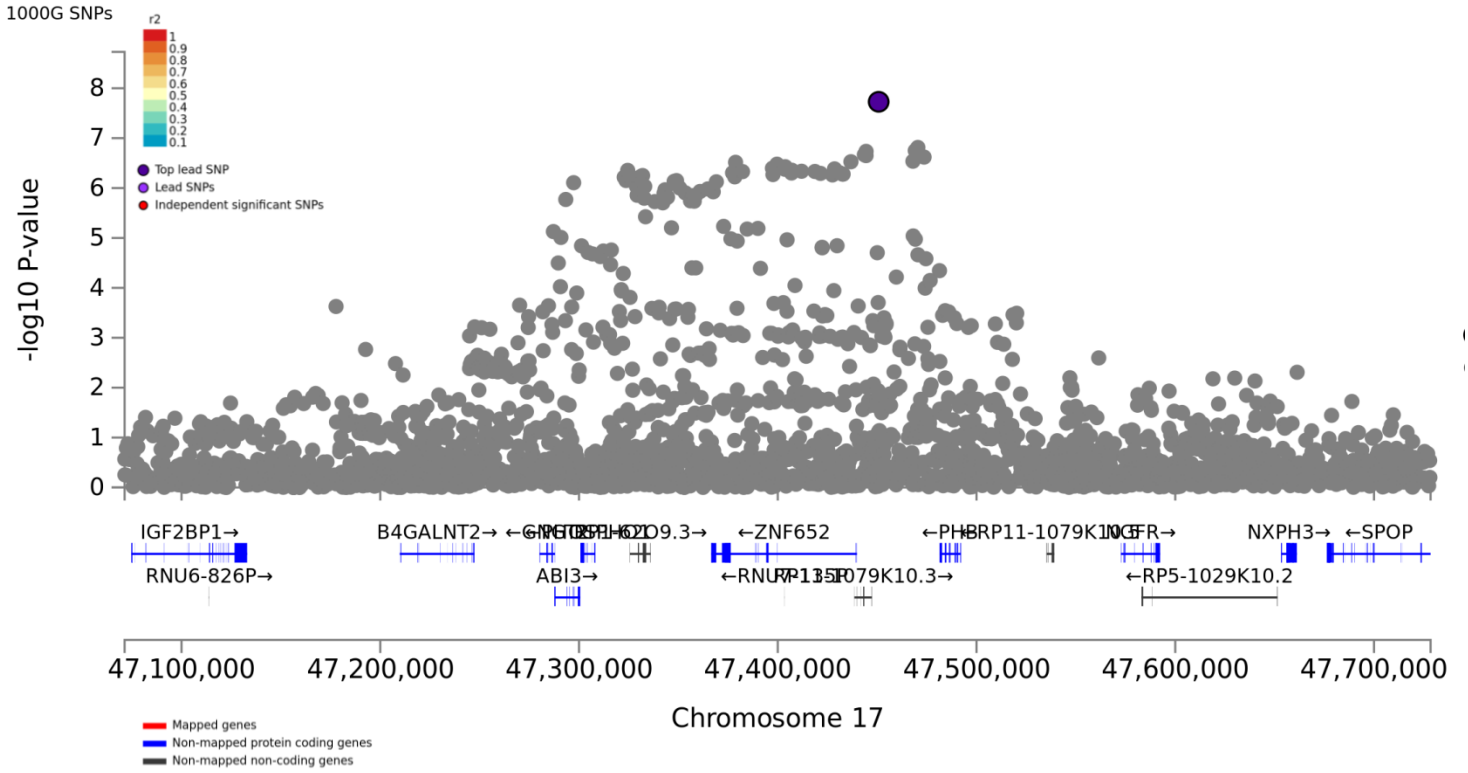
1000G SNPs
r2
1
0.9
0.8
0.7
0.6
0.5
0.4
0.3
0.2
0.1
Top lead SNP
Lead SNPs
Independent significant SNPs
-log10 P-value
0
1
2
3
4
5
6
7
8
IGF2BP1→
RNU6-826P→
B4GALNT2→
ABI3→
←ZNF652
←RP5-1029K10.2
NXPH3→
←SPOP
47,100,000
47,200,000
47,300,000
47,400,000
47,500,000
47,600,000
47,700,000
Chromosome 17
Mapped genes
Non-mapped protein coding genes
Non-mapped non-coding genes

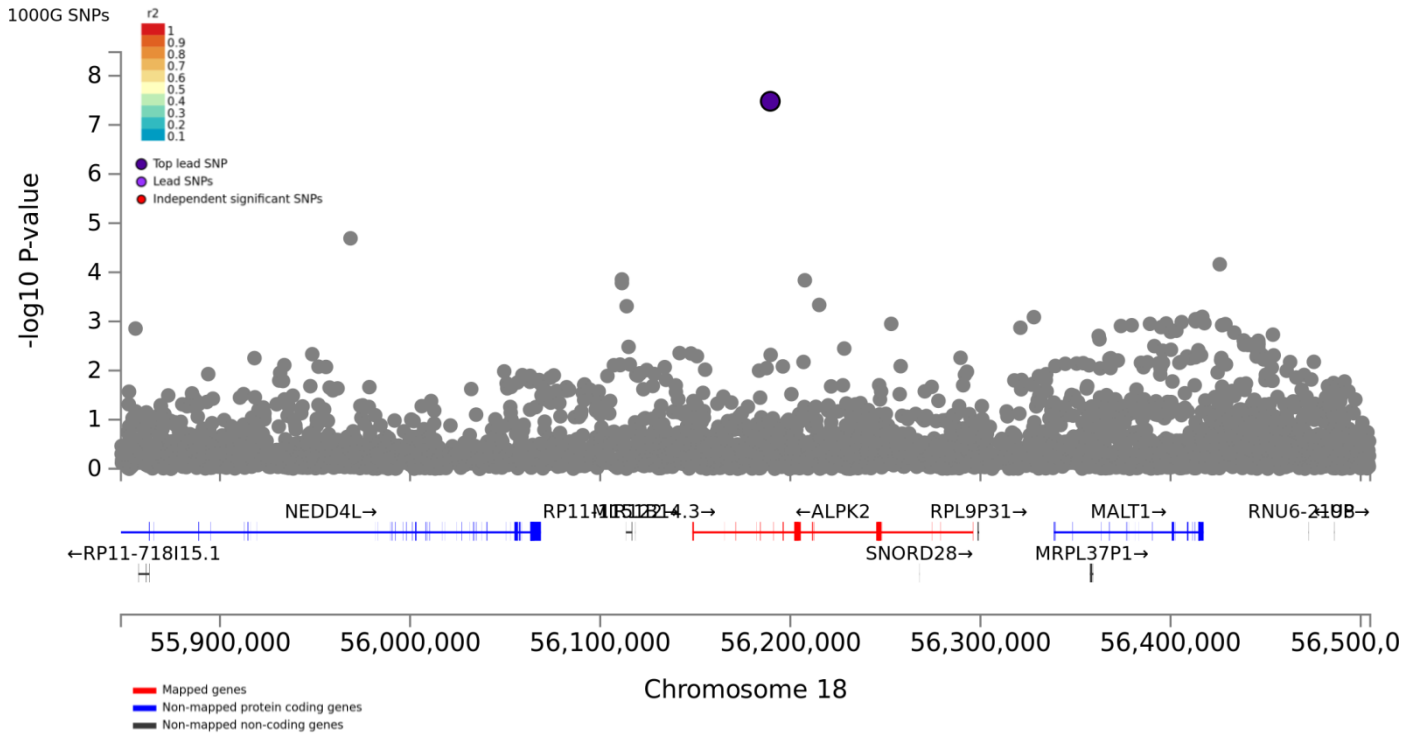
1000G SNPs
r2
1
0.9
0.8
0.7
0.6
0.5
0.4
0.3
0.2
0.1
Top lead SNP
Lead SNPs
Independent significant SNPs
-log10 P-value
0
1
2
3
4
5
6
7
8
NEDD4L→
←RP11-718I15.1
←ALPK2
RPL9P31→
SNORD28→
MALT1→
MRPL37P1→
55,900,000
56,000,000
56,100,000
56,200,000
56,300,000
56,400,000
Chromosome 18
Mapped genes
Non-mapped protein coding genes
Non-mapped non-coding genes

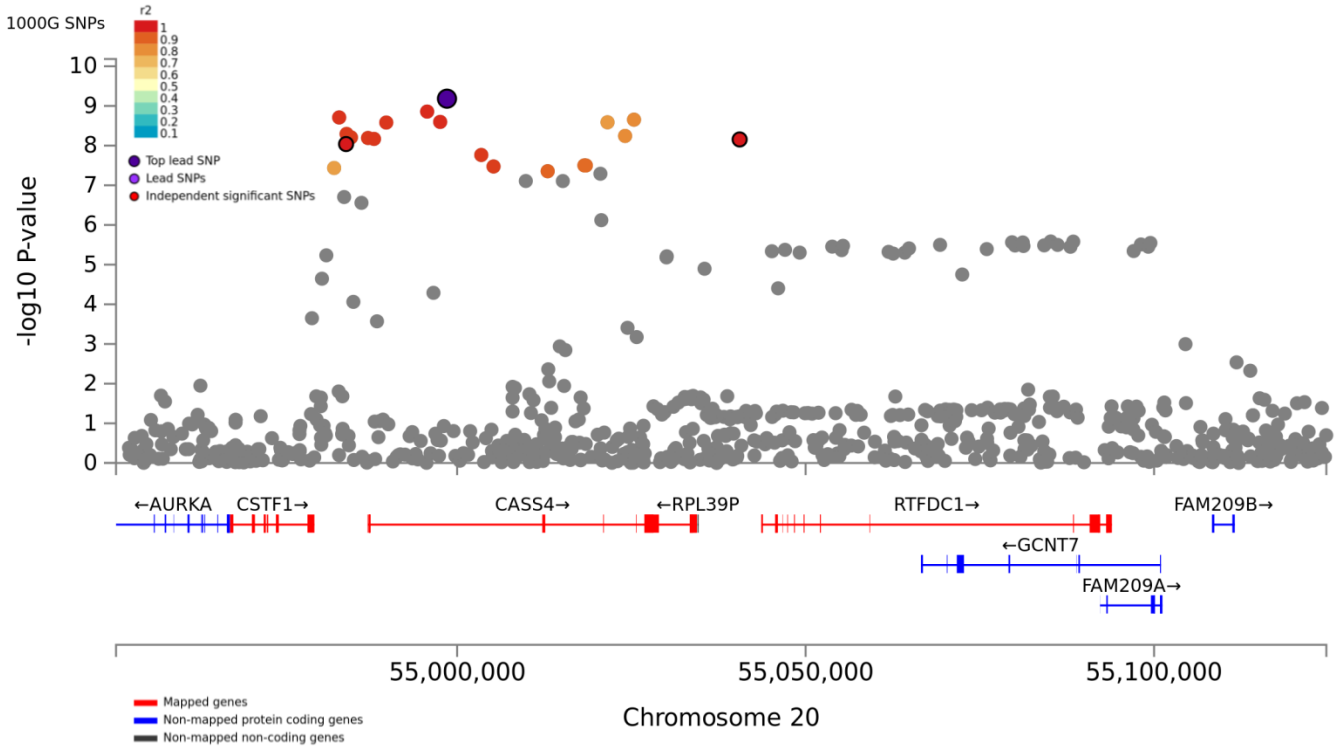
1000G SNPs
r2
1
0.9
0.8
0.7
0.6
0.5
0.4
0.3
0.2
0.1
Top lead SNP
Lead SNPs
Independent significant SNPs
-log10 P-value
10
9
8
7
6
5
4
3
2
1
0
←AURKA
CSTF1→
CASS4→
←RPL39P
RTFDC1→
FAM209B→
←GCNT7
FAM209A→
55,000,000
55,050,000
55,100,000
Chromosome 20
Mapped genes
Non-mapped protein coding genes
Non-mapped non-coding genes

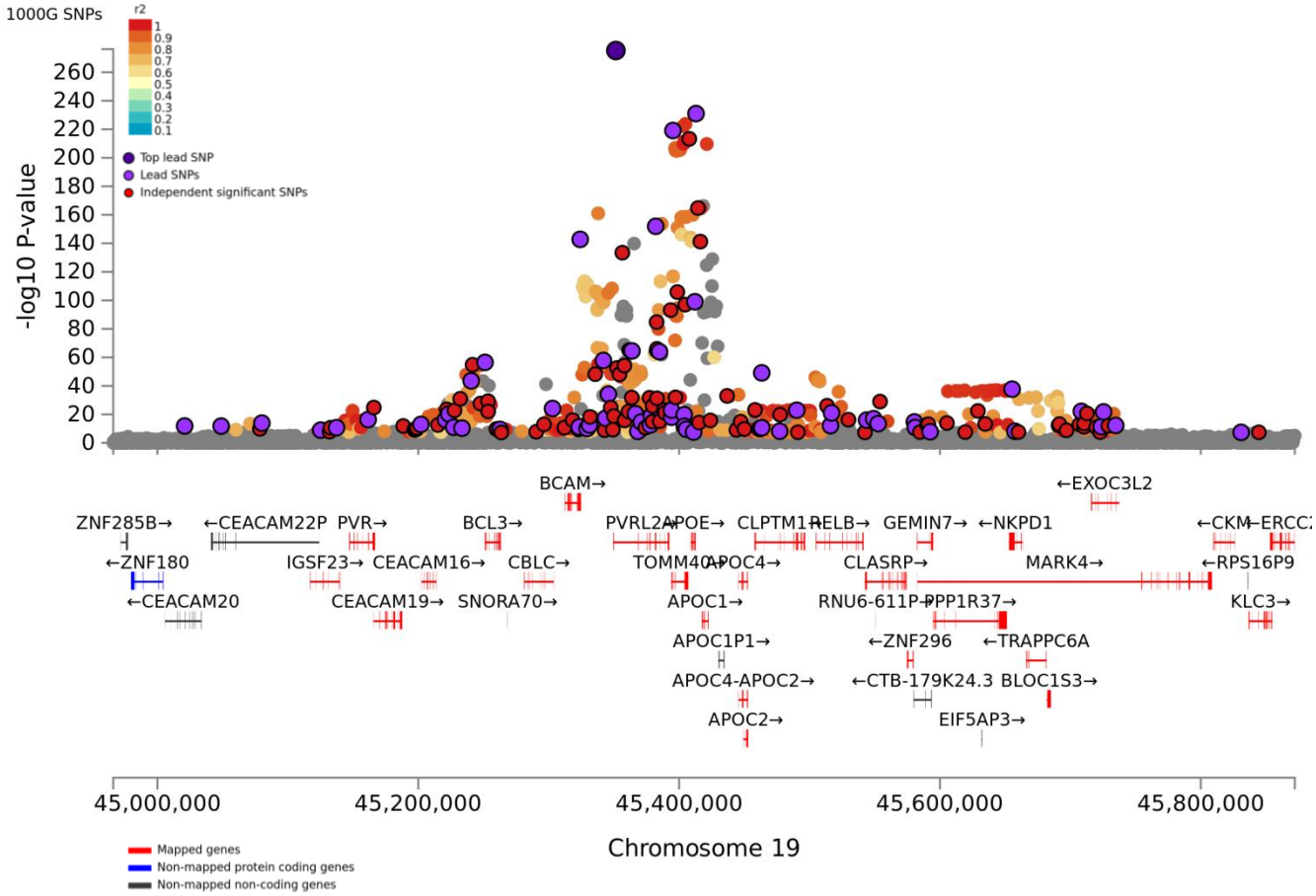
1000G SNPs
r2
1
0.9
0.8
0.7
0.6
0.5
0.4
0.3
0.2
0.1
Top lead SNP
Lead SNPs
Independent significant SNPs
-log10 P-value
260
240
220
200
180
160
140
120
100
80
60
40
20
0
BCAM→
←EXOC3L2
ZNF285B→
←CEACAM22P
PVR→
BCL3→
PVRL2
APOE→
CLPTM1
RELB→
GEMIN7→
←NKPD1
←CKM
←ERCC
←ZNF180
IGSF23→
CEACAM16→
CBLC→
TOMM40
APOC4→
CLASRP→
MARK4→
←RPS16P9
←CEACAM20
CEACAM19→
SNORA70→
APOC1→
RNU6-611P
PPP1R37→
KLC3→
APOC1P1→
←ZNF296
←TRAPPC6A
APOC4-APOC2→
←CTB-179K24.3
BLOC1S3→
APOC2→
EIF5AP3→
45,000,000
45,200,000
45,400,000
45,600,000
45,800,000
Chromosome 19
Mapped genes
Non-mapped protein coding genes
Non-mapped non-coding genes

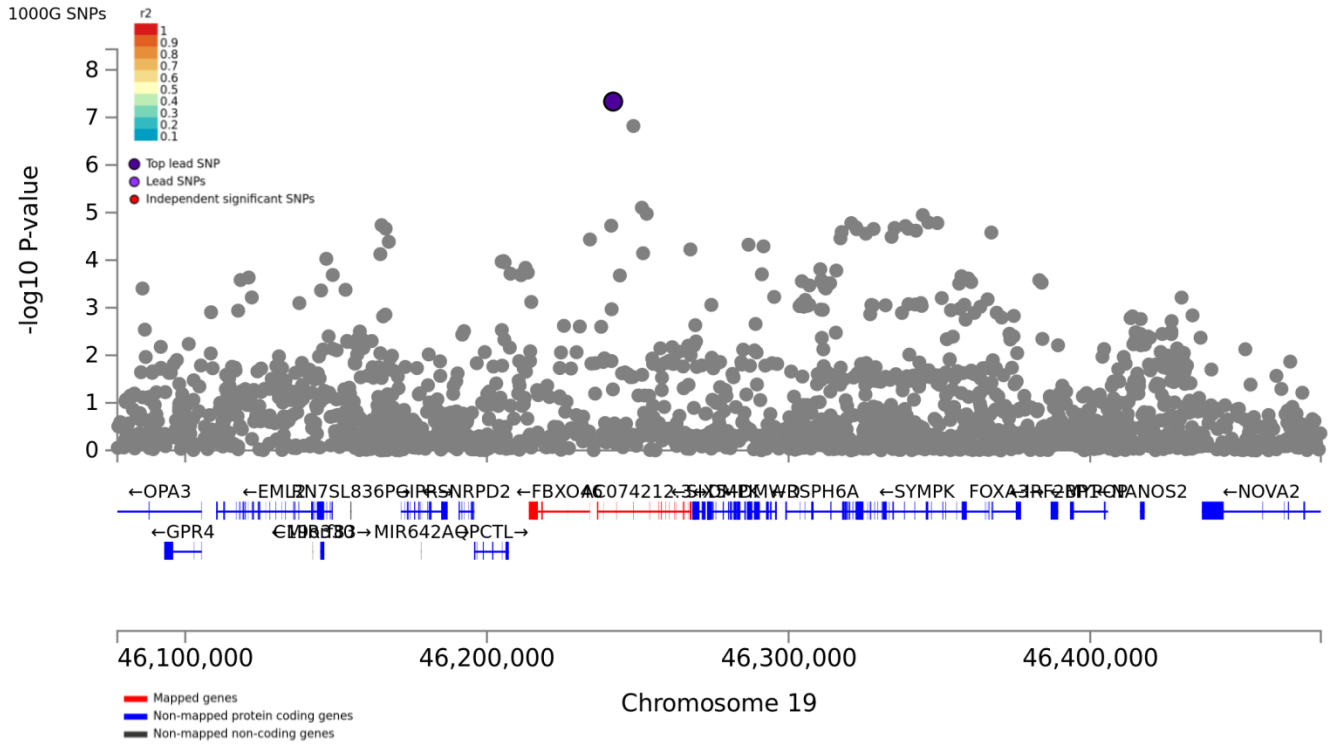
1000G SNPs
r2
1
0.9
0.8
0.7
0.6
0.5
0.4
0.3
0.2
0.1
Top lead SNP
Lead SNPs
Independent significant SNPs
-log10 P-value
0
1
2
3
4
5
6
7
8
←OPA3
←GPR4
←NOVA2
46,100,000
46,200,000
46,300,000
46,400,000
Chromosome 19
Mapped genes
Non-mapped protein coding genes
Non-mapped non-coding genes

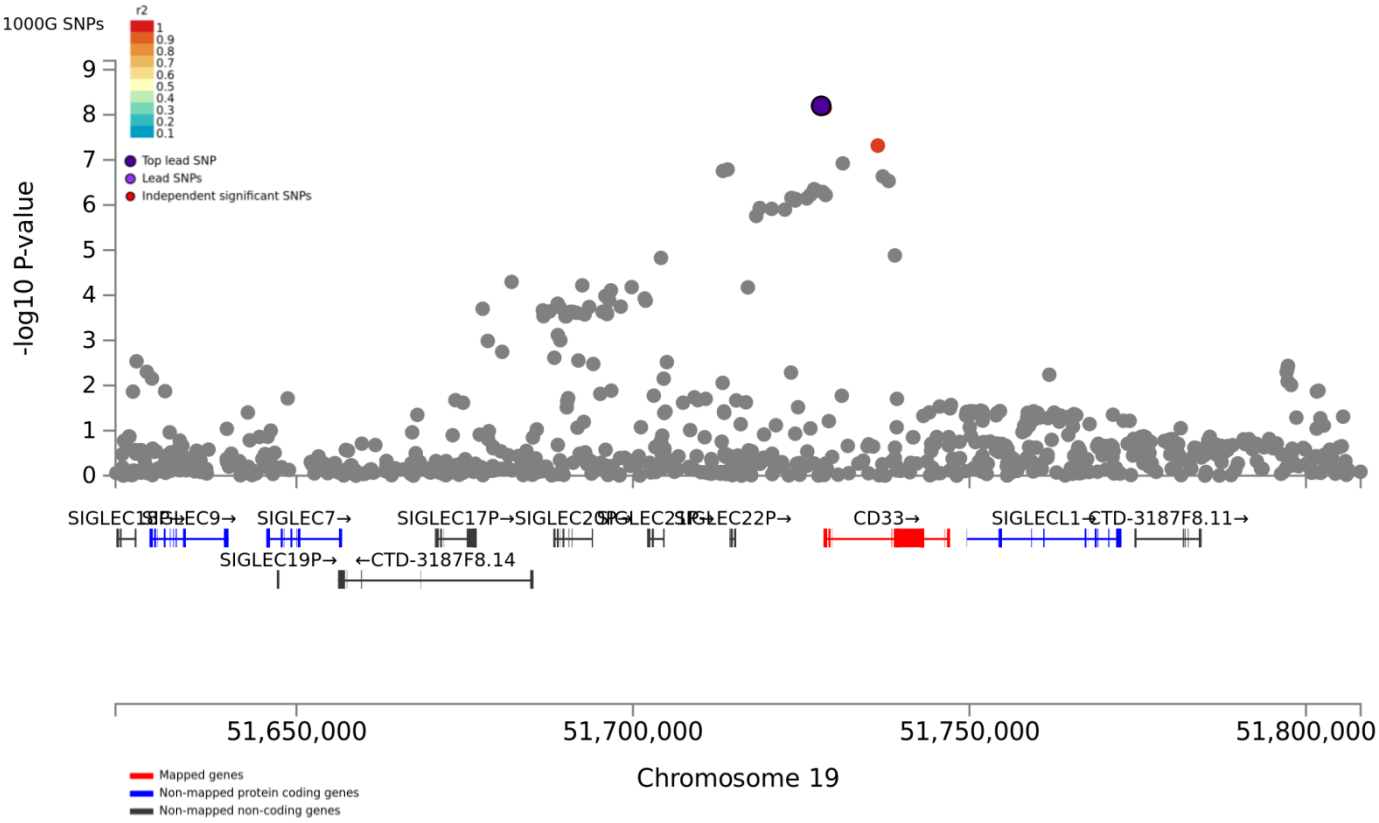
1000G SNPs
r2
1
0.9
0.8
0.7
0.6
0.5
0.4
0.3
0.2
0.1
Top lead SNP
Lead SNPs
Independent significant SNPs
-log10 P-value
0
1
2
3
4
5
6
7
8
9
SIGLEC7→
SIGLEC17P→
CD33→
SIGLECL1→
CTD-3187F8.11→
SIGLEC19P→
←CTD-3187F8.14
51,650,000
51,700,000
51,750,000
51,800,000
Chromosome 19
Mapped genes
Non-mapped protein coding genes
Non-mapped non-coding genes

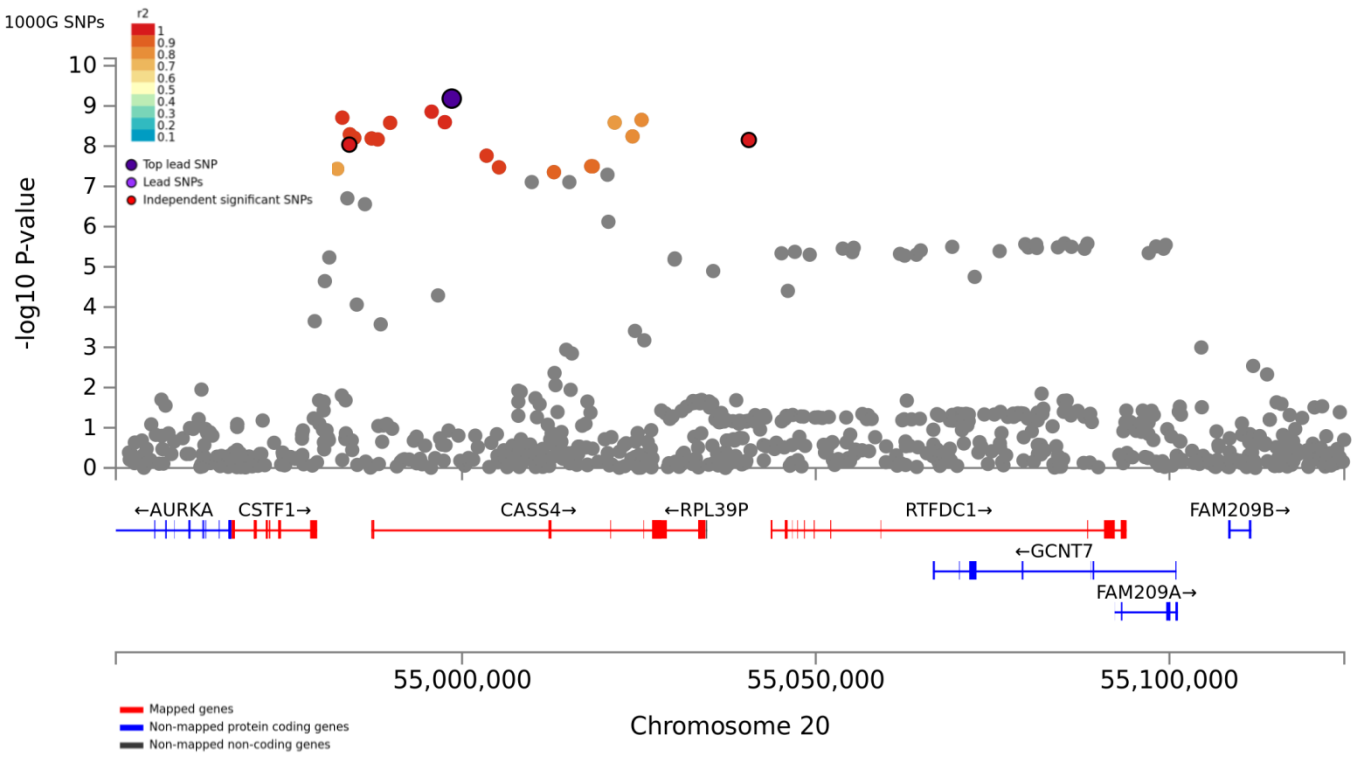
1000G SNPs
r2
1
0.9
0.8
0.7
0.6
0.5
0.4
0.3
0.2
0.1
Top lead SNP
Lead SNPs
Independent significant SNPs
-log10 P-value
10
9
8
7
6
5
4
3
2
1
0
←AURKA
CSTF1→
CASS4→
←RPL39P
RTFDC1→
FAM209B→
←GCNT7
FAM209A→
55,000,000
55,050,000
55,100,000
Chromosome 20
Mapped genes
Non-mapped protein coding genes
Non-mapped non-coding genes

Supplementary Figure 3. Partitioned heritability results for the meta-analysis. Variants were binned by chromosome or minor allele frequency and tested for a significant over- or underrepresentation as to what is expected by chance. A) Enrichment results for heritability calculations where variants have been partitioned per chromosome. B) Enrichment results for heritability calculations where variants have been partitioned into multiple categories based on minor allele frequency.

A

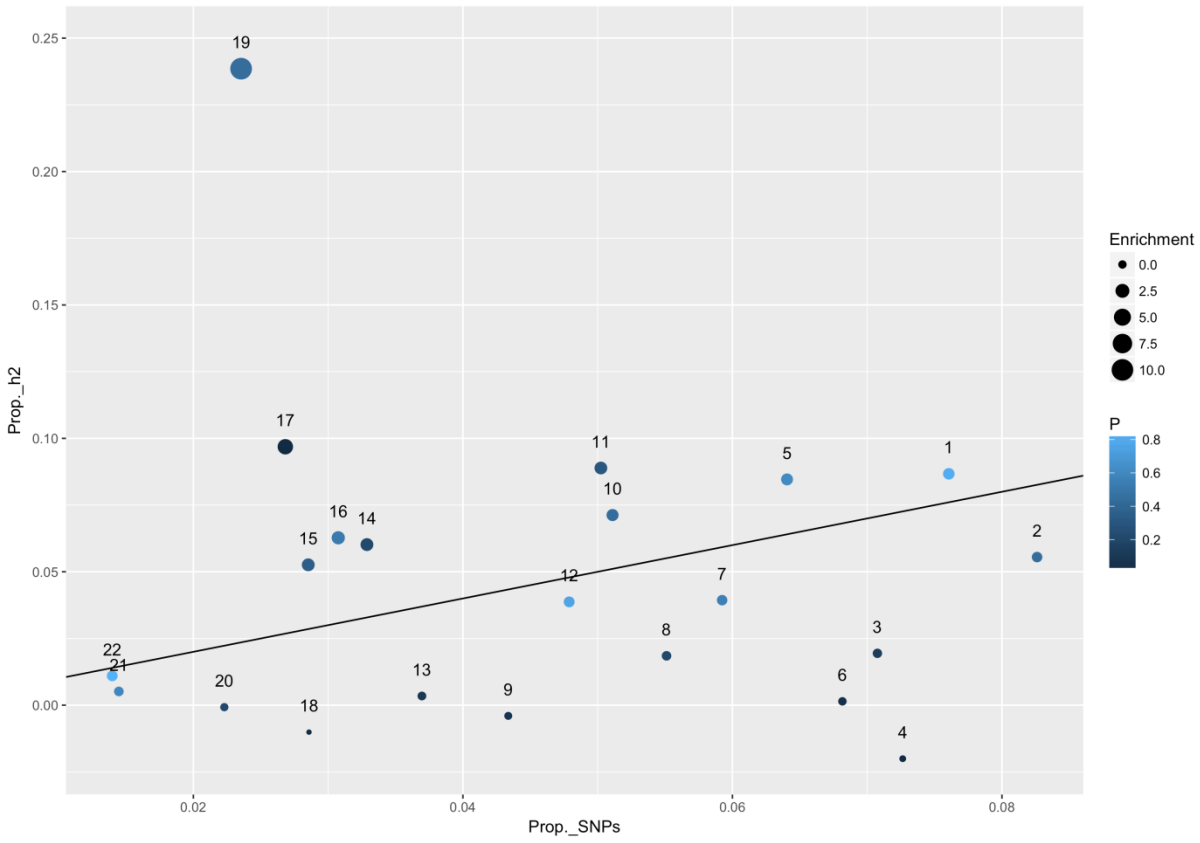

B

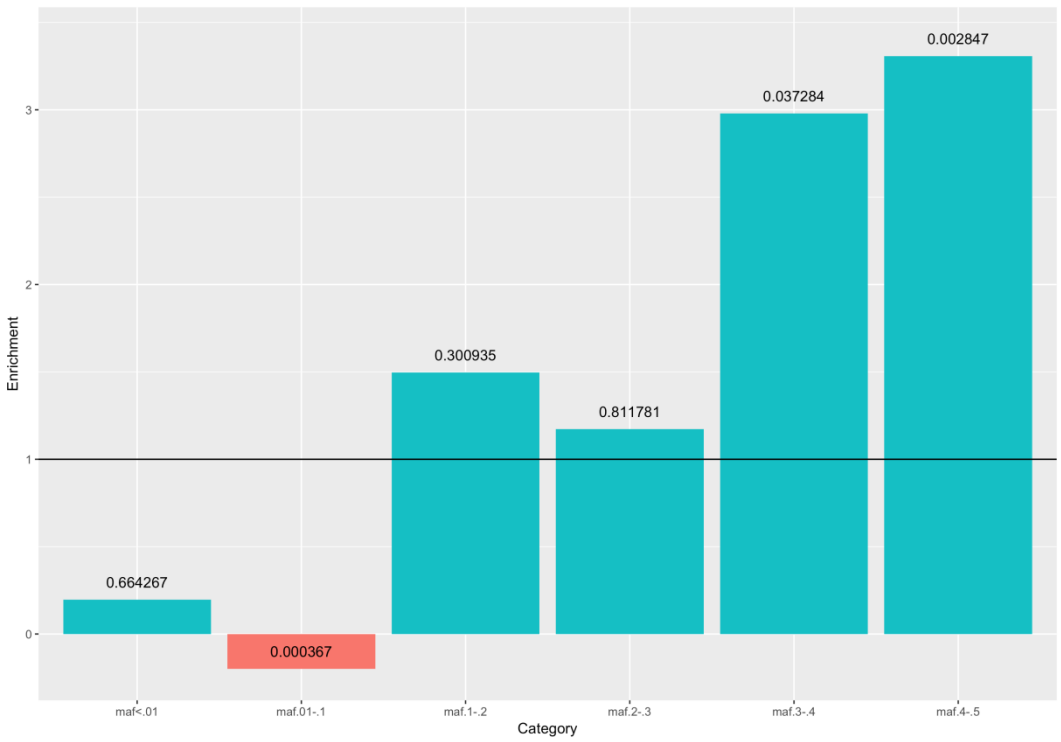

Supplementary Figure 4. Full circos plots of chromatin interactions and eQTLs for all chromosomes with significantly associated loci. The distinct layers and colors correspond to various features. The outer layer contains zoomed in Manhattan plots containing only SNPs with P < 0.05. SNPs in genomic risk loci are color-coded as a function of their maximum r2 to the one of the independent significant SNPs in the locus, as follows: red (r2 > 0.8), orange (r2 > 0.6), green (r2 > 0.4) and blue (r2 > 0.2). SNPs that are not in LD with any of the independent significant SNPs (with r2 ≤ 0.2) are grey. The second layer displays the position of the genomic risk loci in blue. The third layer contains the mapped genes that are implicated by chromatin interactions and/or eQTL analysis (orange = chromatin interaction; green = eQTL; red = chromatin interaction and eQTL).

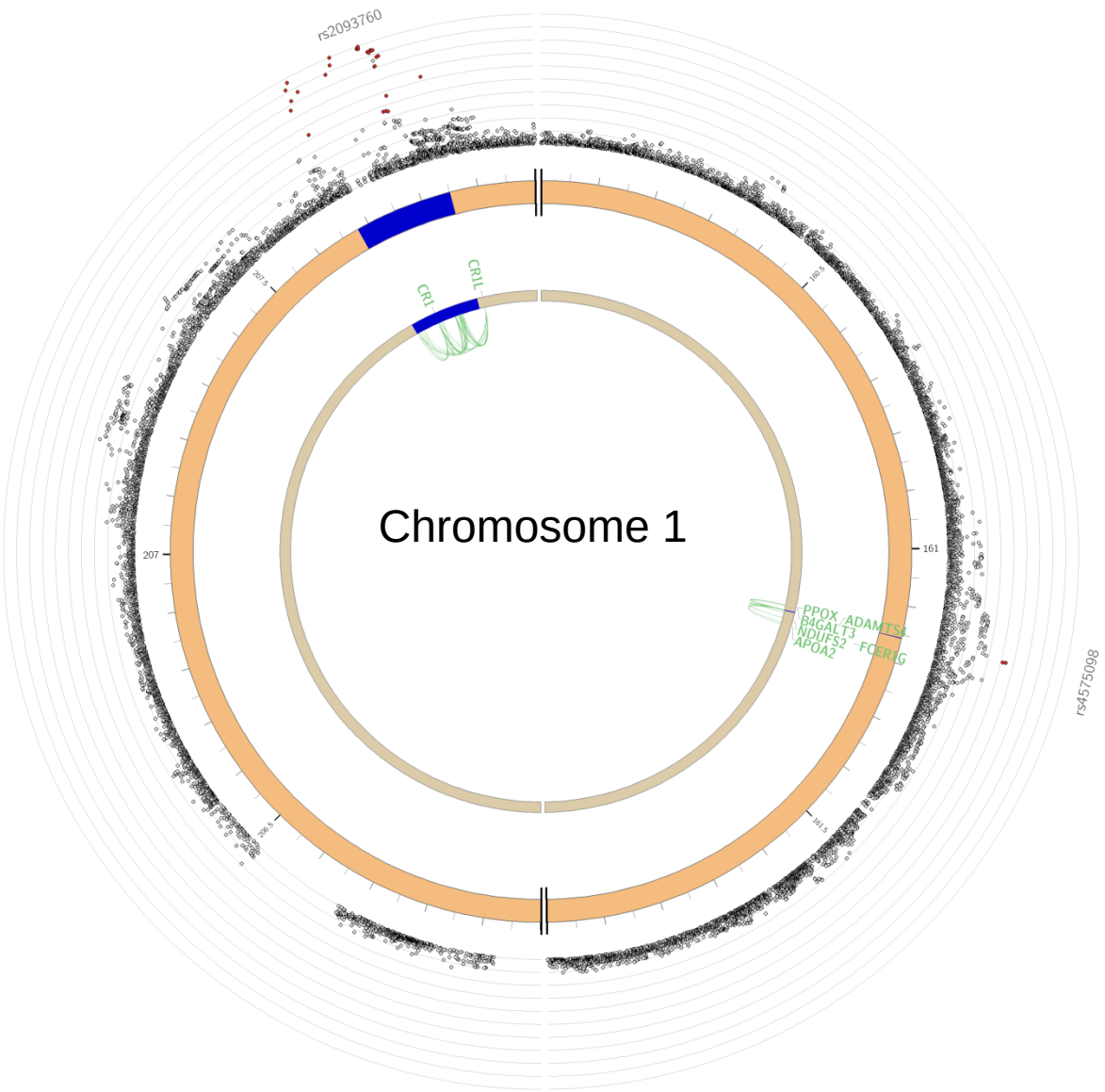

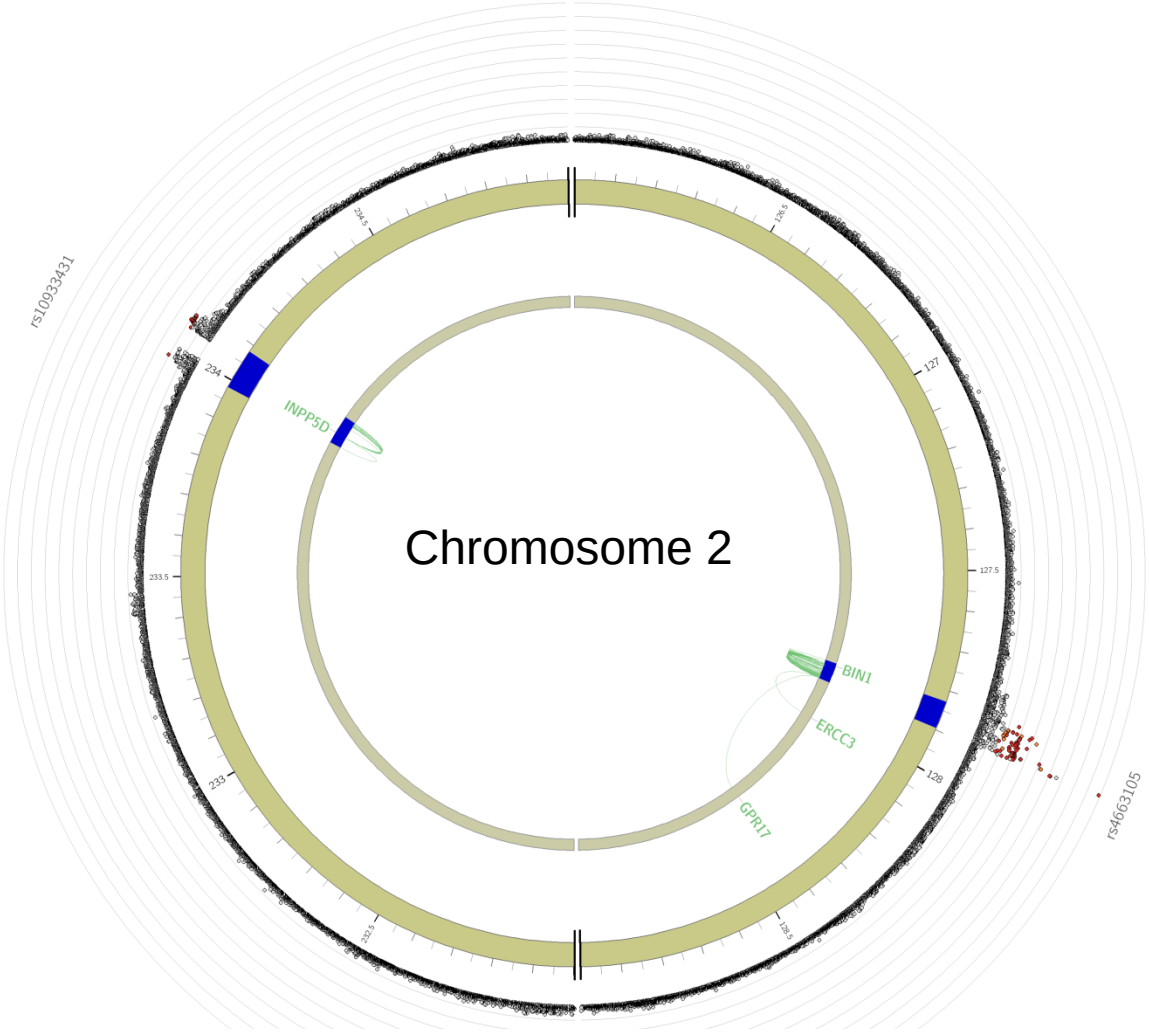
Chromosome 2
rs10933431
rs4663105
INPP5D
BIN1
ERCC3
GPR17
234
233.5
233
234.5
232.5
126.5
127
127.5
128
128.5

Chromosome 3
57.5
56.5
57

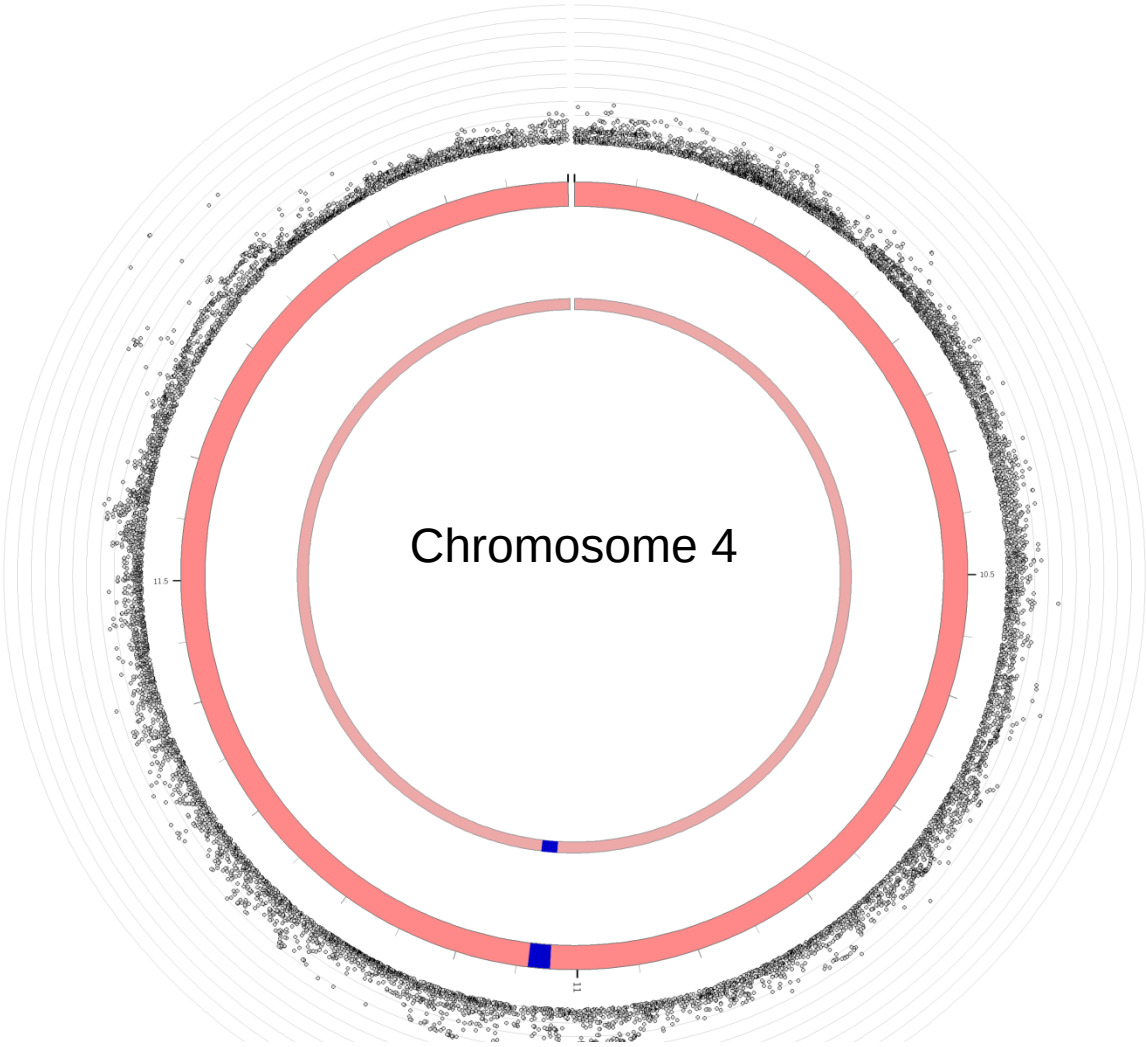
Chromosome 4
11.5
10.5
11

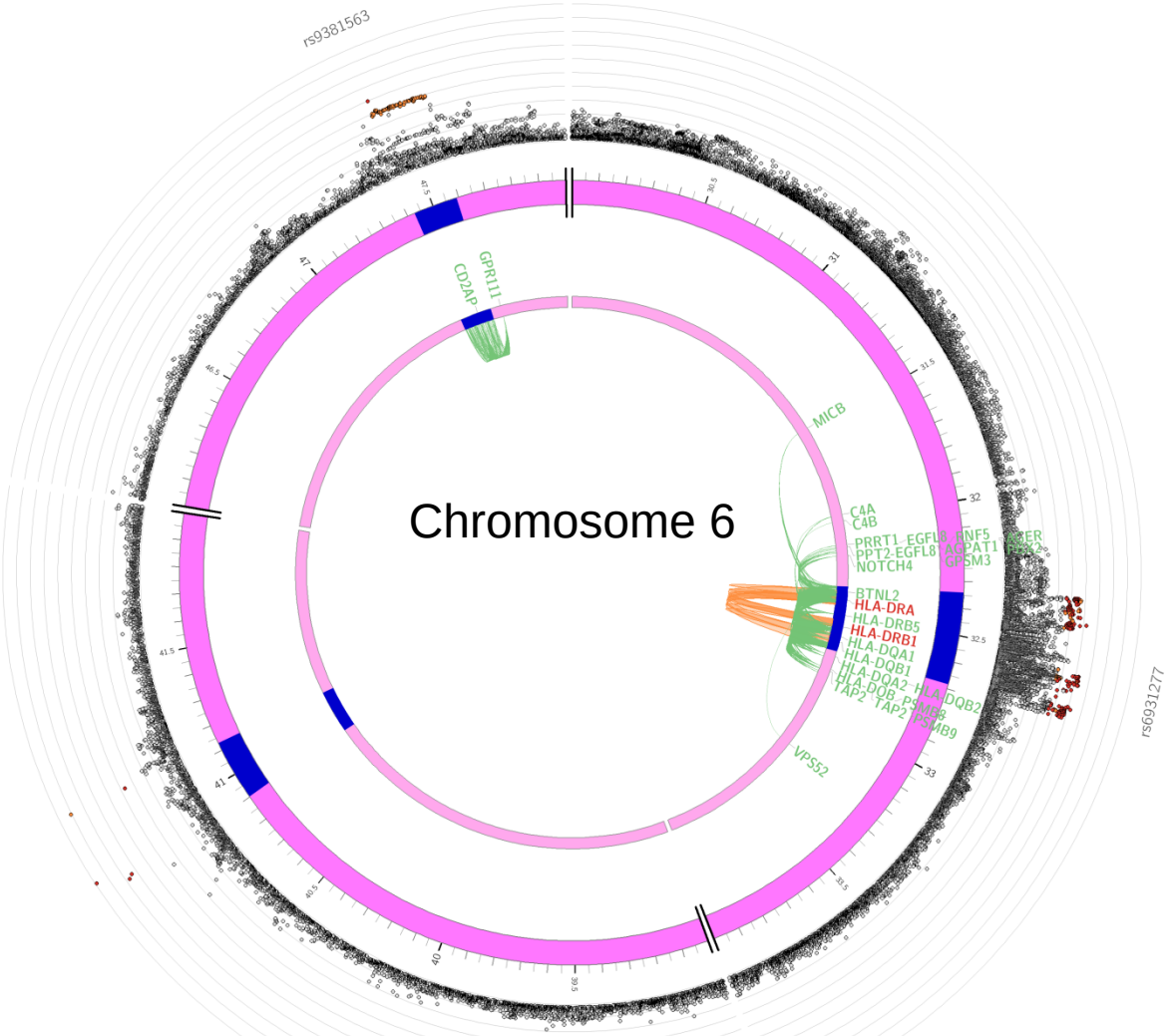
rs9381563
Chromosome 6
47.5
47
46.5
41.5
41
40.5
40
39.5
30.5
31
31.5
32
32.5
33
33.5
GPR111
CD2AP
MICB
C4A
C4B
PRRT1-EGFL8
PPT2-EGFL8
NOTCH4
TNF5
AGPAT1
GPSM3
BTNL2
HLA-DRA
HLA-DRB5
HLA-DRB1
HLA-DQA1
HLA-DQB1
HLA-DQA2
HLA-DQB2
TAP2
TAP2
VPS52
rs6931277

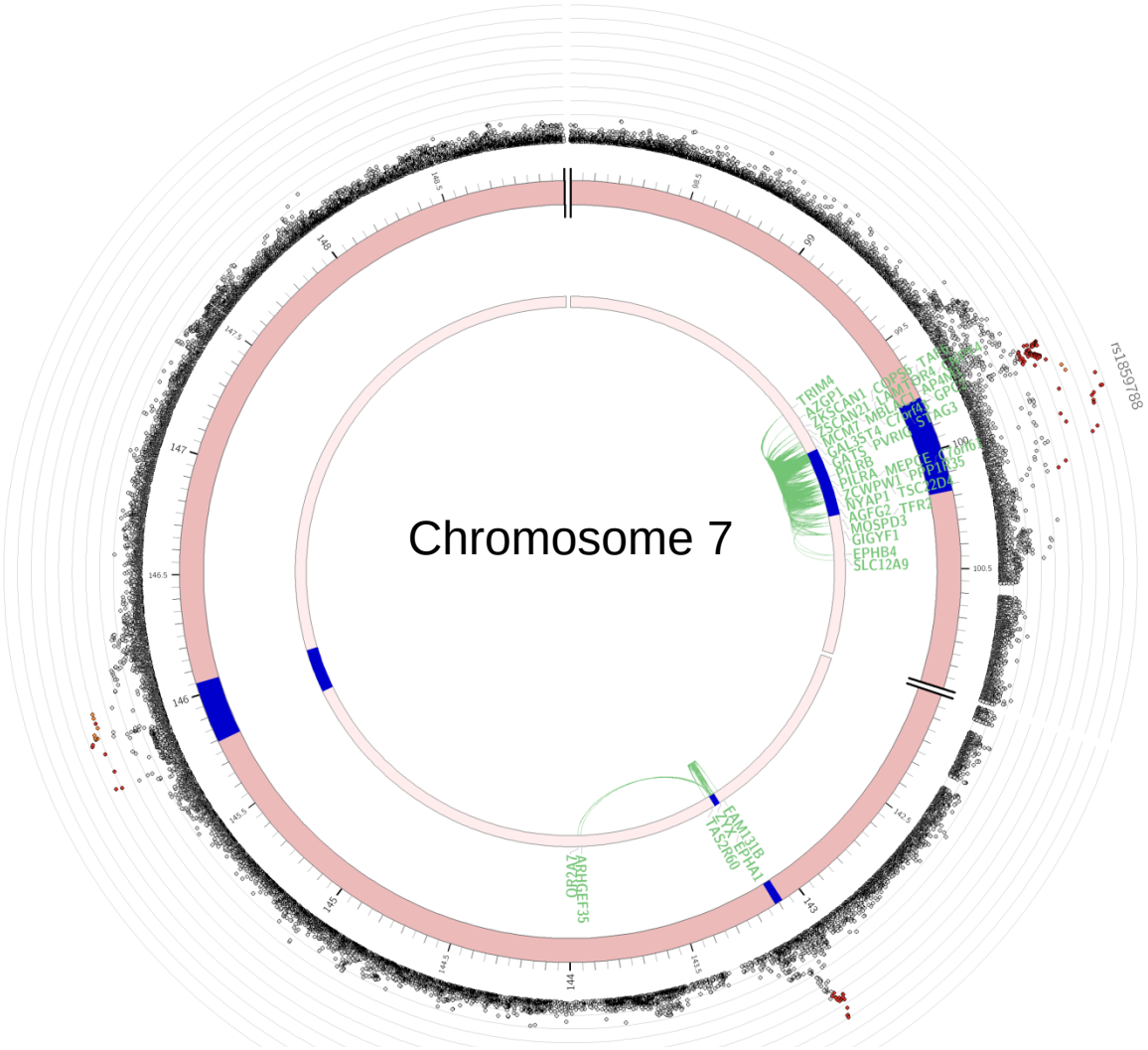
Chromosome 7
rs1859788
TRIM4
AZGP1
ZKSCAN1
ZSCAN21
MCM7
GALS3
GATS
PILRB
PILRA
ZCWPW1
NYAP1
AGFG2
MOSPD3
GIGYF1
EPHB4
SLC12A9
FAM131B
TAS2R60
ARHGEF35

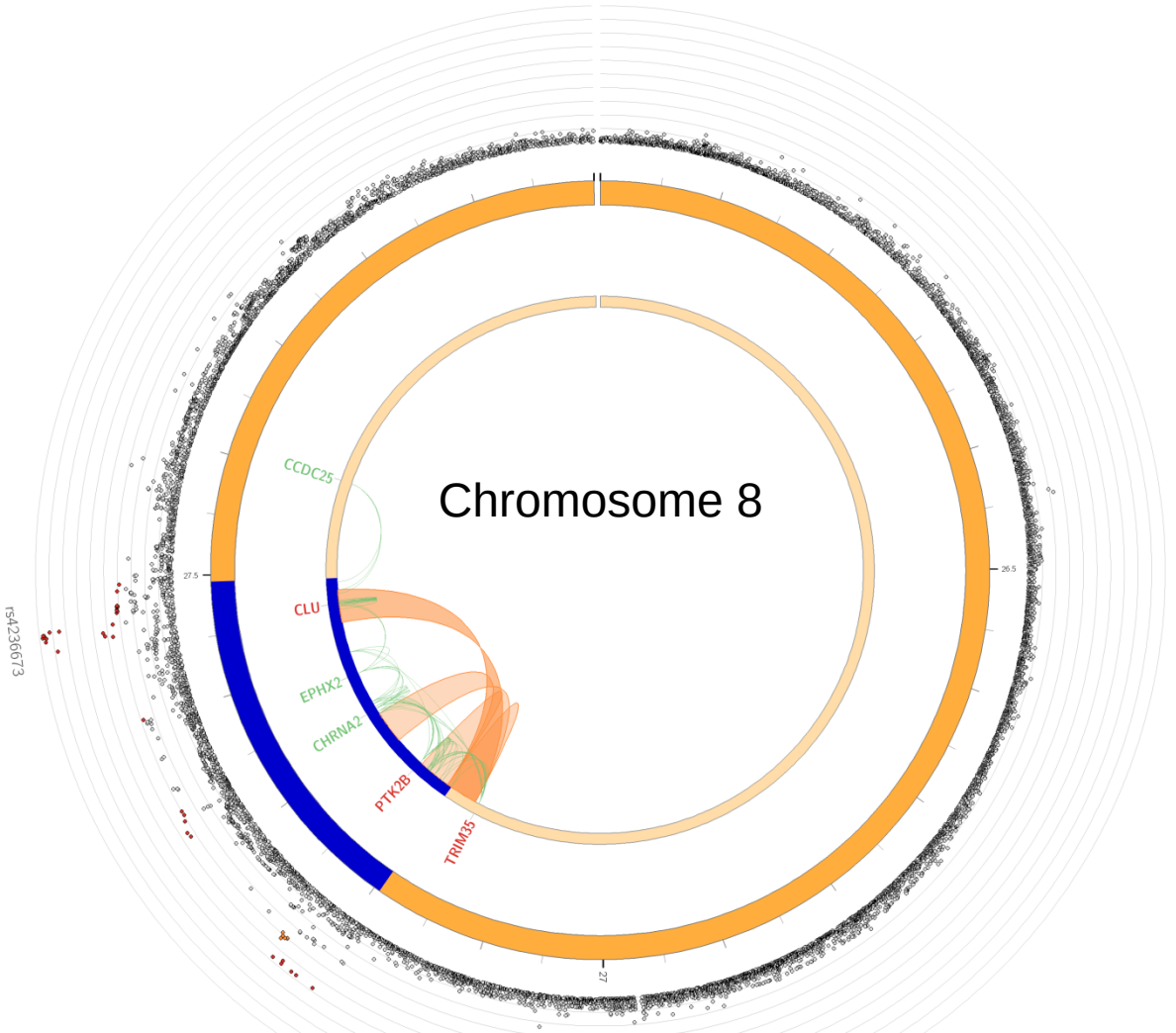
Chromosome 8
rs4236673
CCDC25
CLU
EPHX2
CHRNA2
PTK2B
TRIM35

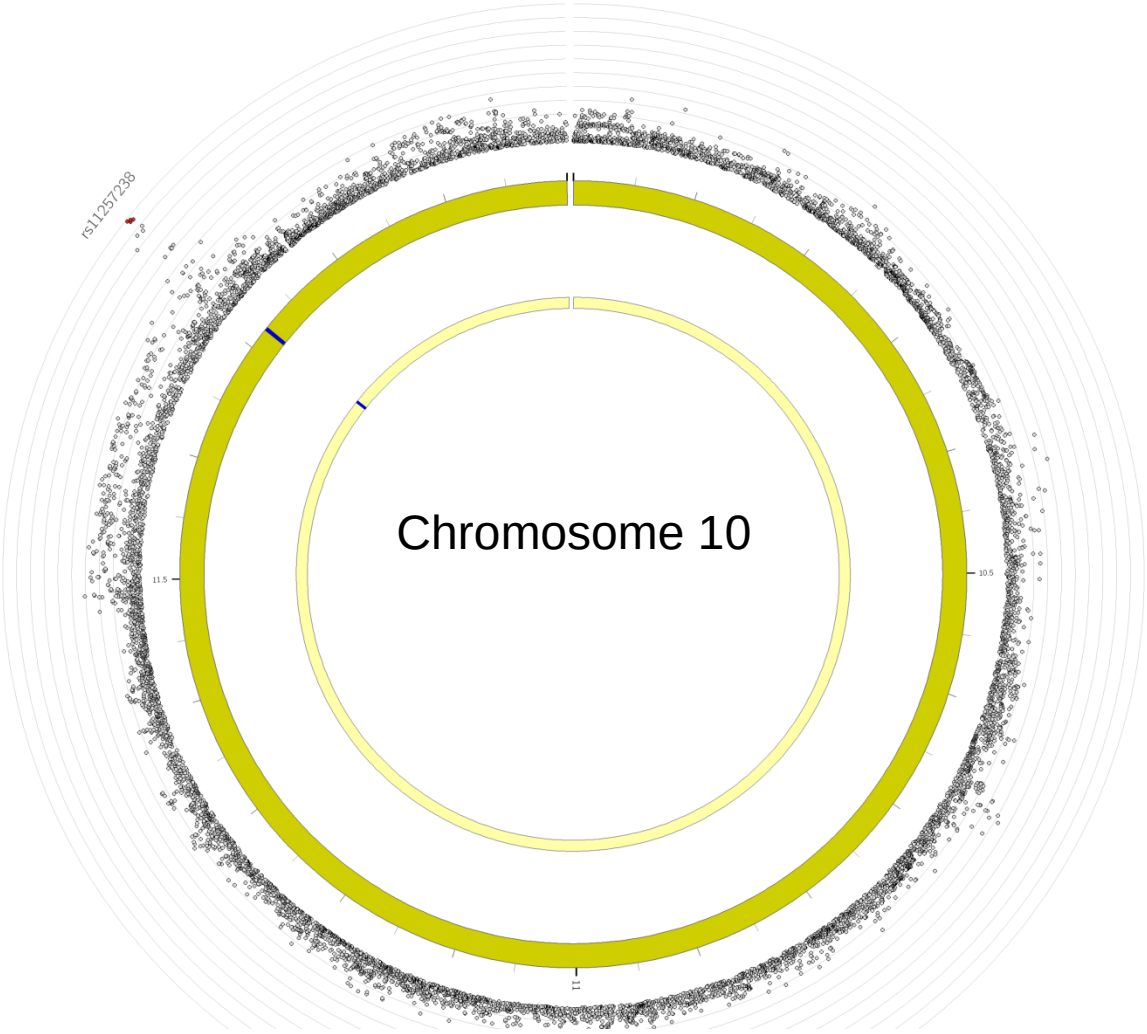
rs11257238
Chromosome 10
11.5
10.5
11

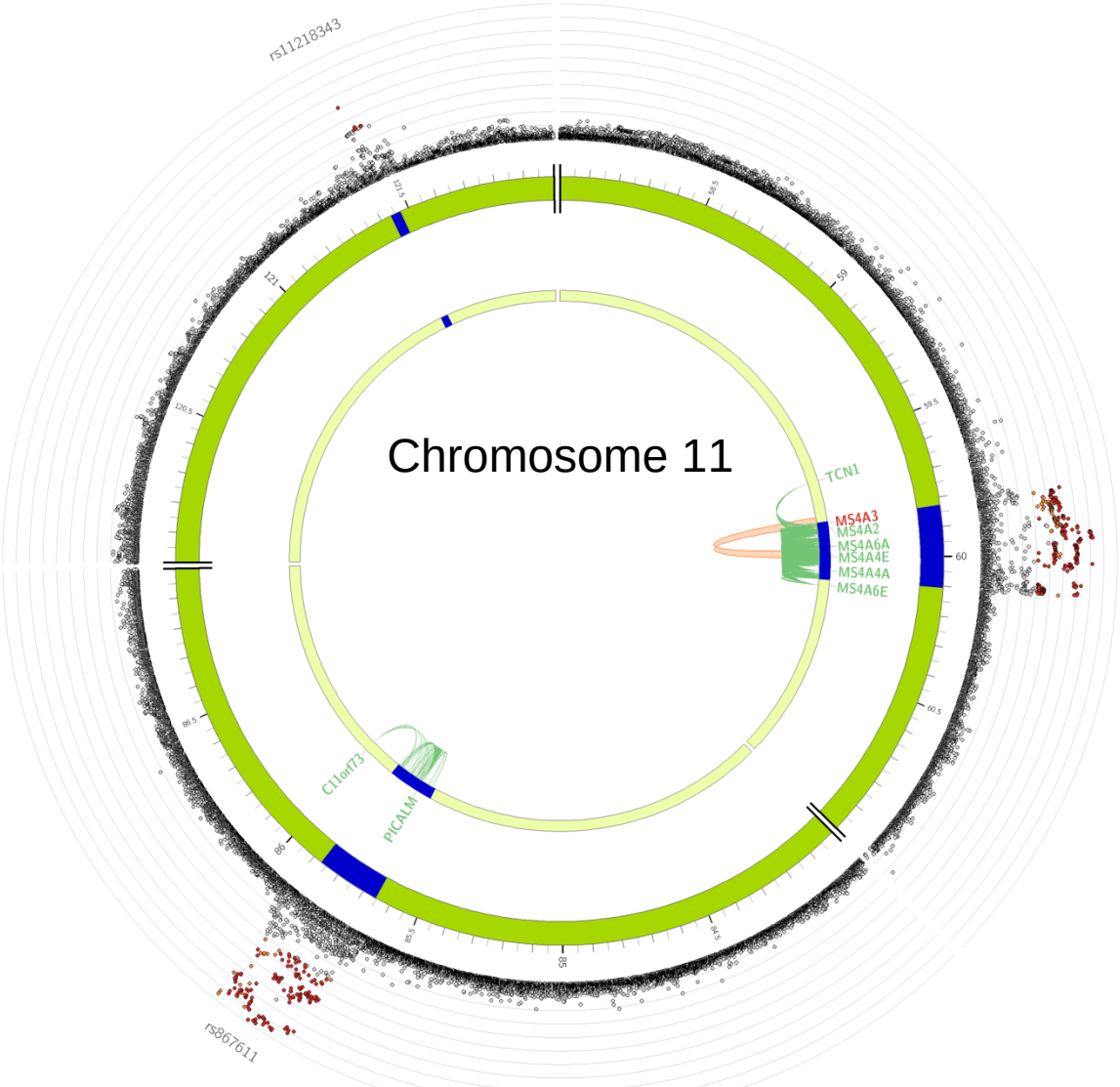
rs11218343
Chromosome 11
TCN1
MS4A3
MS4A2
MS4A6A
MS4A4E
MS4A4A
MS4A6E
C11orf73
PICALM
rs2081545
rs867611
121
120.5
86
85
60
59

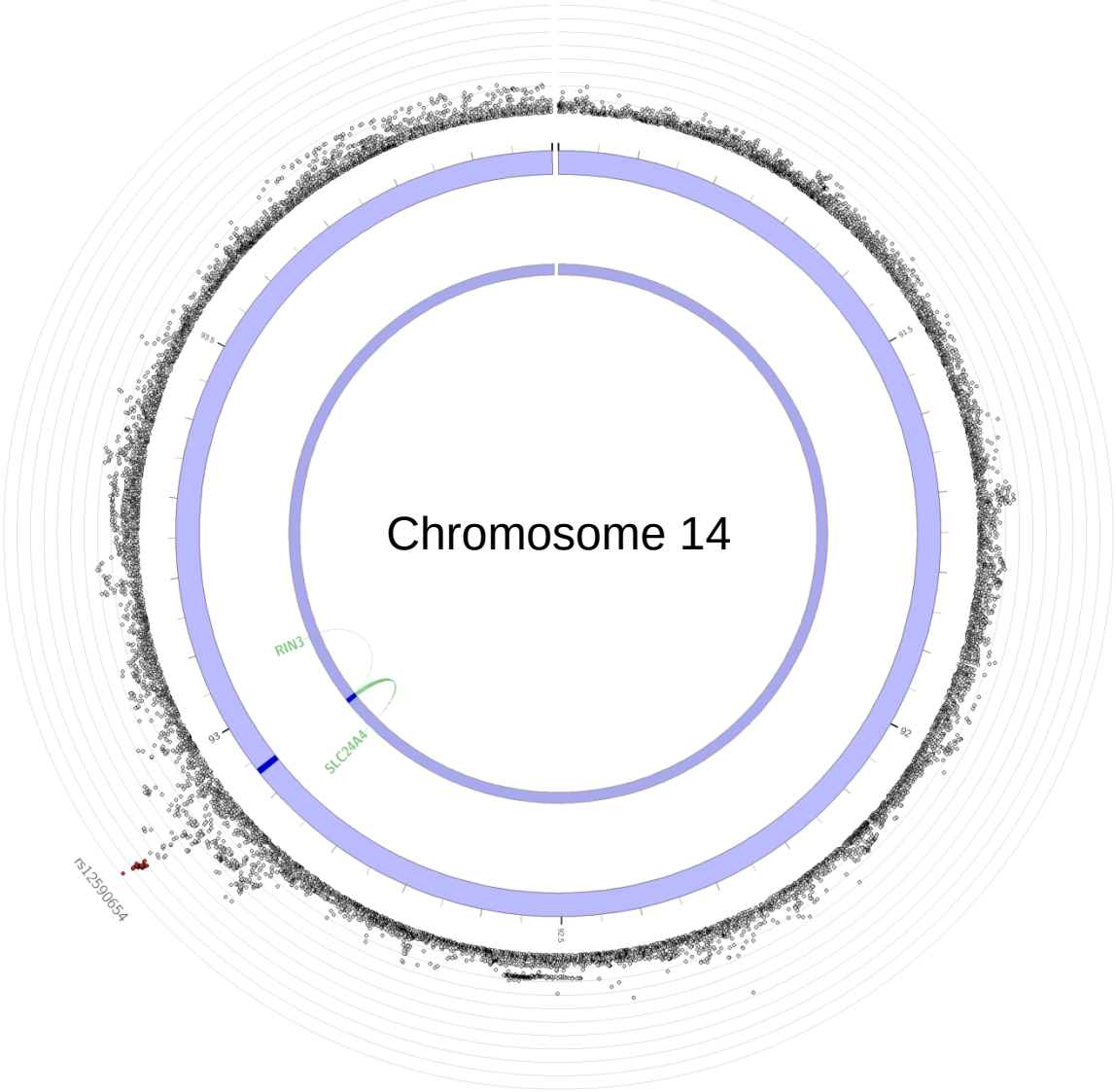
Chromosome 14
RIN3
SLC24A4
rs12590654
93.5
93
92.5
92
91.5

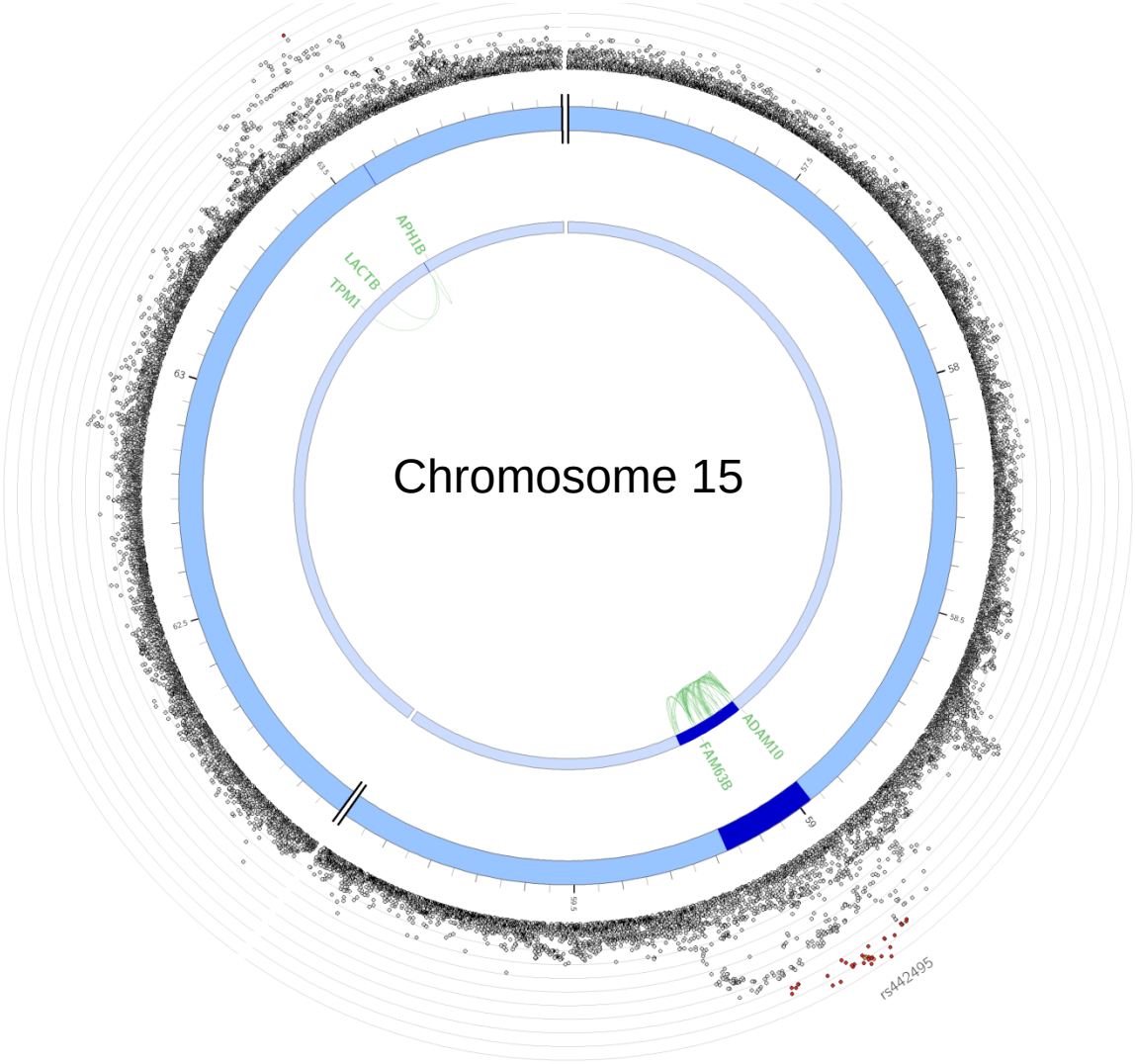
Chromosome 15
APH1B
LACTB
TPM1
ADAM10
FAM63B
rs442495
63.5
63
62.5
59.5
59
58.5
58
57.5

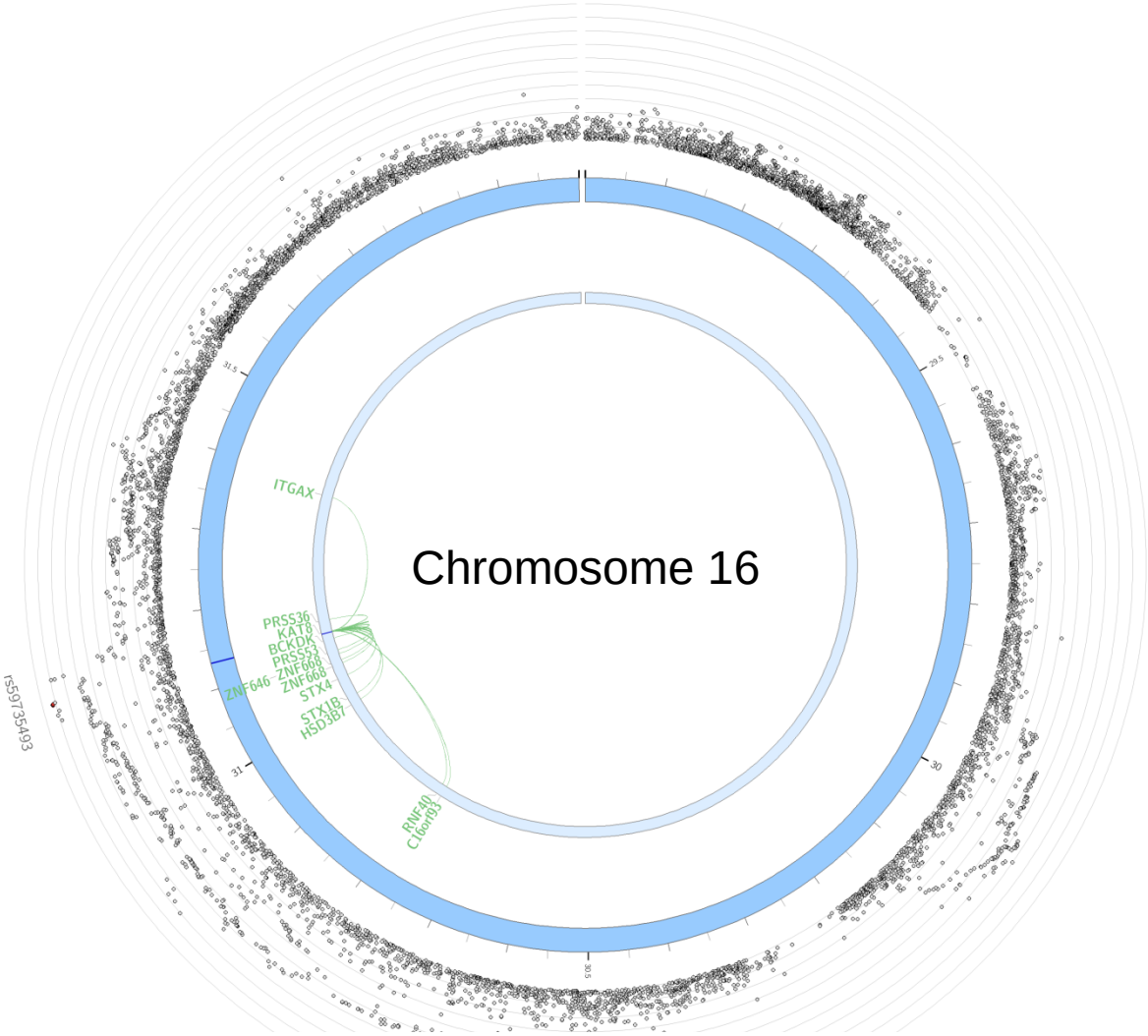
Chromosome 16
ITGAX
PRSS36
KAT8
BCKDK
PRSS53
ZNF668
ZNF646
STX4
STX1B
HSD3B7
RNF40
C16orf93
rs59735493

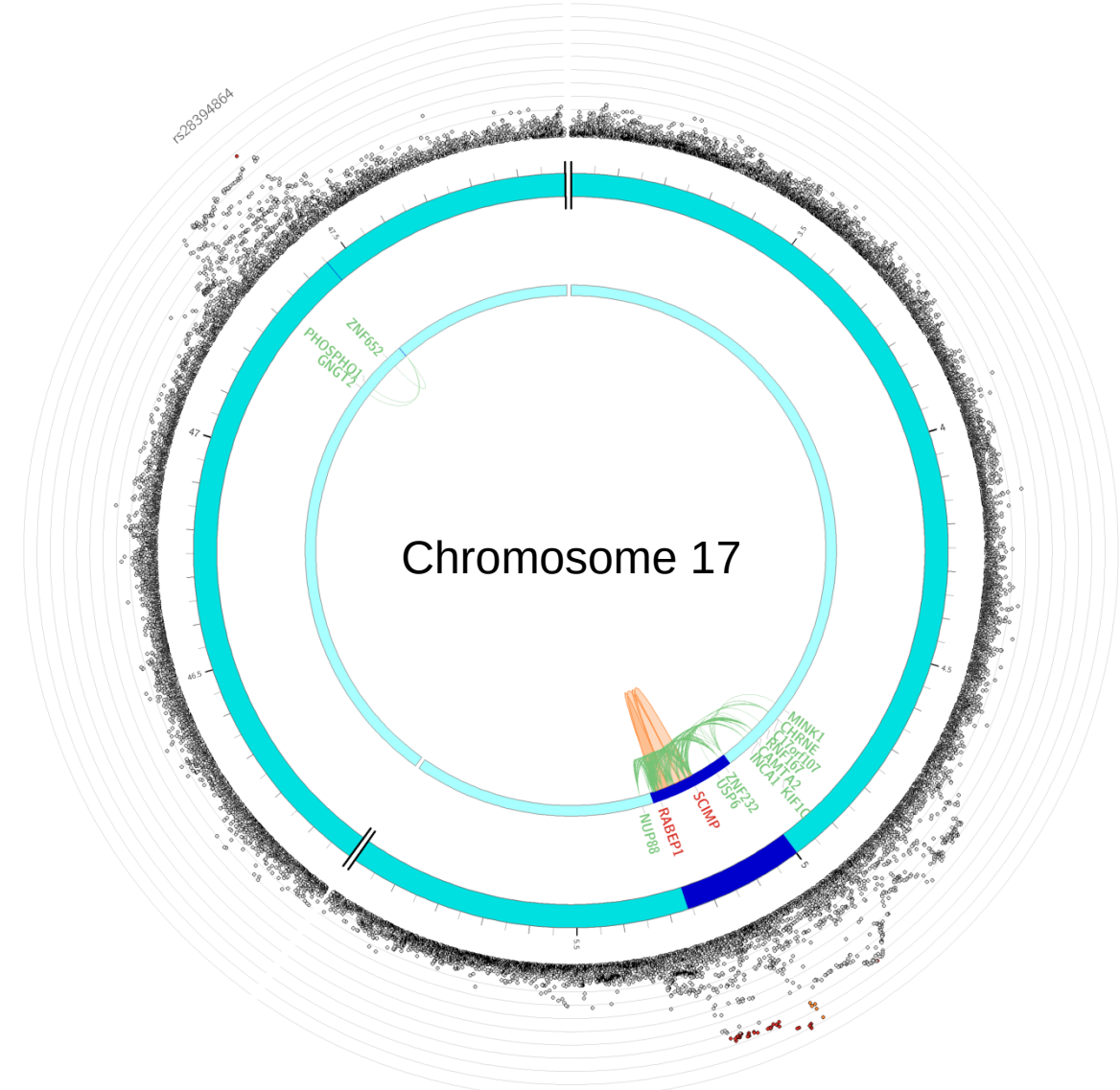
Chromosome 17
ZNF652
PHOSPHO1
GNGT2
MINK1
CHRNE
RNF167
CAMTA2
INCA1
ZNF232
USP6
SCIMP
RABEP1
NUP88
rs28394864

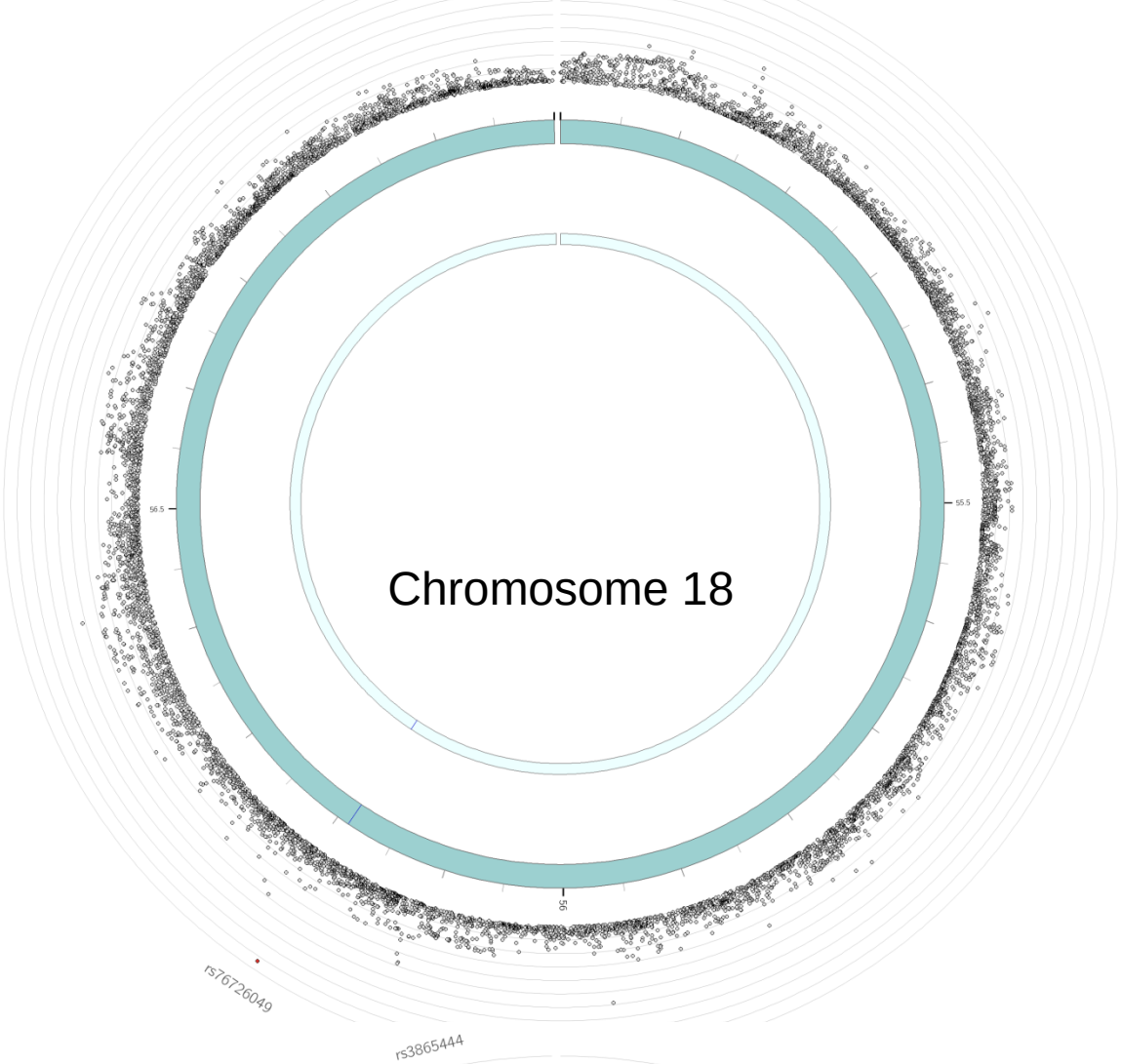
Chromosome 18
rs76726049
rs3865444

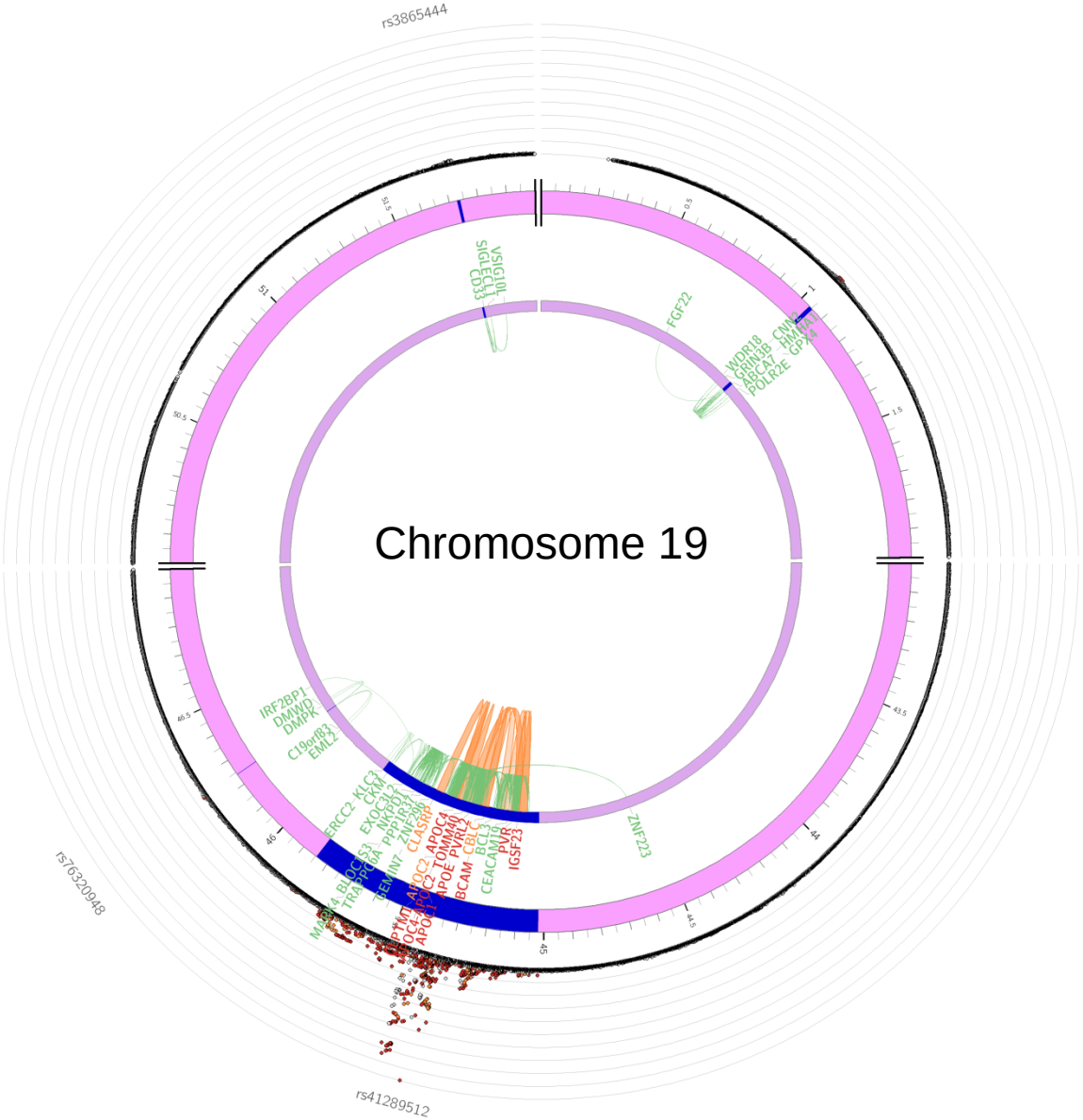
Chromosome 19
rs76320948
rs41289512

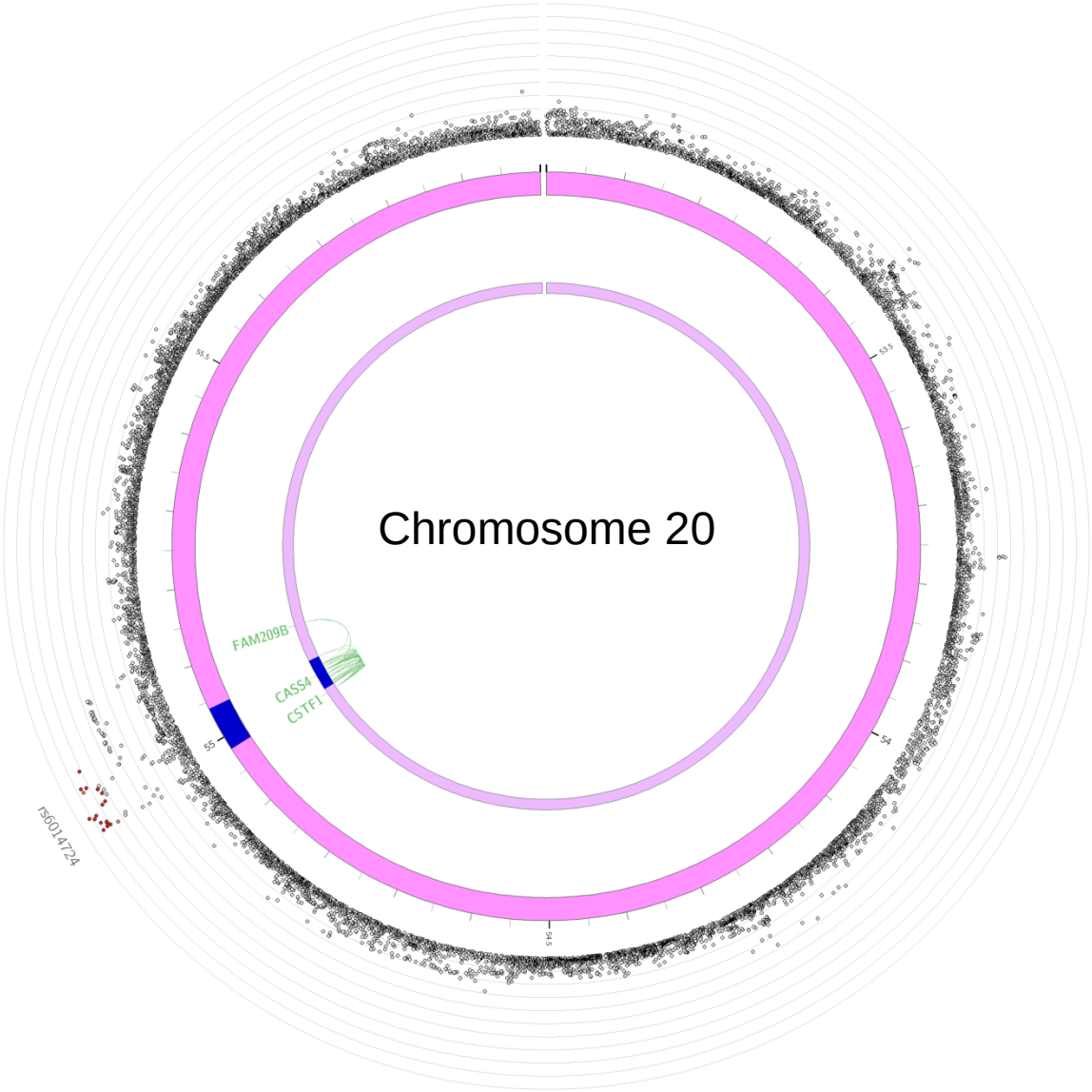
Chromosome 20
FAM209B
CASS4
CSTF1
rs6014724
55.5
55
54.5
54
53.5

Supplementary Figure 5. Gene-based association results with MAGMA. A) The Manhattan plot displays all associations per gene ordered according to their genomic position (start of gene) on the x-axis and showing the strength of the association with the –log10 transformed *P*-values on the y-axis. B) The QQ plot displays the expected –log10 transformed *p*-values on the x-axis and the observed –log10 transformed *p*-values on the y-axis.

A

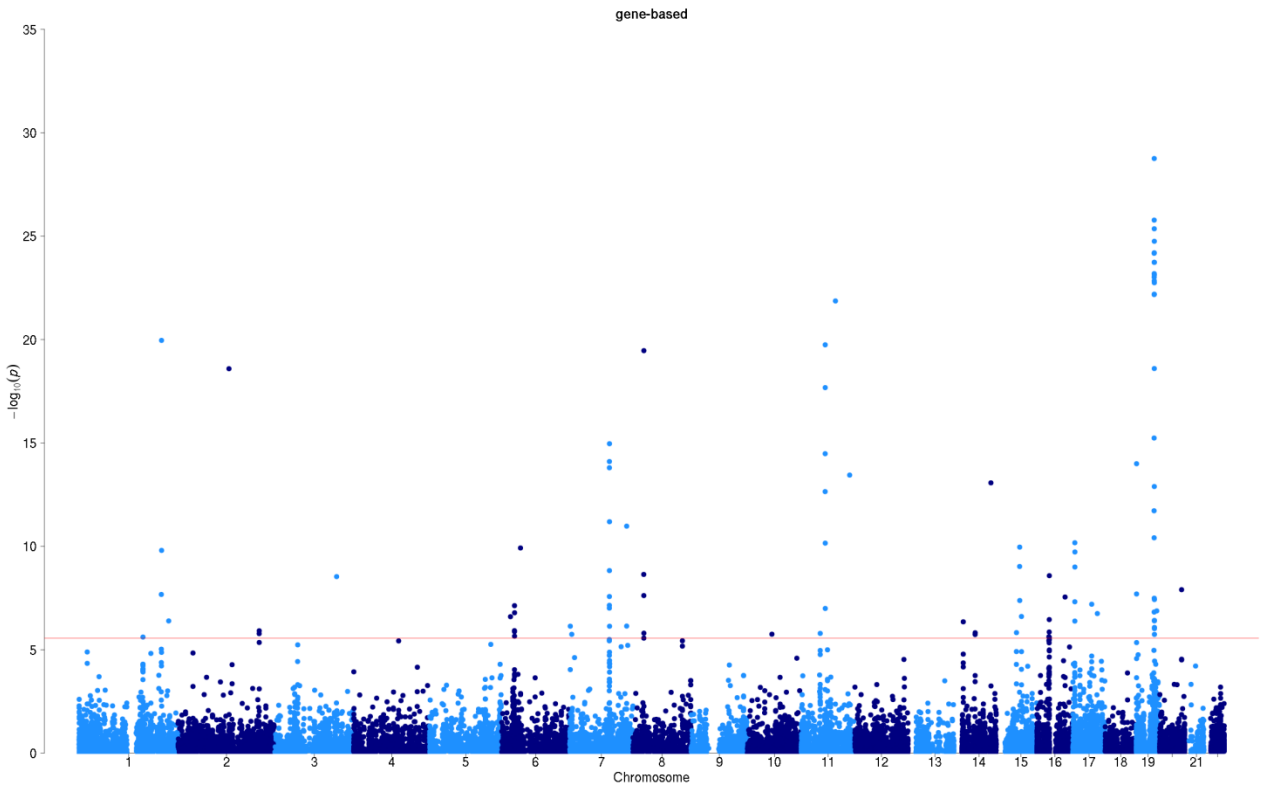

B

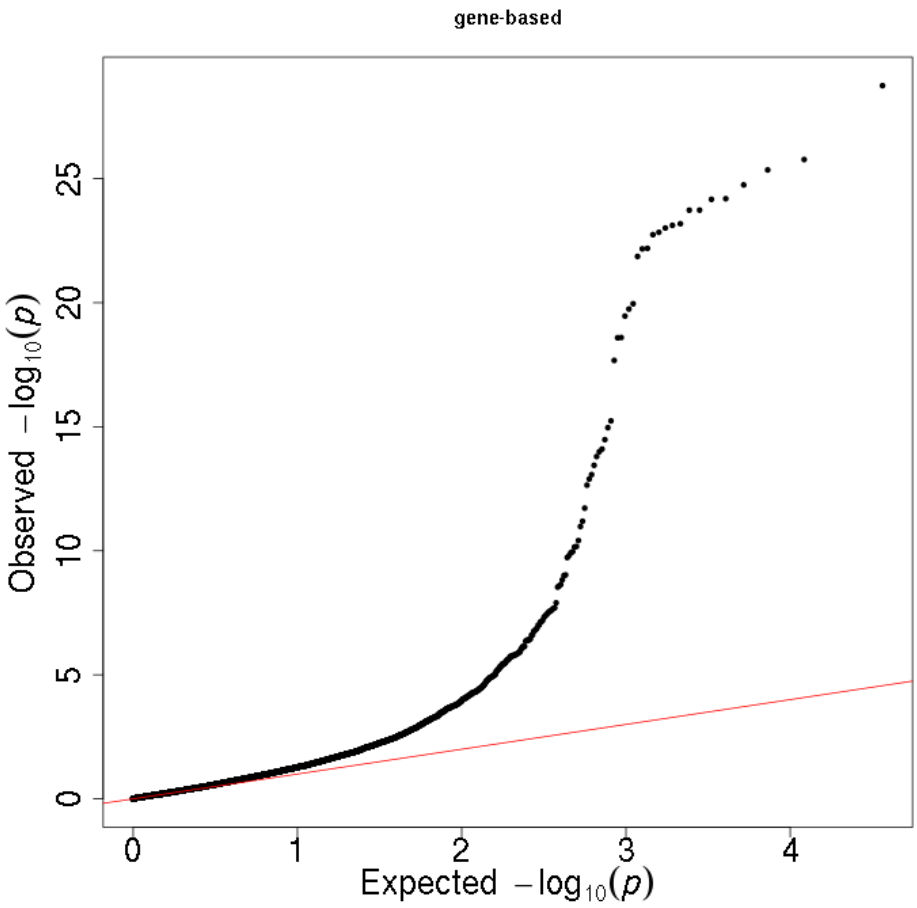

Supplementary Figure 6. Single-cell expression gene-set results of human brain tissue. The black vertical line indicates the significance threshold correcting for number of tests within category. MG = microglia; ExCA1 = Hippocampal CA 1 pyramidal neurons; END = Endothelial cells; ExPFC2 = Prefrontal glutamergic neurons 2; ExPFC1 = Prefrontal glutamergic neurons 1; ODC1 = Oligodendrocytes; ASC2 = Astrocytes 2; OPC = Oligodendrocyte precursor cells 1; GABA1 = GABAergic interneurons 1; NSC = Neuronal stem cells; GABA2 = GABAergic interneurons 2; OPC2 = Oligodendrocyte precursor cells 2; ExCA3 = Hippocampal CA 3 pyramidal neurons; ASC1 = Astrocytes 1; ExDG = Dentate gyrus granule neurons.

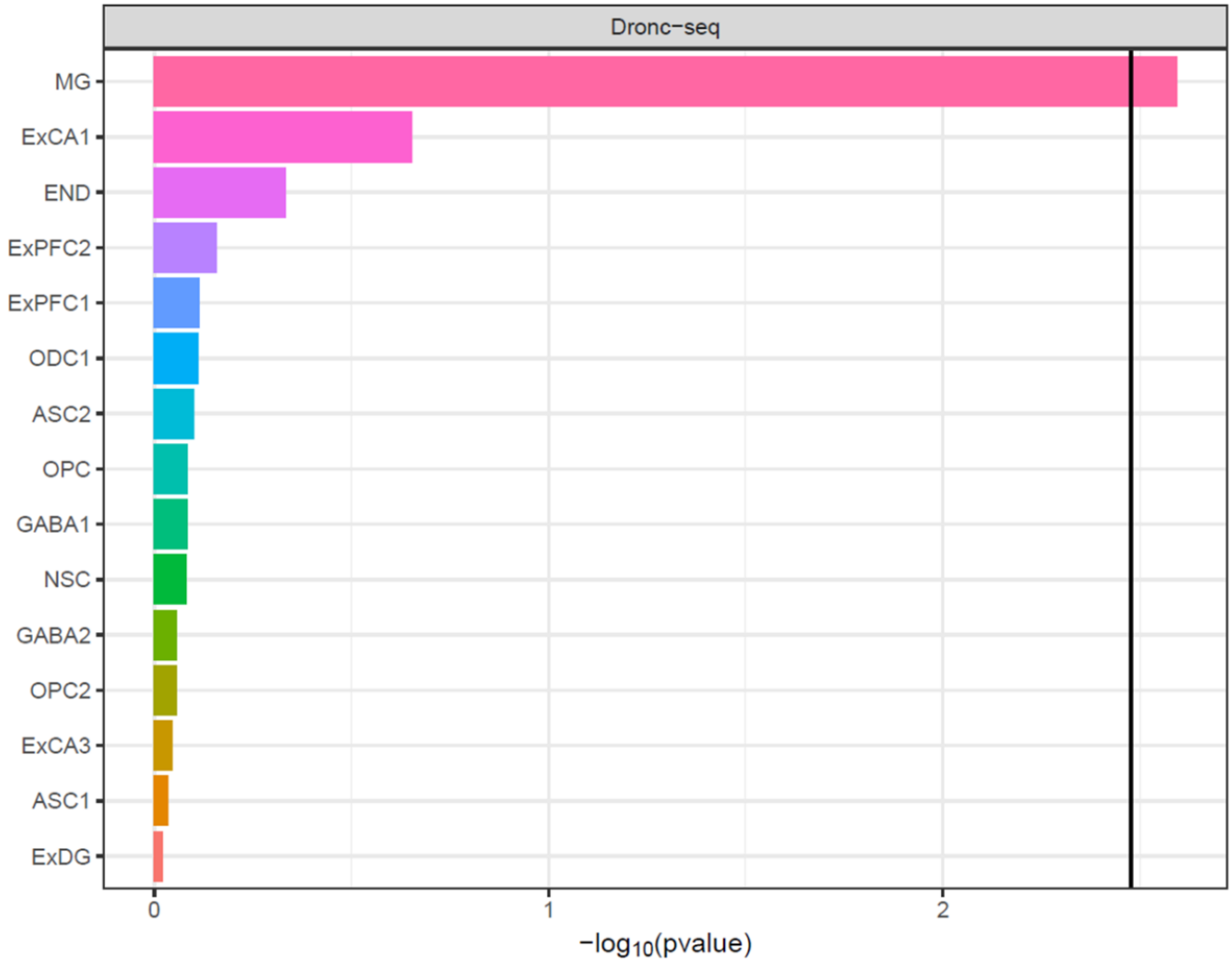

Supplementary Figure 7. Mendelian Randomization tests for the effect of correlated phenotypes on risk for Alzheimer's disease. For independent significant SNPs from each correlated phenotype, effect sizes of the SNPs for Alzheimer's disease (b_{zy}) are shown on the x-axis and effect sizes for correlated phenotypes are on the y-axis (b_{zx}). The dotted line represents a line with slope of (b_{xy}) and an intercept of 0.Red dots represent outliers that were excluded for the Mendelian Randomization analysis.

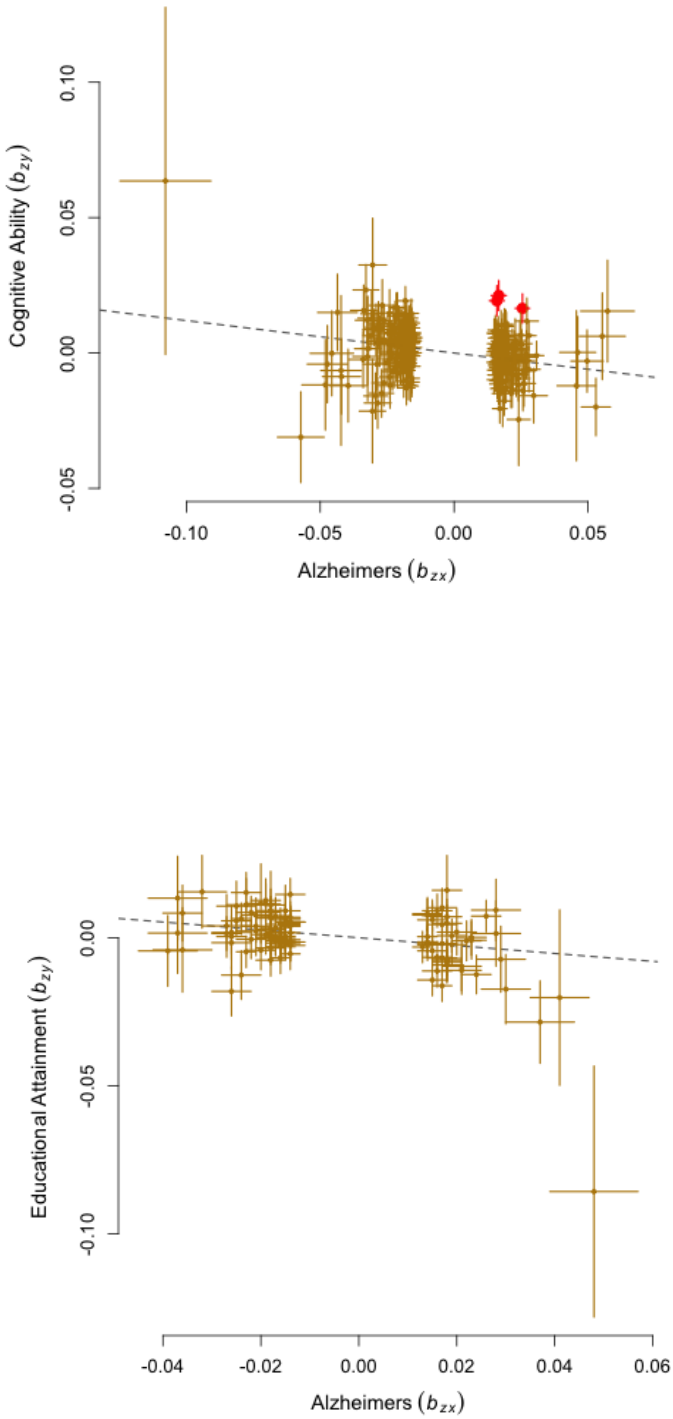

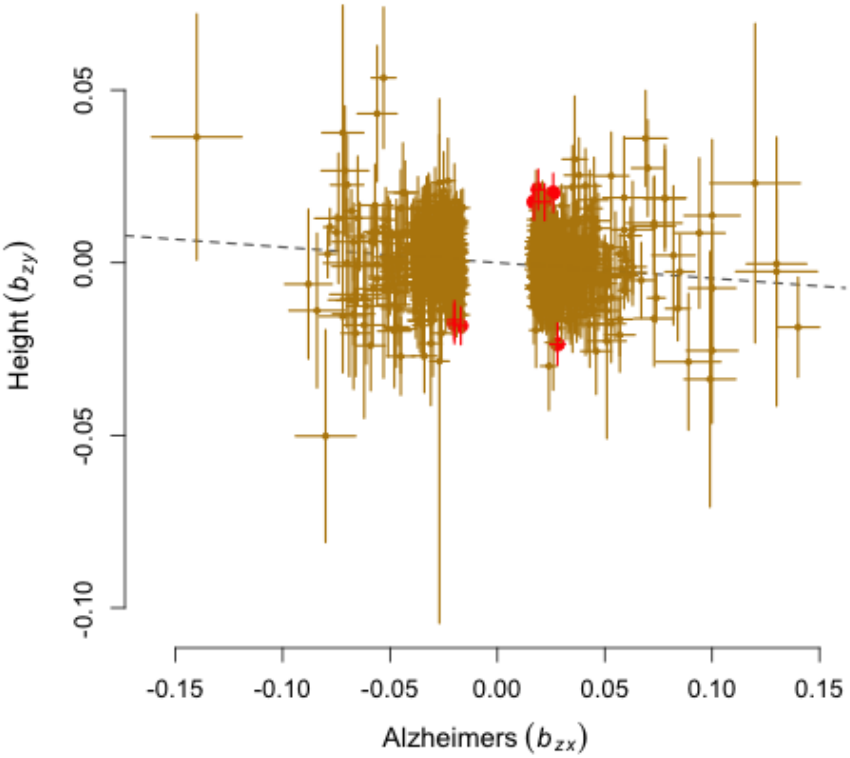
Height (b_{zy})
0.05
0.00
-0.05
-0.10
-0.15
-0.10
-0.05
0.00
0.05
0.10
0.15
Alzheimers (b_{zx})

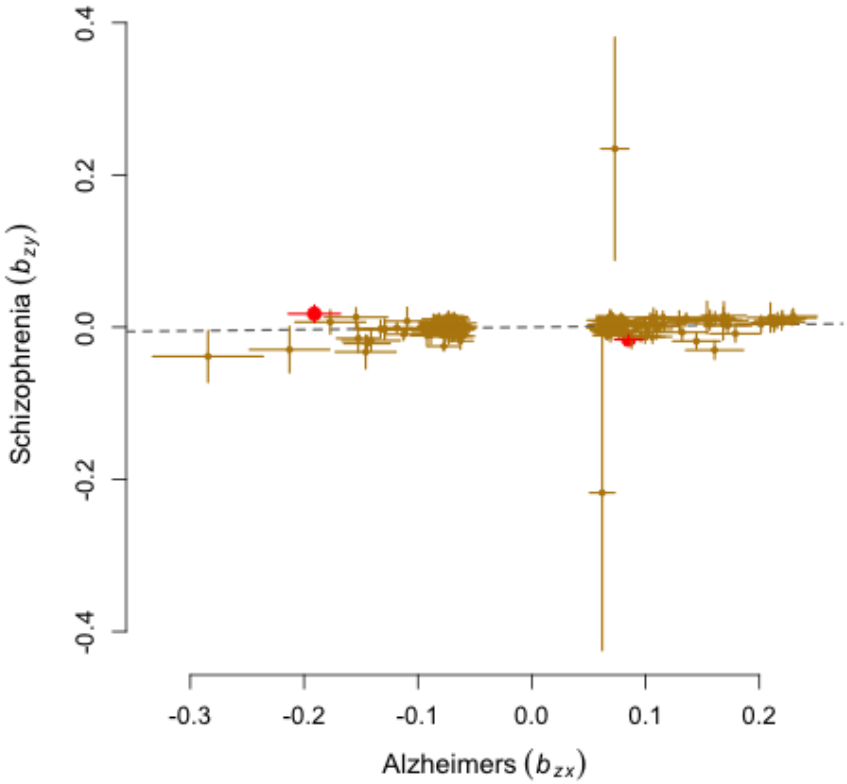
Schizophrenia (b_{zy})
0.4
0.2
0.0
-0.2
-0.4
-0.3
-0.2
-0.1
0.0
0.1
0.2
Alzheimers (b_{zx})

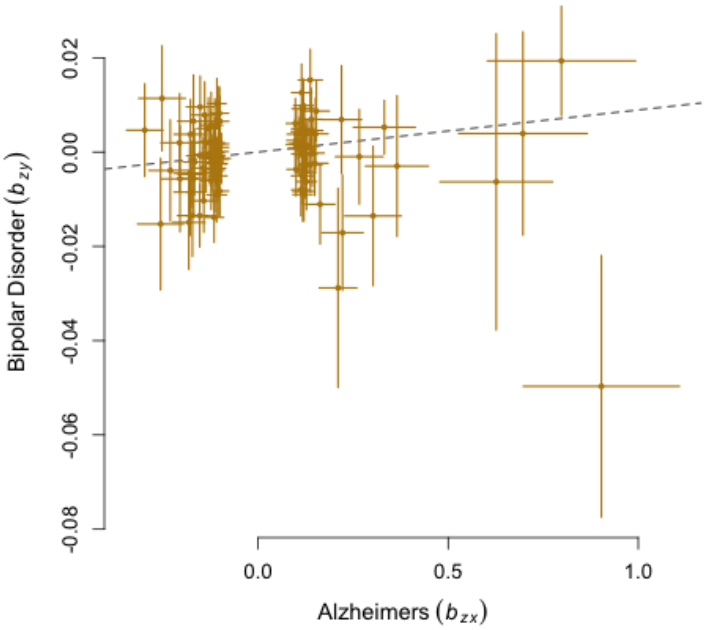
Bipolar Disorder (b_{zy})
0.02
0.00
-0.02
-0.04
-0.06
-0.08
0.0
0.5
1.0
Alzheimers (b_{zx})

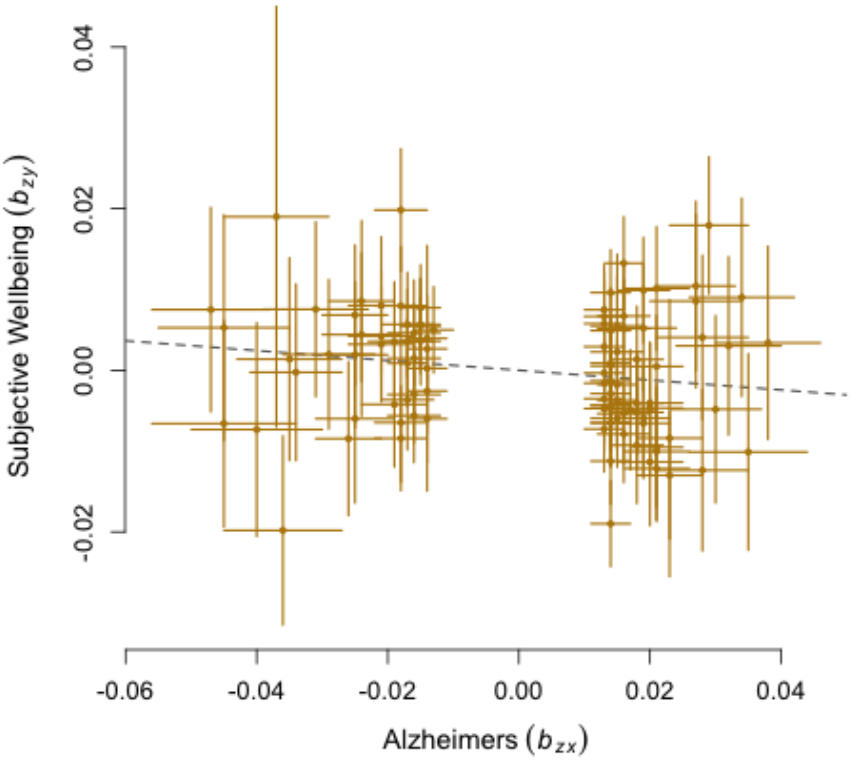
Subjective Wellbeing (b_{zy})
0.04
0.02
0.00
-0.02
-0.06
-0.04
-0.02
0.00
0.02
0.04
Alzheimers (b_{zx})

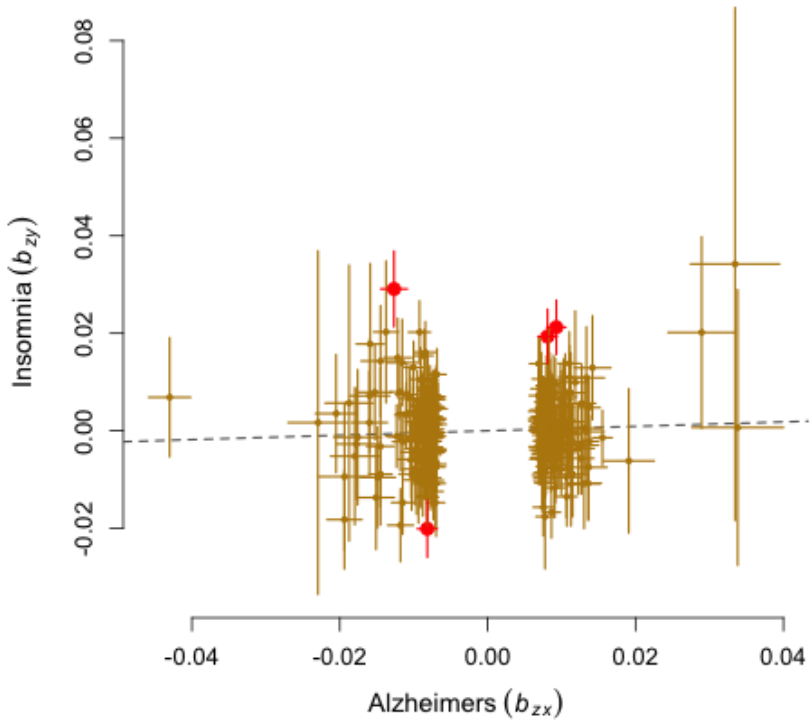
Insomnia (b_{zy})
0.08
0.06
0.04
0.02
0.00
-0.02
-0.04
-0.02
0.00
0.02
0.04
Alzheimers (b_{zx})

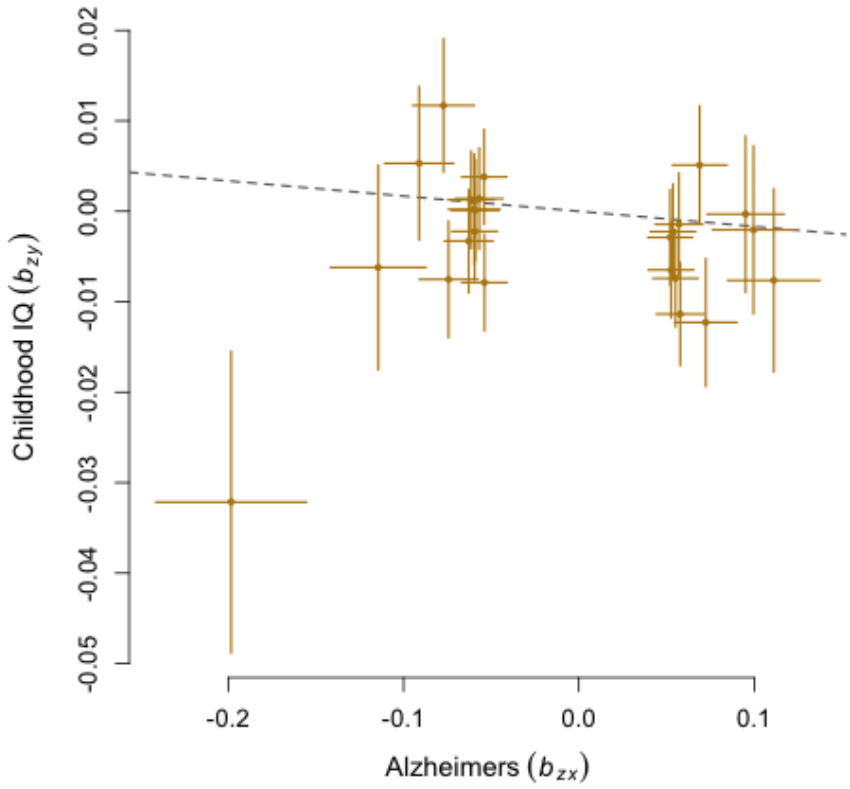
Childhood IQ (b_{zy})
0.02
0.01
0.00
-0.01
-0.02
-0.03
-0.04
-0.05
-0.2
-0.1
0.0
0.1
Alzheimers (b_{zx})

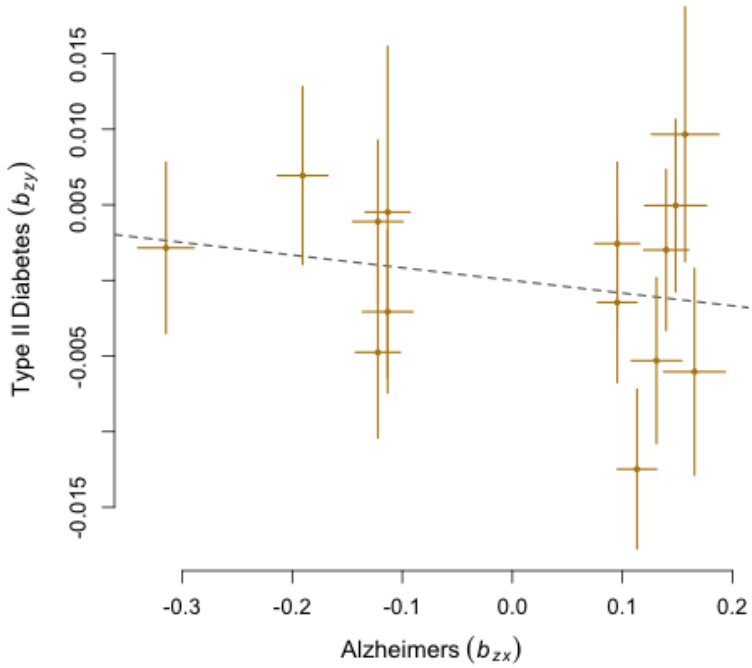
Type II Diabetes (b_{zy})
-0.015
-0.005
0.005
0.010
0.015
-0.3
-0.2
-0.1
0.0
0.1
0.2
Alzheimers (b_{zx})

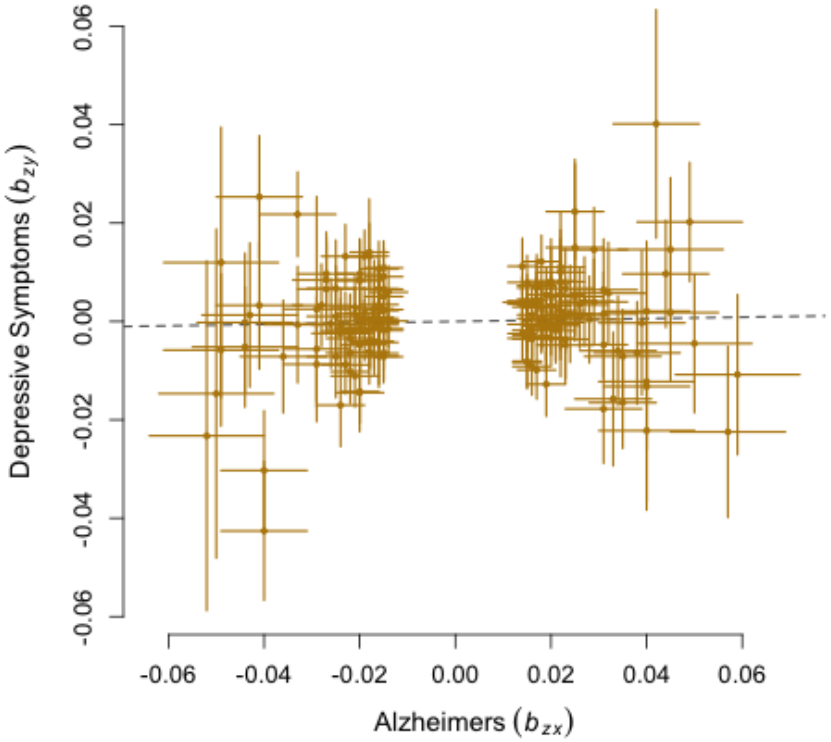
Depressive Symptoms (b_{zy})
-0.06
-0.04
-0.02
0.00
0.02
0.04
0.06
-0.06
-0.04
-0.02
0.00
0.02
0.04
0.06
Alzheimers (b_{zx})

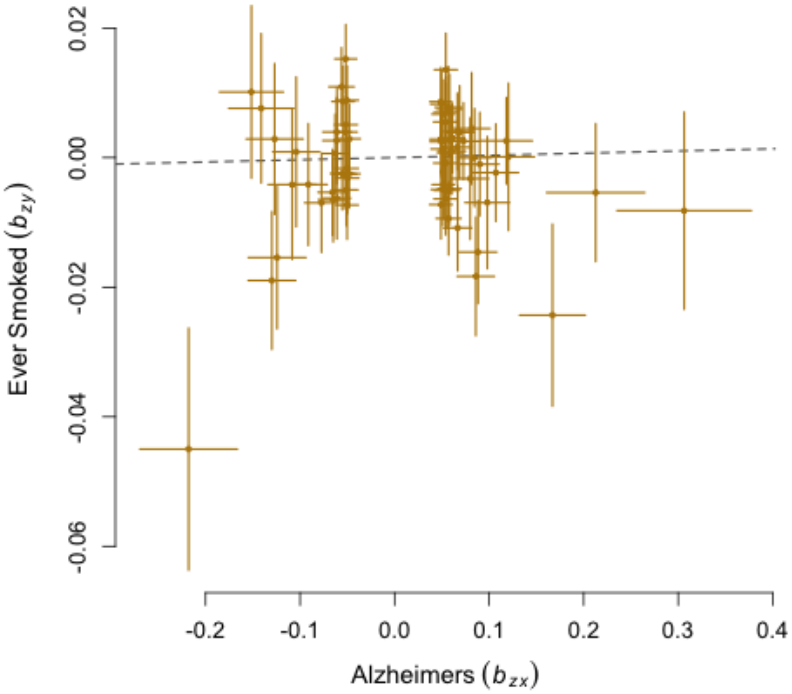
Ever Smoked (b_{zy})
0.02
0.00
-0.02
-0.04
-0.06
-0.2
-0.1
0.0
0.1
0.2
0.3
0.4
Alzheimers (b_{zx})

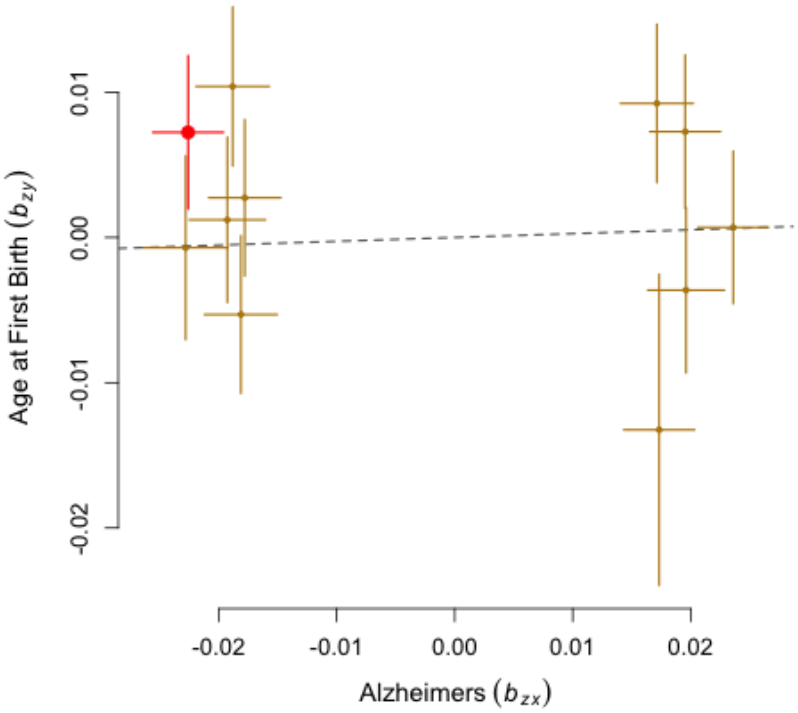
Age at First Birth (b_{zy})
0.01
0.00
-0.01
-0.02
-0.02
-0.01
0.00
0.01
0.02
Alzheimers (b_{zx})

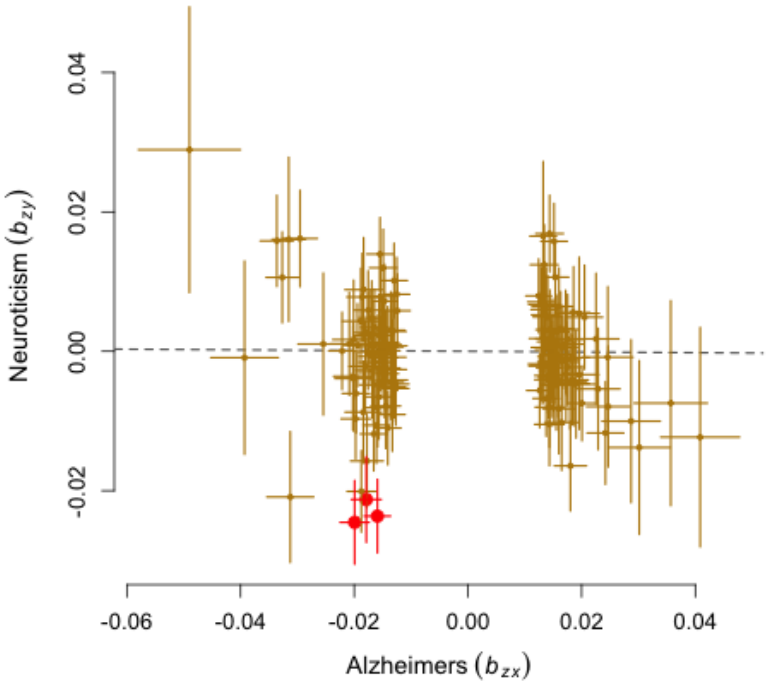
Neuroticism (b_{zy})
0.04
0.02
0.00
-0.02
-0.06
-0.04
-0.02
0.00
0.02
0.04
Alzheimers (b_{zx})